UNIVERSITÄT
BERN

Graduate School for Cellular and Biomedical Sciences

University of Bern

Early detection of degeneration of the equine joint cartilage using quantitative MRI techniques

PhD Thesis submitted by

Andrea Simone Bischofberger

from **Heiden, AR**

for the degree of

Doctor of Veterinary Medicine and Philosophy (DVM,PhD)

Supervisor
Prof. Dr. Patrick Kircher
Clinic for Diagnostic Imaging, Small Animal Department,
Vetsuisse Faculty of the University of Zurich

Co-advisor
Prof. Dr. Anton Fürst
Equine Hospital, Equine Department,
Vetsuisse Faculty of the University of Zurich

Accepted by the Faculty of Medicine, the Faculty of Science and the Vetsuisse Faculty of the University of Bern at the request of the Graduate School for Cellular and Biomedical Sciences

Bern, Dean of the Faculty of Medicine

Bern, Dean of the Faculty of Science

Bern, Dean of the Vetsuisse Faculty Bern

1 Table of contents

2 List of abbreviations

CC: calcified cartilage thickness

dGEMRIC: delayed gadolinium enhanced magnetic resonance imaging of cartilage

DIPJ: distal interphalangeal joint

DP: distal phalanx

EDTA: ethylene diamine tetraacetic acid

FLASH: fast low angle shot

FSE: fast spin echo

GAG: glycosaminoglycan

Gd-DTPA^{2-}: gadolinium diethylene triamine pentaacetic acid

HC: hyaline cartilage thickness

ICC: intraclass correlation coefficient

IL: interleukin

MMP: matrix-metalloproteinase

MP: middle phalanx

MRI: magnetic resonance imaging

OA: osteoarthritis

ROI: region of interest

SD: standard deviation

SPGR: spoiled gradient recalled acquisition at steady state

TC: total cartilage thickness

TE: echo time

TNF: tumor necrosis factor

TR: repetition time

3 Abstract of the thesis

Osteoarthritis (OA) is one of the principal causes of lameness and leads to early retirement of equine athletes. The distal interphalangeal joint (DIPJ) experiences considerable loads during exercise and is commonly affected with OA in sport horses. Since early articular cartilage degeneration may not result in lameness, it is essential to use imaging modalities that can identify cartilage lesions early, especially if prevention and repair of damaged cartilage is to occur. Delayed gadolinium enhanced magnetic resonance imaging of cartilage (dGEMRIC) and T2 mapping are quantitative MRI-techniques, which have been shown to reliably identify early cartilage degeneration in humans.

In dGEMRIC, gadolinium, a negative contrast agent is used. In the event of OA, glycosaminoglycans (GAGs) are lost and the negative charge decreases, allowing proportional uptake of the contrast media into the cartilage. T2 mapping is a reliable technique to visualize cartilage hydration, collagen integrity and orientation. Cartilage collagen structure and water content are other important organic cartilage components, which are affected by early cartilage degeneration.

The premise that hyaline cartilage degeneration may be identified early holds considerable promise and warrants investigation of these MRI-techniques in horses. The project aims at 1) establishing dGEMRIC and T2 mapping techniques in the normal and osteoarthritic equine DIPJ, 2) investigating whether dGEMRIC or T2 maps can identify OA and 3) correlating dGEMRIC and T2 maps with the biochemical cartilage data (collagen type II structure, water and GAG content).

The study was performed on twelve Warmblood cadaver limbs. The mean T1 and T2 weighted relaxation times before (T1) and after ($T1_{Gd}$) intraarticular gadolinium administration of predetermined sites (n = 122) of the DIPJ cartilage were obtained. Cartilage thickness measurements were obtained on T1 and T2 weighted images at the same sites. Corresponding cartilage sites were examined macroscopically, histologically (Safranin-

O-Fast green, picrosirius red, toluidine blue, haematoxylin and eosin) and immunohistochemically (collagen type II). Cartilage health was graded macroscopically and histologically. Cartilage thickness was measured histologically. The sites' GAG (µg/mg) and water content (%) were determined. The T1-, $T1_{Gd}$- and T2 values were correlated to the histological, macroscopic and biochemical data. The cartilage thickness measurements obtained on dGEMRIC and T2 maps were correlated with the histomorphology. Generalized linear mixed models analysed the effects of cartilage sites, articular surface and cartilage health (histologic and macroscopic scores) on the relaxation times (T1, $T1_{Gd}$ and T2) as well as the cartilage thickness measurements.

The main results from this study related to the DIPJ are that dGEMRIC and T2 mapping was established. DGEMRIC and T2 maps are reliable to visualize the true articular cartilage thickness in the normal and osteoarthritic equine DIPJ at areas of opposing and non-opposing cartilage surfaces. A topical variation of T1-, $T1_{Gd}$- and T2 values and cartilage thickness measurements were shown. Varying degrees of naturally occurring DIPJ OA significantly affected dGEMRIC relaxation times, potentially having important consequences in early recognition of equine OA. However against our hypothesis T2 maps were not sensitive enough to depict the varying degrees of OA in these cadaver DIPJs, needing follow-up investigation. The GAG and water content correlated with the T1 value and the cartilage macroscopic and histologic findings, however not with the $T1_{Gd}$ value. The water content negatively correlated with the T2 values, however not the GAG content or the collagen structure evaluated by means of immunohistochemistry or polarized microscopy.

Limitations of the study include small deviations between MRI data and histological data despite having used a template to match the sites. In terms of OA distribution within the cartilage specimens there was a relatively small size of cartilage specimens with a severe grade of OA, potentially explaining the lack of the sensitivity of the T2 maps. In spite of these limitations this study lays a foundation for future studies investigating promising cartilage specific MRI sequences. The study provides technical information and reference values for dGEMRIC and T2 mapping in the normal and osteoarthritic equine DIPJ, having important

consequences in early recognition of OA in a research and later potentially in a clinical setting. Future studies need to further examine the use of intravenous administration of gadolinium and develop a dGEMRIC scanning protocol in the live horse. The effect of differing degrees of OA on T2 values needs to be further investigated and finally dGEMRIC and T2 maps of horse DIPJs with differing degrees of OA and lameness need to be performed in order to relate the MR lesions to the clinical symptoms.

4 Introduction

In horses, musculoskeletal soundness is crucial, as most horses are ultimately kept for athletic performance. When a horse is unable to perform, emotional and financial implications arise.

Lameness due to articular disease is the primary cause of poor performance in horses; [1] indeed, 60% of lameness problems in horses are related to osteoarthritis (OA). For example: The U.S. horse population is currently estimated to be 7.3 million according to the American Veterinary Medical Association. This means that over 4 million horses are affected by OA. Considering direct and indirect medical expenses, the cost of one horse suffering from OA per year amounts to $15 000. [2] Thus articular disease constitutes the largest, single economic loss to the equine industry and arthritic pain represents a serious animal welfare concern. [3]

4.1 The distal interphalangeal joint

Each joint in the horse can be affected by OA. Depending on the horses breed, age and its use certain joints may be more likely affected than others. Racing is a large source of revenue and employment in many countries; therefore lameness in Thoroughbred racehorses is often studied. Twenty-five per cent of racing Thoroughbreds experience pain in the proximal metacarpo/metatarsophalangeal joint, [4] with this joint being the most commonly affected by traumatic and degenerative lesions of the appendicular skeleton, often referred to as overload arthritis, resulting in OA. [5,6]

In sport horses the distal interphalangeal joint (DIPJ) of the forelimb is a commonly affected joint. [7] Despite this joint being commonly affected, it remains under reported in the current veterinary literature. [7-11] The DIPJ is a classical hinge joint, where flexion and extension, latero-medial excursion, rotation and sliding are possible joint movements. During normal weight bearing and propulsion on flat ground the DIPJ joint moves in a

sagittal plane (flexion and extension). When weight bearing on the circle or on uneven ground there is a rotational and sliding movement in the joint. [12] The DIPJ is a complex joint consisting of the articulation between the middle (MP) and the distal phalanges (DP) as well as the articulation with the navicular bone. The distal sesamoidean impar ligament, the collateral sesamoidean ligaments, the navicular bursa and the deep digital flexor tendon are soft tissue structures closely associated with the DIPJ and are shown in Figure 1.

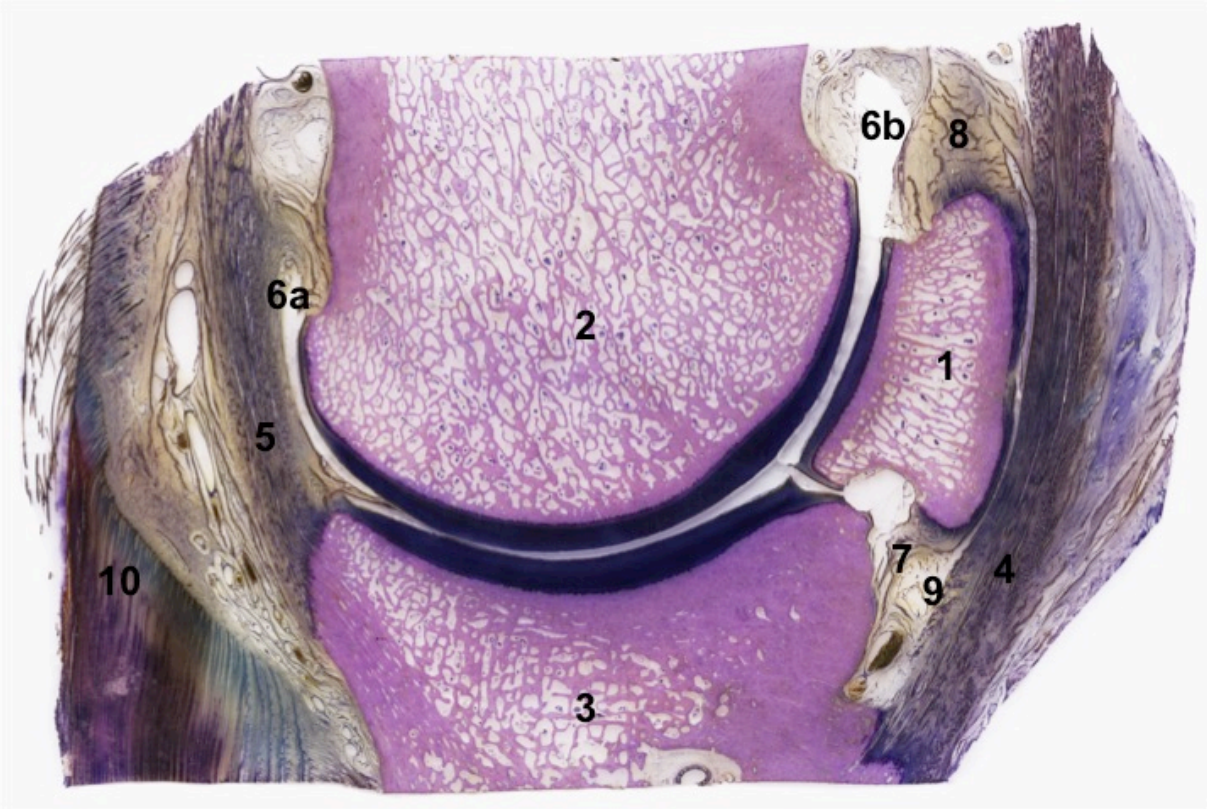

Figure 1: *Histologic sagittal view of a DIPJ of a Warmblood horse stained with Giemsa courtesy of Prof. H. Geyer, Section of Anatomy, Vetsuisse-Faculty, University of Zürich.*
1= navicular bone, 2 = second phalanx, 3 = distal phalanx, 4 = deep digital flexor tendon, 5 = Common digital extensor tendon, 6 = Dorsal (a) and palmar (b) recess of the distal interphalangeal joint, 7 = impar ligament, 8 = suspensory ligament of the navicular bone, 9 = bursa podotrochelaris, 10 = dorsal hoof wall.

Pain associated with the DIPJ itself can be caused by synovitis, joint capsule and/or subchondral bone trauma, osteoarthritis, osseous cyst like lesions, osseous fragments

located at the extensor process of the DP or at either condyles of the distal MP as well as injuries to the distal sesamoidean impar ligament. [12] Pathologies of the DIPJ are often associated with conditions of the foot [13] and/or the podotrochlear apparatus. Medio-lateral or dorso-palmar foot imbalances influence the load distribution and range of movements of the DIPJ. In horses with joint effusion (i.e. synovitis) foot imbalances can result in increased intraarticular pressures leading to damage of the articular cartilage and ultimately to lameness. [13] Further, the degree of sliding and axial rotation within the DIPJ have been found linked to a possible predisposition of horses to injure this joint. [12]

4.2 Synovial joints: anatomic overview

The major components of a synovial joint include: the articular cartilage, the subchondral bone, the synovial membrane, the synovial fluid, the fibrous joint capsule and the periarticular ligamentous structures. [14]

4.2.1 *Articular cartilage*

The central structure, which constitutes the joint surface and its function, is the articular cartilage. Together with the synovial fluid articular cartilage enables frictionless movement of synovial joints. The articular cartilage is composed of water (75 %), type II collagen (15 %), proteoglycans (10 %) and chondrocytes (2 %). [15] Figure 2 shows the normal morphology and orientation of chondrocytes and collagen in the specific cartilage zones.

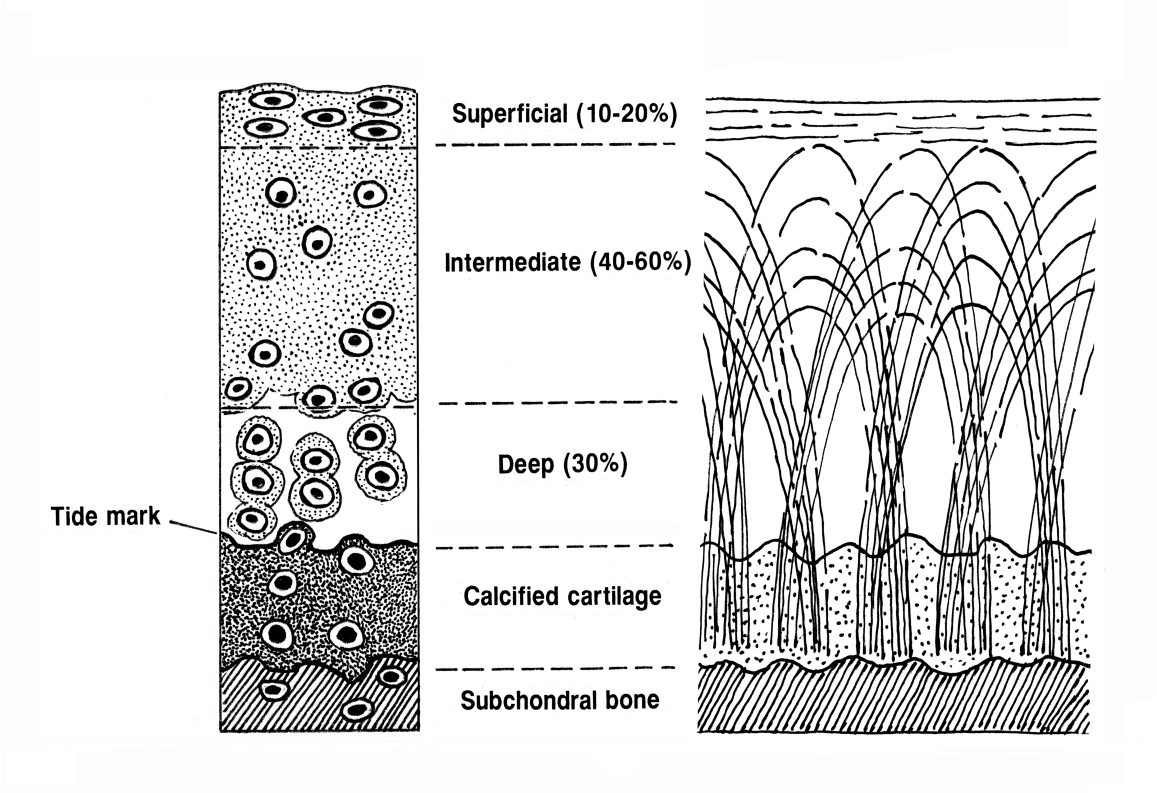

Figure 2: *Schematic illustration of the different contiguous cartilage zones and the characteristic morphology and orientation of the chondrocytes (left side) as well as the typical orientation of the collagen type II fibers (right side). Illustrated by M. Haab, Equine Department, Vetsuisse-Faculty, University of Zürich. Adapted from March L.: Articular Cartilage in Health and Disease. P. 86. In Sambrook P.: The Muskuloskeletal Sytsem. Churchhill Livigstone, New York, 2001.*

Collagen type II fibers are secreted into the extracellular space as propeptides. In the extracellular space, procollagen peptidases remove their excess endings. [16] Mature collagen type II fibers form fibrils, which are composed of three identical alpha I (II)-chains, organised in an alpha helix. [17,18] Further these fibrils are organised in a 3-dimensional framework, which accounts for the tensile strength of the articular cartilage. [18] In the superficial layer (tangential zone) (10 - 20 % of the total cartilage thickness) the collagen fibers are tightly packed, oriented parallel to the cartilage surface and are small in diameter. This layer is also named the armor plate layer referring to its toughness, resilience and skin like cartilage surface. [14] The resistance of the articular cartilage to tensile and shear forces is most pronounced in the superficial cartilage layer, due to their parallel orientation. [18] Another

important factor regarding the magnitude of resistance to tensile strength is the amount of crosslinks between the molecules. A decreased number of crosslinks results in a decline of the articular cartilages` tensile property. [19] The predominant crosslinks are 3 - hydroxypyridinium crosslinks. [18] There are small pores between the fibers of the superfical cartilage layer (diameter 6 nm). These pores allow small molecules such as glucose and ions to pass through, while large proteins such as hyaluronan cannot penetrate. [14] In the intermediate layer (tangential zone) the collagen is randomly arranged (40 - 60 % of the total cartilage thickness). In the deep layer (radiate zone) collagen type II fibrils are fewer, more loosely spaced and of larger diameter. They are arranged perpendicular to the articular surface forming arcades of Benninghoff, they transverse the calcified cartilage layer and are anchored in the subchondral bone (30 % of the total cartilage thickness). [14]

Proteoglycans are literally a combination of proteins and polysaccharides. Proteoglycans are interspersed between the above-described collagen-framework. The content of proteoglycans regulate the stiffness of the cartilage, and provide resistance to compressive forces. [14] In contrast to collagen fibers, the biggest amount of proteoglycans can be found in the deep zone and its content decreases towards the surface. [19] Eighty-five per cent of proteoglycans are aggrecans. [14] Aggrecan molecules are made up of a protein backbone and glycosaminoglycans, which attach radially to the protein. Chondroitin-4-sulfate, chondroitin-6-sulfate and keratan sulphate are the main glycosaminoglycans (GAGs) of equine articular cartilage. [14,16,19,20] In mature articular cartilage chondroitin-6-sulfate, and keratan sulphate, are the predominant types. In immature articular cartilage chondroitin-4-sulfate is the major type and its amount decreases during maturation. Aggrecan molecules then bond to a hyaluronan molecule and form large aggregates. [14] These aggregates can comprise over 100 aggrecan molecules. Such an aggrecan aggregate is shown in Figure 3.

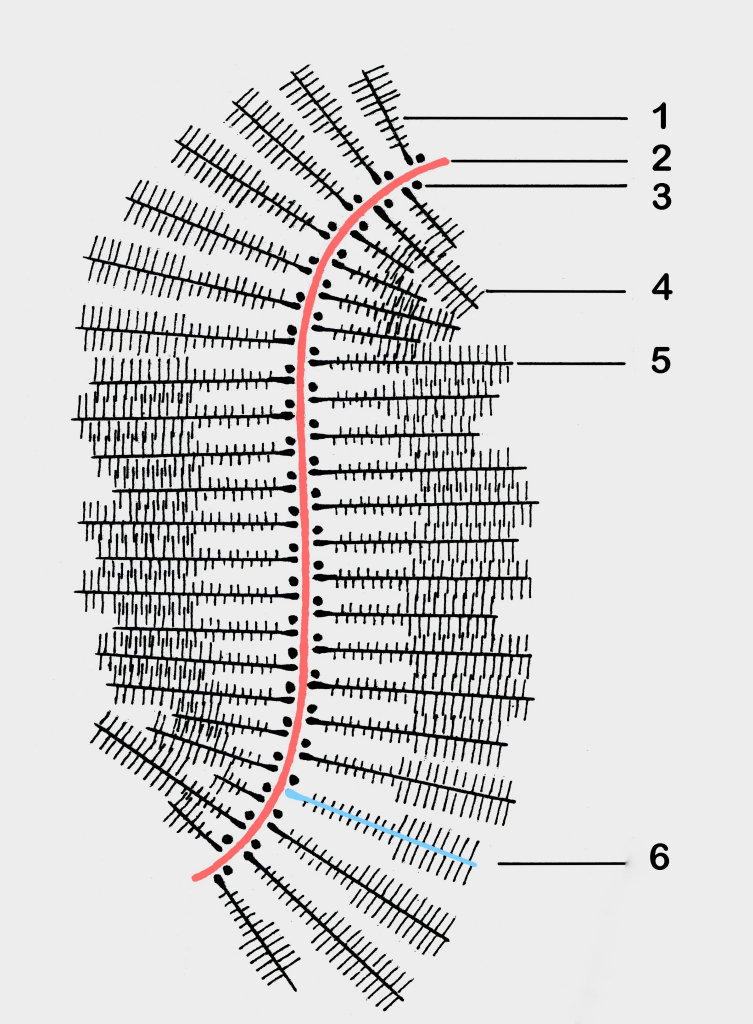

Figure 3: *Aggrecan aggregate consitent of multiple single aggrecan molecules linked to hyaluronan. 1 = keratan sulfate, 2 = hyaluronan, 3 = link protein, 4 = chondroitin sulfate, 5 = core protein, 6 = a single aggrecan molecule. Illustration by M. Haab, Equine Department, Vetsuisse-Faculty, University of Zürich. Adapted from Rosenberg L.: Structure of Cartilage Proteoglycan. In Simon WH.: The Human Joint in Health and Disease. University of Pennsylvania Press, Philadelphia, 1978.*

Water is the most abundant molecule in the extracellular matrix of the cartilage. The GAG itself is constituted of repeating units of disaccharides. They are charged negatively because of the sulphated and carboxylated radicals in chondroitin sulphate, and sulphated radicals in keratan sulphate. The charges of the polyanionic side chains repeal each other and bind cations, mainly sodium, increasing the osmolarity of the extracellular matrix,

resulting in water molecules to be drawn into the extracellular matrix. [19] The collagen arrangement also limits the amount of water that is attracted by the proteoglycans. [21] This results in the constrained cartilage swelling giving the cartilage its compressive stiffness vital for its normal function. [19]

Cartilage is a relatively acellular type of tissue with only few chondrocytes. The chondrocyte morphology is different and characteristic for each cartilage layer (see Figure 2). The superficial layer consists of flattened chondrocytes oriented parallel to the joint surface and densely packed collagen. In the intermediate layer the chondrocytes are larger and more round to ovoid shaped, whereas towards to deep layer the chondrocytes are the largest and oriented perpendicular to the joint. The tidemark separates the non-calcified radiate zone from the calcified zone, where mineralized cells and extracellular matrix are predominant. Chondrocytes possess cytoplasmatic processes through which they can respond to loading of the articular cartilage during exercise. During physiological cartilage loading chondrocytes have an anabolic metabolism, whereas during superphysiologic levels of cartilage loading the chondrocyte metabolism turns into a catabolic state. [14]

4.2.2 *Subchondral bone*

The subchondral bone is a thin plate of bone situated under the articular cartilage providing contour and stability to the articular cartilage. It consists of cortical bone with the Haversian system. The histologic appearance is similar to other cortical bone, however the subchondral bone plate has been found to be much more deformable than other cortical bone. [14] Remodelling and stiffening of the subchondral bone plate determine the amount of forces, which the articular cartilage is subjected to. [21] The subchondral bone plate vasculature also supplies the cartilage with nutrients and the subchondral bone plate cells secrete peptides regulating the chondrocytes. [22]

4.2.3 *Synovial membrane and synovial fluid*

The synovial membrane, consisting of the intimal - and subintimal layer, lines the joint

cavity. Synoviocytes of the intimal layer determine the content of the synovial fluid by either phagocytosis, pinocytosis or protein secretion. There are different types of synoviocytes based on their ultrastructure and their immunohistological characteristics. Synoviocytes type B are responsible for protein secretion and synoviocytes type A are responsible for phagocytosis or pinocytosis. Synoviocytes are dynamic cells and can transition from one type to another. The transitional type of synoviocyte is termed the C type. The proteins secreted by synoviocytes making up the composition of the synovial fluid include hyaluronan, collagen, lubricin, pro-matrix metalloproteinases, interleukins and eicosanoids. The subintimal layer is made of fibrous tissue and has a good blood supply and innervation.

Synovial fluid is a dialysate of blood plasma with important proteins added by the synoviocytes. Molecules less than 10 000 Dalton can pass through the endothelium of the vasculature of the subintima. Larger molecules such as hyaluronan and lubricin are important as boundary lubricants of the joint surfaces and in the steric exclusion of larger molecules from the synovial cavity. [14]

4.2.4 *Joint capsule and the periarticular ligamentous structures*

The fibrous joint capsule and the periarticular ligamentous structures stabilise the joints. [14] The fibrous joint capsule and the ligaments are mainly composed of type I collagen and some elastin fibers, which are organised in parallel fascicles dispersed by fibrocytes and blood vessels as well as occasional nerve fibers. The comparison to Sharpey fibers has been made to describe the attachment of the joint capsule and the periarticular ligaments to the bone. It is important to keep in mind that the joint capsule and the periarticular ligamentous structures are metabolically active tissues, which may hypertrophy or atrophy with exercise or immobilization, respectively.

4.3 Pathogenesis of osteoarthritis: brief overview

Osteoarthropathy, derived from the Greek, is the general term defined as disease of the joints and bones. Disease of the articular cartilage is more specifically described by the term OA. The term OA may be used in the clinical, diagnostic imaging, macroscopic,

histological and biochemical fields. Within the past decade research in these areas has progressed enormously. All of the above named anatomic structures play an important role in the disease of OA and contribute to its overall pathogenesis. OA can originate from different causes:

a) Degenerated or defective articular cartilage itself may be an essential inciting cause of OA. [21] Cartilage degeneration results in abnormal biomechanical properties of the cartilage leading to it`s failure under physiological loads.

b) Overuse or conformational abnormalities (i.e. in younger athletic horses) can lead to excessive biomechanical forces acting on normal articular cartilage. The abnormal forces overwhelm the normal metabolic repair mechanisms of the articular cartilage and failure of the articular cartilage is the consequence. The abnormal loads may either be repetitive in nature resulting in cartilage micro damage or be a single traumatic event. Micro damage accumulates over time and leads to cartilage failure when the normal repair process of the tissue is overwhelmed. A single traumatic event, immediately leads to failure without a chance for repair.

c) Physiologically the density of the subchondral bone increases under load. If bone densitiy increases excessively in response to superphysiological loads and a specific threshold is reached, the subchondral bone becomes less compliant. As a consequence the articular cartilage may undergo damage.

From the primarily injured tissue (articular cartilage, subchondral bone, synovial membrane) inflammation starts and the inflammatory cascade perpetuates and affects the neighbouring joint tissues. Cytokines play a fundamental role in this cascade. The primarily upregulated cytokine is interleukin (IL) - 1β. [17] IL - 1β has a multitude of pathogenic properties including the upregulation of the production of matrix-metalloproteinases (MMP's), inhibition of the synthesis of their natural inhibitors and prevention of the synthesis of the major extracellular matrix components, such as collagens and proteoglycans. Moreover IL - 1 activates fibroblasts to secrete type I and III collagen, resulting in fibrosis of the joint capsule observed in chronically inflammed joints. [23] Another

cytokine which is central in the pathogenesis of OA is tumor necrosis factor - α (TNF - α). TNF - α leads to the upregulation of MMP's. [24] MMP's are degradative enzymes. Both synoviocytes and chondrocytes release MMP's. [14] The different MMP's as a collective are able to degrade every single component of the articular cartilage. MMP's can further be divided into three different subtypes, [19] according to their preferential substrate including collagenases, stromelysins and gelatinases. [19] Of the enzyme collagenase three different forms have been isolated: MMP - 1, MMP - 8 and MMP - 13. [17] MMP - 13 is most commonly involved in degradation of collagen type II fibers in horses and humans. Beside MMP's there are additional enzymes not mentioned here possessing the ability to break down the extracellular matrix components. Proteoglycans, predominantely aggrecans are degraded by "aggrecanases", enzymes which have also been named a disintegrin and metalloproteinase with thrombospondin motifs (ADAMTS)- 4 and 11. [19]

On a biochemical level, one of the first indications of OA is decreased proteoglycan content and increased water content of the extracellular matrix. [25] Physiologically the collagen framework limits the amount of water that can be attracted by the GAGs. [22] In the early stages of OA the collagen framework loses its organisation [25] allowing the GAGs to attract more water and the water content of the extracellular matrix increases. [25] In the later stage of the disease, superficial cartilage fibrillation as well as breakdown of the collagenous framework occurs. [25] If superficial changes occur, the deeper layers are also more susceptible to damage because they are less resistant to the physiological forces. [19]

4.4 Assessing the degree of osteoarthritis

OA has been scored using macroscopic and microscopic scoring systems. Spontaneously or termed naturally occurring OA must be clearly distinguished from experimentally created OA.

4.4.1 *Macroscopic cartilage assessment*

Macroscopically articular cartilage appears smooth, milky or glasslike. In thinner areas the cartilage has a slightly pink appearance, because of the translucent subchondral bone plate. Macroscopically the surface of the articular cartilage looks flawless, however when assessed electron microscopically small depressions with a diameter of 20 - 40 µm can be seen. [14,19,20] The articular cartilage is approximately 1 - 4 mm thick. This however depends on the joint itself, the location within the joint, the individual's age and whether the joint is under load or not. Due to the non-existence of a vascular, lymphatic and neural supply, the nutrition of the adult articular cartilage occurs solely via diffusion of the synovia. [14]

In cases of spontaneous OA macroscopic changes of the articular cartilage have been scored using descriptive terms such as partial- and or/full-thickness erosions, wear lines or palmar arthrosis on the third metacarpal bone condyle in horses. [26-28] The Neundorf scoring system is a specific grading system, which has also been used in horses specifically for the metacarpophalangeal joint cartilage. [29] Additionally the Outerbridge scoring system, originally developed for the grading of chondromalacia of human patellae [30] may be used. A technique using India ink stain of the articular cartilage surface has also been reported to help detect spontaneous OA. [31] India ink particles will not enter intact articular cartilage surface. However when the surface of the articular cartilage is fibrillated and the proteoglycans are depleted the stain has a high affinity to the damaged cartilage. Use of India ink stain has been combined with digital imaging techniques in the equine proximal phalanx articular cartilage [32] or the stained area has been transferred to plastic in the medial femoral condyle to assess the affected area and stage the progression of disease. [33]

4.4.1 *Microscopic cartilage assessment*

Histologically, the articular cartilage can be divided into the four morphologically different zones as shown above in Figure 2. The surface of healthy articular cartilage appears smooth and constant under light microscopy. In early stages of OA, histological changes include fibrillation and irregularities of the cartilage surface. Further the decreased

proteoglycan content results in loss of staining of the superficial zone in Safranin-O-Fast green or toluidine blue stained sections. In further stages, fissures of the superficial zone can be noted. As OA progresses erosions with destruction of the cartilage surface may occur. In early stages erosions are superficial and in later stages erosions may expand up to the subchondral bone ("full thickness erosions"). The subchondral bone may form microcracks or collapse and pits may form. [34] Blood vessels may break through the tidemark, with loss of its integrity. [22]

Microscopic scoring systems used for grading spontaneously/naturally occurred OA include the Mankin grading system [35] or modifications thereof. [34] Criteria include structure of the cartilage, density of chondrocytes, cluster formation and the amount of staining with the Safranin-O-Fast green colorant. Further the Osteoarthritis Research Society International scoring system has also been used in experimental and also spontaneously/naturally occurring OA. [27]

4.5 Diagnosing osteoarthritis of the distal interphalangeal joint

Horses suffering from DIPJ OA show an acute or chronic lameness. Lameness may be unilateral or bilateral. In bilaterally lame horses clinical signs such as shortened strides, reluctance to jump and poor performance may occur. Upon palpation the dorsal DIPJ outpouching may be effused reflecting a certain degree of synovitis. Horses may show signs of pain upon hyperflexion and rotation of the DIPJ. The lameness may be localised to the DIPJ via perineural - and/or intraarticular anaesthesia.

Diagnostic imaging particularly radiography and ultrasonography have been the next step in confirming the cause of lameness until a few decades ago. In the early stages OA of the DIPJ is frequently associated with none to little radiographic changes. In the later stages these may include periarticular osteophytes and enthesiophytes, joint incongruity and joint space narrowing. [36] The ultrasonographic evaluation of the DIPJ is difficult and limited to evaluating the degree of joint effusion, [9] synovial proliferation, tears of the origin of the

collateral ligaments of the DIPJ, lesions of the deep digital flexor tendons in the pastern area and limited areas of the joint surfaces. By using the frog and bulbs of the heel as a window, ultrasonography can be used to image the central soft tissue structures within the hoof capsule. [37] This simple method allows imaging of the digital cushion, the deep digital flexor tendon, the distal recess of the podotrochlear bursa and the distal sesamoidean impar ligament. The flexor surface of the DP and distal sesamoidean bone can also be imaged. Unfortunately the frog only allows visualization of the central structures of the ventral foot and not the structures medial, lateral and dorsal to the frog as the hoof capsule is impenetrable by ultrasound.

Arthroscopy has been judged as a valuable tool diagnosing articular cartilage lesions, however the arthroscopic examination of the DIPJ is limited due to anatomic constraints and a large portion of the weight-bearing surface of the articular cartilage cannot be assessed despite joint flexion and extension during the procedure. [38] Additionally only the superficial portion of the articular cartilage can be inspected. This emphasizes the need for imaging tools for the assessment of articular cartilage, especially in the DIPJ.

4.6 Conventional magnetic resonance imaging of the equine distal interphalangeal joint

Magnetic resonance imaging (MRI) has emerged as a valuable diagnostic tool in these cases. T2 - weighted images are of interest in OA because T2 relaxation times are highly sensitive to tissue hydration. Generally on T2 - weighted sequences subchondral bone, tendinous and ligamentous structures are hypointense and fat, synovial fluid and cartilage are hyperintense. In degenerated cartilage the T2 relaxation time increases, [39] due to the degradation of the collagen network and due to the increase in the overall content and mobility of water. Focal areas of increased T2 relaxation times have been found to correlate to arthroscopically detected cartilage lesions. [40,41] T2 relaxation times have also been linked to collagen content changes and have been found to inversely correlate with cartilage volume and thickness. [39] However, T2 is less correlated with the cartilage proteoglycan content. [42] Generally on T1 weighted sequences cartilage, subchondral bone, tendinous and

ligamentous structures are hypointense and fat relatively hyperintense. T1 relaxation time without contrast enhancement has also been shown to correlate with cartilage water content. [43]

Magnetic field strength is the main determinant of image contrast and image resolution. [44] Currently clinically used magnets range from 0.5 - 3 tesla. [45] Depending on the field strength, rated in tesla, magnets are divided into low- (0.1 - 0.5 tesla) and high field (1.5 tesla) systems. The disadvantages of a lower strength magnet include decreased signal to noise ratio, thicker images slices, longer scanning times and patient motion ending in inferior image resolution and quality compared to higher strength magnets. [45,46]

MRI of the equine DIPJ has been described in low-field systems. [10] Superficial erosions and fibrillations of the articular cartilage have been unreliably detected in low-field systems in cadaver limbs, [10] whereas experimentally created full thickness erosions (8 mm in diameter) were always detected using T1 weighted gradient-recalled echo sequences. [10] No comparable studies using high-field systems for the DIPJ are available. The equine metacarpophalangeal articular cartilage was examined using a 1.5 tesla scanner using fat-suppressed spoiled gradient-recalled imaging, where full-thickness cartilage erosions were detected consistently with a moderate sensitivity and high specificity. Non-structural (early) cartilage alterations were limited in this joint in the examined technique. [48] The reliability of both low- and high field systems for the detection of cartilage and bone lesions has been investigated in the equine proximal metacarpo/metatarso phalangeal joint. [49] It was found that there was a high likelihood of false positive results using both low- or high-field systems for the detection of cartilage lesions and a moderate to high likelihood for false positive results when detecting subchondral bone lesions compared to histopathology. [49] Despite using high-field systems evaluation of the thin equine articular cartilage still remains a challenge.

4.7 Articular cartilage thickness measurements

Imaging modalities such as MRI provide a non-invasive approach for visualizing and measuring the articular cartilage, which is important when understanding osteochondral adaptation and injury. In humans cartilage thickness measurements are used for assessing the progression of OA. [50] OA leads to thinning of the articular cartilage [14] and this thinning can be quantified. For example, in humans with symptomatic osteoarthritis of the knee joint MRI cartilage thickness and volume measurements were found to decrease. [51]

In horses joint cartilage thickness is on average 1 - 4 mm. This however depends on the joint itself, the location within the joint, the individual's age and whether the joint is under load or not. The specific cartilage thickness in horses has only been described in a few joints including the metacarpo/metatarsophalangeal joint, [48,52] the carpal joints [53] and the DIPJ. [10] The equine cadaver DIPJ cartilage of the DP appeared as trilaminar structure with a mean thickness of 3.1 mm palmar and 2.1 mm dorsally when evaluated in a low-field system using dorsal T1 weighted gradient-recalled echo sequences and sagittal dual echo sequences. [10] Abrupt thinning of the articular cartilage was noted at the most abaxial palmar aspects of the distal phalanx and should not be confused with cartilage erosions in this particular region. On the distal aspect of the MP the articular cartilage was 2.3 mm palmar and 1.7 mm dorsal. In this study no comparison was made with histological measurements. [10]

To ensure that the cartilage-bone interface and the cartilage surface of MR images are consistent with true anatomical areas validation studies comparing MRI measurements to histological measurements as the gold standard are necessary. In equine articular cartilage of the carpal joints [53] and the metacarpophalangeal joint, [48,52] there was a good and moderate correlation between MRI and histological measurements, respectively. However it is debatable whether the articular cartilage layer measured on MRI represents the hyaline and the calcified cartilage layer, or whether it represents only the hyaline cartilage layer. [54] Measurements from cadaveric equine carpal joints using 3-dimensional fast spoiled gradient echo sequences have shown that the cartilage thickness measured on MRIs was a better

representation of hyaline and calcified cartilage combined. [53]

4.8 Quantitative magnetic resonance imaging of the articular cartilage

Early lesions in the articular cartilage generally do not show signs of pain or lameness due to the lack of nociceptive receptors in this type of tissue. This implies that cartilage damage can and does progress while no clinical signs such as lameness are yet apparent, [55] therefore it is imperative to use modalities that can detect cartilage injury early, enabling pathologic conditions to be addressed before they have progressed and allowing timely therapy to be instigated.

In humans more is known about imaging articular cartilage than horses or small animals. Cartilage lesions have been semi-quantitatively scored in T1 weighted spoiled gradient recalled acquisition at steady state (SPGR) or fast low-angle shot (FLASH) with fast suppression, T2- or intermediate weighted fast spin echo (FSE), or fat-supressed driven equilibrium Fourier transform and steady state free precession imaging. [56,57] Conventional MRI methods are based on imaging water content and have shown morphologic changes of the cartilage, which probably represent already progressed stages of OA. [58] Such morphological changes are preceded by biochemical and structural changes in the extracellular cartilage matrix, which can be evaluated by parametric mapping of cartilage. Post-processing of the images results in relaxation time-coded colour-maps. Mapping techniques have been described in T2, T2*, T1rho and delayed gadolinium enhanced MRI of cartilage. [58,59] To obtain relaxation time maps several images of one area are acquired, whereby a certain sequence parameter is varied. For T1 mapping (delayed gadolinium-enhanced magnetic resonance imaging of cartilage (dGEMRIC) this is the “inversion time” and for T2 mapping this is the “time to echo”. The change of image intensity as a function of this sequence parameter is fitted pixel by pixel into mono-exponential equations, resulting in a relaxation time value for each pixel. [58, a]

4.8.1 *T2 mapping*

T2 mapping is sensitive to cartilage composition such as hydration status, collagen content and collagen orientation. [58,60] In vitro studies have investigated the relationship between T2 measurements and the biochemical composition of cartilage showing that increased T2 values correlated with histologically present degeneration, both in tissue samples and in animal models (rats and rhesus macaque). [61-66] In vivo studies have been conducted in the human knee joint, [67,68-72] the human hip joint, [73,74] the human ankle, [75] and the human proximal interphalangeal joint of the hands. [76] In T2 mapping cartilage stratification (tangential zone, transitional zone, radiate zone) has been well visualized. It has been recognized that superficial cartilage has significantly longer T2 relaxation time values than deeper cartilage. [70,63] Additionally superficial cartilage was more sensitive to the presence of cartilage lesions than deep cartilage, and it was therefore found potentially more sensitive in detecting compositional differences in the cartilage in early knee OA. [70,77]

Studies have explored the relationship between cartilage biomechanics and T2 values. A strong relationship between the change in collagen fiber orientation and T2 values was noted: T2 values decreased under static compression of the cartilage. [78-80] Mosher *et al.* [81] reported that training (running) resulted in a decrease of cartilage thickness and a decrease in T2 values in the superficial cartilage layers. Similarly after running T2 values were found lower, suspected to correspond with loss of cartilage water due to cartilage compression. [82]

T2 mapping has also been used to evaluate cartilage repair techniques and study results show that it is a useful technique in post-operative evaluation of repaired articular cartilage. [58] Following autologous chondrocyte implantation with a fibrin-based scaffold in the human knee T2 mapping showed that the spatial variation of the T2 values was similar in repaired and in normal articular cartilage. [83] Welsch *et al.* [84] reported similar findings following repair of femoral condyle defect with autologous chondrocytes implanted in a hyaluronan scaffold. The spatial variation of T2 values was similar in normal articular cartilage and in the repaired articular cartilage, making T2 mapping a promising tool in the

assessment of articular cartilage ultrastructure following cartilage repair techniques. [84]

4.8.2 *Delayed gadolinium-enhanced magnetic resonance imaging of cartilage*

With degeneration, cartilage loses essential GAGs, which are negatively charged and responsible for maintaining adequate fluid content of the cartilage. [14] DGEMRIC uses gadolinium diethylene triamine pentaacetic acid (Gd-DTPA^{2-}), an intravenously or intraarticularly administered contrast agent that is also negatively charged. With progressive GAG loss, as seen in OA, Gd-DTPA^{2-} penetrates the cartilage and adheres to the positively charged cartilage matrix. T1 mapping can then be used to quantify the amount of cartilage degeneration in the joint. [55,58] Areas with lower GAG concentrations will accumulate a higher concentration of Gd-DTPA^{2-} resulting in a more rapid T1 relaxation time. [58] The dGEMRIC technique has been validated by in vitro and in vivo studies with dGEMRIC values corresponding to gold standard measures for GAGs. [85-87] It has been found that GAG measures correlate better with MR imaging in the superficial cartilage layers than in the deeper ones, where the GAG measure can be overestimated. [88] Similar to T2 mapping the gradient zonal variation in GAGs and the laminated appearance of articular cartilage has been reported. [89]

Reports also show the successful use of the dGEMRIC technique to evaluate cartilage regeneration after cartilage grafting techniques. [90-93] Osteochondral lesions at the human femoral condyle were treated with TruFit plugs and evaluated 1 year following treatment, using dGEMRIC. Similar $T1_{Gd}$ relaxation times were noted in repaired cartilage and normal cartilage. [93]

dGEMRIC may also provide a non-invasive way to measure the cartilage`s biomechanical properties. dGEMRIC values, as a non invasive measure of GAG content, were strongly correlated with the cartilage`s compressibility and site-matched stiffness measurements. [88,94-96]

The contrast agent may be administered intravenously or direct intraarticularly. In humans typically a double dose of contrast agent (0.2 mmol/kg) is administered intravenously followed by 10 - 15 minutes of light exercise and delayed MR imaging 90 - 120 minutes following contrast media administration. [97,98] Vascular distribution and the thickness of the articular cartilage affect the rate of equilibration between the articular cartilage and the contrast media. [55] When administered directly intraarticularly the dilute solution of Gd-DTPA^{2-} improves the visualization of the cartilage because of the contrast between the cartilage and the injected fluid. The delineation of the cartilage in the human hip joint [99] and in the canine stifle joint [89] was superior using a direct intraarticular administration versus an intravenous administration.

4.8.3 *T2 and T1 mapping of the equine articular cartilage*

In humans quantitative MRI techniques such as T2 mapping and to a lesser extent dGEMRIC have rapidly developed in recent years and have been used to identify OA early in the disease process. [100,101] Only a handful of quantitative MRI techniques have been reported in equine subjects. [52,a,102-105]

Carstens *et al.* [102] tested the feasibility of dGEMRIC following intraarticular administration of Gd-DPTA^{2-} into the normal proximal metacarpo/metatarso phalangeal joint in normal equine cadaver limbs in a 1.5 tesla scanner. The authors showed that it is a feasible technique to map T1 relaxation times in the equine distal third metacarpal/metatarsal bone articular cartilage with recommendations to delay scanning 60 - 120 minutes following intraarticular contrast administration. These investigations were limited by the thin cartilage of the distal third metacarpal/metatarsal bone and the low magnet strength (1.5 tesla) resulting in images of poor spatial resolution. Due to the thin cartilage (approximately 0.67 mm) [52] a combined analysis of synovial fluid and adjacent articulating cartilages was performed. [102] Further it was shown that dGEMRIC and T2 mapping were accurate techniques for measuring cartilage thickness of the equine distal third metacarpal/metatarsal bone at locations where the cartilage was not in direct contact

with the proximal phalanx cartilage. [52] Much veterinary and human research is performed on cadavers. The effects of freezing and chilling have been described in horses for certain MRI sequences before. [106-108] Carstens and colleagues established that dGEMRIC T1 relaxation times and T2 relaxation times were similar in fresh, chilled and frozen equine cadaver limbs. [62] To date these are the only published fundamental investigations of dGEMRIC and T2 mapping of equine cartilage.

Quantitative mapping techniques in the horse T2 mapping of experimentally made defects in articular cartilage of equine stifles using a 1.5 tesla scanner, revealed that T2 mapping helped to differentiate hyaline cartilage from reparative fibrocartilage. [105] Use of dGEMRIC in a 3 tesla machine has been reported once in a group of ponies, where it helped to assess the effects of administered bone morphogenic protein in experimentally created femoral condyle lesions. [103] T2 mapping of full-thickness cartilage defects repaired with concentrated bone marrow aspirate versus microfracture indicated that treatment with bone marrow aspirate resulted in increased fill of the defects and improved integration of repair tissue into surrounding normal cartilage. [104] Similar to humans these reports are promising and clearly show the benefits of a non-invasive tool to determine the biological consequence of an intervention.

5 Hypotheses and aims of the thesis

Based on the issues noted above. The following **hypotheses** were put forward:

1. dGEMRIC and T2 mapping techniques are feasible in equine cadaver DIPJ cartilage.

2. Cartilage thickness measured on dGEMRIC and T2 maps is representative of the true histomorphometric thickness of the normal and diseased articular cartilage.

3. Joint disease state and site within the joint will have a significant effect on cartilage thickness measurements.

4. dGEMRIC and T2 mapping are accurate techniques at identifying differing degrees of naturally occurring OA in equine cadaver DIPJs.

5. dGEMRIC (T1 and $T1_{Gd}$) and T2 relaxation times correlate with the cartilage`s GAG concentration and water content.

The project **aims** were as follows:

1. To establish dGEMRIC and T2 mapping of normal equine DIPJ cartilage.

2. To measure cartilage thickness on histology and correlate it to the thickness measurements obtained on dGEMRIC and T2 maps at select ROI in the equine DIPJ.

3. To analyse whether cartilage health status (determined histologically) and site within the joint (condylar/intercondylar; dorsal/central/palmar) effects cartilage thickness measured histomorphologically and on dGEMRIC and T2 maps.

4. To test whether dGEMRIC and T2 mapping can identify differing degrees of naturally occurring OA by correlating histological and macroscopic findings with dGEMRIC and T2 relaxation times.

5. To determine the cartilage`s GAG concentration and water content and correlate it to the dGEMRIC and T2 relaxation times.

6 Results

6.1 Chapter I:

Validation of delayed gadolinium – enhanced magnetic resonance imaging of cartilage and T2 mapping for quantifying normal and naturally occurring osteoarthritic distal interphalangeal joint cartilage thickness in Warmblood horses

Regula Fürst, Dr. vet. med.[1]; Anton E. Fürst, Prof., Dr. med. vet., DECVS[1]; Paul R. Torgerson, Prof., PhD, VetMB, DECVPH, DEVPC[2]; Andrea Bachmann, med. vet.[1]; Muriel Federici, med. vet.[1]; Patrick Kircher, Prof., Dr. med. vet., PhD, DECVDI[3]; **Andrea S. Bischofberger, Dr. med. vet., DACVS, DECVS[1].**

From the [1]Equine Hospital, the [2]Section of Veterinary Epidemiology and the [3]Division of Diagnostic Imaging, Vetsuisse-Faculty, University of Zürich, Zürich, Switzerland.

The authors have no financial or personal interests to declare.

Contribution:

Study design, study execution, shared contribution to data collection, shared contribution to data analysis, shared contribution to data interpretation, shared contribution to manuscript writing, arrangement and formatting. Design of figures 1 and 2, shared contribution to figure 3 and to tables.

6.1.1 *Abstract*

Objective - To establish whether dGEMRIC and T2 mapping are accurate techniques for measuring cartilage thickness in the normal and osteoarthritic equine DIPJ

Animals - 12 Warmblood cadaver DIPJs

Procedures - Twelve cadaver forelimbs were acquired from twelve horses without signs of lameness. Cartilage thickness was measured from dGEMRIC images, T2 maps and histological slides at 11 matching regions of interest (ROIs) of the distal MP and the proximal DP. The ROIs were histologically graded and classified into three groups of cartilage health (normal, mild-moderate OA, severe OA). The MRI cartilage thickness measurements (dGEMRIC, T2-maps) were correlated with the histological measurements. The effects of cartilage health and site within the joint ((condylar, intercondylar) (dorsal, central, palmar)) on cartilage thickness were analysed using generalized linear mixed models.

Results –There was a good correlation between the MRI and histological cartilage thickness measurements. However, the correlation between the T1 measurements and the histological measurements was superior to the correlation of the T2 measurements to the histological measurements. There were regional differences in cartilage thickness depending on the cartilage site within the joint. The distal MP cartilage was thinner than the proximal DP cartilage, cartilage in the central areas was thickest and cartilage in dorsal areas was thinnest. On T2 maps the cartilage of the condyles was thinner than the intercondylar cartilage, this was however not the case on histology or T1 maps.

Conclusions and clinical relevance - T1 and T2 maps are reliable to evaluate the thickness of normal and osteoarthritic equine articular cartilage at areas of opposing or non-opposing cartilage surfaces. In doing so, the T1 measurements are more suitable than the T2.

6.1.2 *Introduction*

Each joint can be affected by OA and there are often multiple joints affected in one horse at the same time. Depending on the breed, the age and the use of the horse individual joints may be affected more often. In sport horses a common site for OA is the DIPJ. [1-3] OA is a degenerative disease characterized by proteolytic breakdown of the cartilage matrix, fibrillation and erosion of the cartilage surface and release of the breakdown products resulting in synovitis. [4,5] Early lesions in the articular cartilage may not show signs of pain due to the lack of nociceptive receptors in this type of tissue. This implies that cartilage damage can and does progress while no clinical signs such as lameness are yet apparent. It is therefore imperative to use modalities that can detect cartilage injury early, enabling pathologic conditions to be addressed before they have progressed and allowing timely therapy to be instigated.

Traditional MR imaging methods have principally shown morphologic articular cartilage changes and were based on imaging the tissue water content. However morphological cartilage changes are preceded by molecular biochemical and structural changes, which can be evaluated by cartilage imaging techniques such as dGEMRIC and T2 cartilage mapping. [6]

In dGEMRIC a negatively charged contrast agent (Gd-DPTA^{2-}) is injected either intraarticularly or intravenously. Gd-DPTA^{2-} permeates the hyaline cartilage and disperses in an inverse relationship to the proteoglycan content of the articular cartilage. In areas of cartilage degeneration, the Gd-DPTA^{2-} uptake increases as a result of the relative decrease in the negative charge of the proteoglycan-depleted cartilage. By post-processing the dGEMRIC images and by producing relaxation time color maps, a detailed visual representation of the relaxation times within the articular cartilage is obtained.

Collagen fibers are organised in a fashion to maximize the efficiency in the transmission of joint forces and joint lubrication. Loss of this orientation is a hallmark feature of OA. [7,8] Early degenerative changes in the extracellular matrix affect cartilage hydration by both increasing the overall water content via osmosis and increasing the mobility of water.

MRI using T2 relaxation time mapping is sensitive for determining the amount of collagen, the collagen orientation within the cartilage and its water content. Increased signal on T2 weighted images have been found in cartilage swelling due to cartilage edema and increased water content. [9] Also focal areas of increased signal on T2 weighted images have been found to correspond to cartilage lesions upon arthroscopic evaluation. Additionally there is a link between early OA changes in T2 weighted images and the changes in collagen content. [10]

To ensure that the bone-cartilage interface and the cartilage surface of the dGEMRIC and T2 mapping sites are consistent with true anatomical areas, validation studies comparing MRI measurements to histological measurements as the gold standard are needed before the cartilage boundaries can be accurately identified and the cartilage itself can be reliably evaluated. This is especially true for a complex joint like the DIPJ. OA leads to thinning of the articular cartilage and this thinning can visually be appreciated as narrowing of the joint space. Different studies have measured the equine cartilage thickness or the joint space width by MRI in different equine joints. Cartilage thickness of specific areas of 20 metacarpophalangeal joints of 10 mature racing Thoroughbreds was measured on MRI and compared with the histological measurements. This study illustrated that the MRI allows clinically applicable, satisfactory assessment of articular cartilage thickness, structure and to a lesser extent, early biochemical alterations in the osteoarthritic equine metacarpophalangeal joint. [11] DGEMRIC and T2 mapping were found to be accurate techniques for measuring the distal third metacarpal/metatarsal bone cartilage thickness at locations where the cartilage is not in direct contact with the proximal phalanx cartilage. The thin distal third metacarpal/metatarsal bone cartilage and the limit of detection of the measuring device were however the main limitations in this study. [12] Additionally the same author established that dGEMRIC T1 and T2 relaxation times were similar in fresh, chilled and frozen cadaver limbs.[a] However the study was limited by the low number of limbs tested and by the fact that the limb temperature at the time of scanning was not determined. In the current literature there is no information of quantitative MRI sequences in the DIPJ.

The aims of this study were 1) to determine measurements of cartilage thickness on dGEMRIC, T2 maps and histology of predetermined ROIs in normal and osteoarthritic Warmblood cadaver DIPJs, 2) to correlate the histological and MR measurements and to test

the effect of cartilage disease state and cartilage site within the joint on the cartilage thickness (histological and MR measurements).

It was hypothesised that 1) that diseased joint cartilage would be thinner than normal joint cartilage and 2) that there would be site dependent differences in cartilage thickness within the joint.

6.1.3 *Material and methods*

Horses

Twelve Warmblood cadaver forelimbs of horses with a mean age of 15.2 ± 9.2 (6 - 32 years) were included in the study. All horses were euthanized for reasons unrelated to the musculoskeletal tract according to Swiss ethical standards. Warmbloods of any gender, with no age restrictions, showing no signs of lameness at a walk or trot were included in the study. A right or a left forelimb was randomly dissected from the body in the intercarpal joint. The limbs were refrigerated (4°C) until scanning.

MRI

The limbs were scanned within 24 hours after euthanasia at room temperature on different days over a period of four months. A vitamin E oil capsule was taped to the lateral aspect of the hoof and each limb was positioned on the scanner table with the dorsal hoof wall facing downwards and the toe facing towards the gantry. A 16 - channel knee coil was used and the DIPJ of each forelimb was scanned using a three Tesla MRI scanner[b]. A frontal localizer was run to identify the condylar and intercondylar sagittal slices of each DIPJ. Pre contrast T1 maps were obtained using single slice inversion recovery spin echo sequences (Repetition time (TR) 12 ms, echo time (TE) 5.6 ms, field of view 100 x 100 mm, matrix 252 x 244, slice thickness 3 mm, receiver band width 131.6 Hz/pixel) for each lateral and medial mid condylar sagittal slice and the central intercondylar sagittal slice (sagittal groove positioned in the middle of the distal MP). T2 - maps were obtained using multi – slice, multi – echo, spin – echo sequences (TR 2000 ms, TE 6 x 13 ms, field of view 160 x 160 mm, matrix 380 x 311, slice thickness 2.5 mm, receiver band width 291.1 Hz/pixel). By placing a 21 gauge needle into the dorsal recess of the DIPJ, as much synovial fluid as possible was aspirated to minimise dilution of Gd-DTPA^{2-} and to minimize fluid – related sources of variability. Gd-

$DTPA^{2-}$ [c] was injected into the DIPJ at 0.05 ml in 5 ml saline solution (0.025 mmol/joint). After the injection the joints were manually flexed for five minutes to distribute the contrast media in all parts of the joint. The limbs were scanned again using the same mid and central intercondylar slices 120 minutes after the injection of the contrast medium. The T1 relaxation time measurements were repeated.

MRI image analysis

Three ROIs were analysed for each mid condylar and the inter condylar slice as shown in Figure 1.

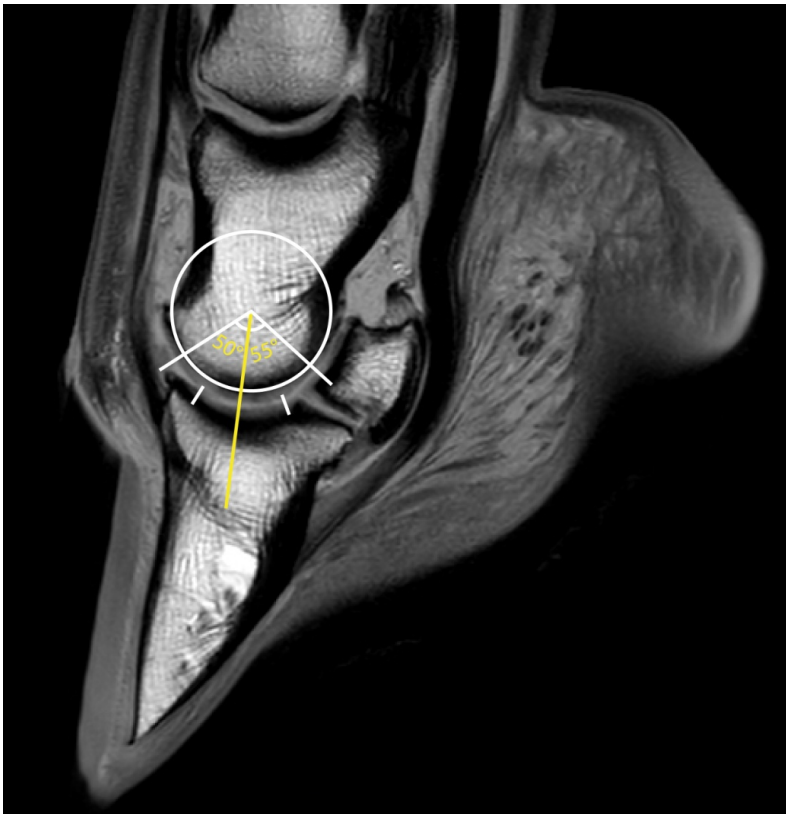

Figure 1: *Region of interest (ROI) 2 was defined as the end of a vertical line through the rotation center point of the DIPJ. ROI 1 was defined at a 50° dorsal angle from the vertical line through the rotation center point. ROI 3 was defined at a 55° palmar angle from the vertical line through the rotation center point.*

Cartilage thickness was measured using a commercially available measuring software[d]. The image was zoomed into an optimal position where a translucent template (as shown in Figure 1) determined the center point in the middle of the condyles of the MP and

the midline that goes vertically through the DIPJ. The optimal window was found by using the windowing tool in the software and the sites were defined where the cartilage, the joint space and the surface of the bone could best be identified. Two observers measured the thickness of the cartilage at each ROI three times and the mean ± standard deviation of each ROI of each observer was calculated. The second observer undertook the measurements one month later, but with the same settings.

Tissue harvesting

The DIPJs were disarticulated. Cartilage and subchondral bone cores (9 mm diameter) were cut from the distal aspect of the MP and from the proximal aspect of the DP. A total of eleven cores were obtained per joint as shown in Figure 2. A central 1000 µm thick osteochondral slice was cut from the core by using a saw and this slice was further processed for histological sections. Briefly the osteochondral samples were fixed in 4% paraformaldehyde for 48 hours, decalcified in 25% EDTA for 4 weeks, embedded in paraffin and sections were cut and stained with haematoxylin and eosin, Safranin-O-Fast green and toluidine blue.

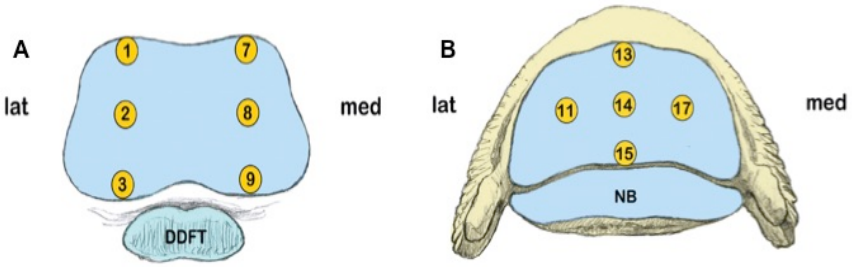

Figure 2: *Schematic drawing of the distal middle phalanx (A) and proximal distal phalanx (B) hyaline cartilage surface, showing the locations of the obtained core biopsies for histological and magnetic resonance image analyses. Abbreviations: lat = lateral; med = medial, NB = navicular bone, DDFT = deep digital flexor tendon.*

Histological analysis

Three months after analyzing the MRIs, the histological measurements of the cartilage thickness were obtained. Again two observers obtained the measurements with an interval of one month. A Leica DM LB2 light microscope equipped with a Leica DC 480 camera was used[e]. The total cartilage thickness (TC), the calcified cartilage thickness (CC)

and hyaline cartilage thickness (HC) were each measured three times (Figure 3). The mean ± standard deviation of the three measurements was calculated and used for further analysis.

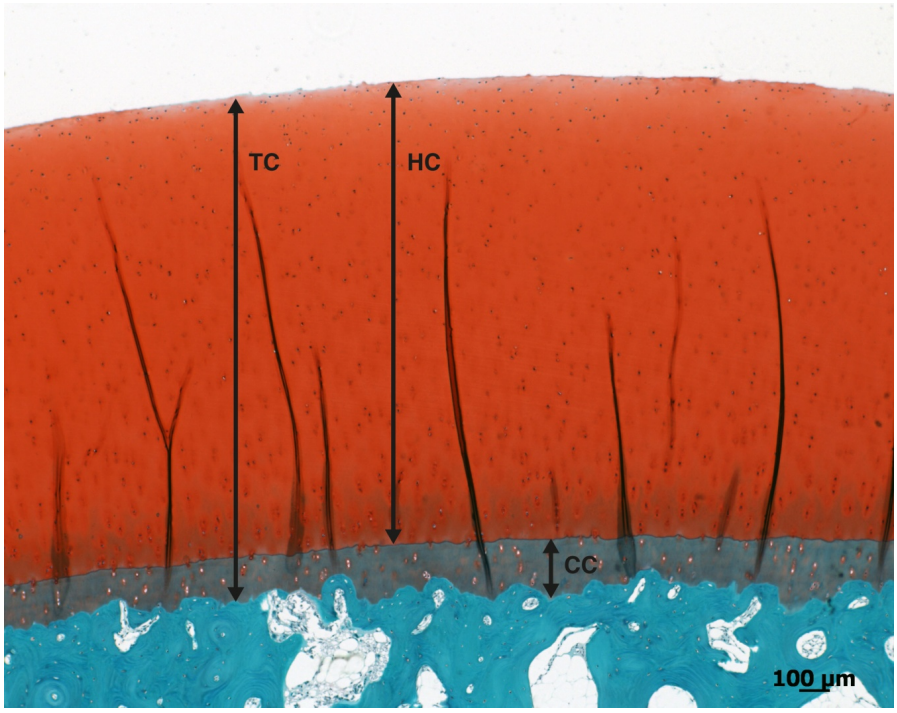

Figure 3: *Safranin-O-Fast green stain of normal cartilage. TC: total cartilage thickness, HC: hyaline cartilage thickness, CC: calcified cartilage thickness.*

Safranin-O-Fast green stained sections were analysed and scored for degenerative changes by three blinded observers using a modified Mankin scoring system. The histological sections of the different ROIs were scored on the basis of the criteria shown in Table 1. An overall cartilage score was given and the ROI was classified into three groups of differing degrees of cartilage change: Normal cartilage: 0 - 1.9 Mankin score; mild to moderate OA: 2.0 - 8.0 Mankin score; severe OA: 8.1 - 16.0 Mankin score.

Structure	
0	Normal
1	Fibrillation
2	Fissures
3	Erosion of 1/3 of depth of the hyaline cartilage
4	Erosion of 2/3 of depth of the hyaline cartilage
5	Full depth erosion of the hyaline cartilage
6	Full depth erosion of the hyaline and calcified cartilage
Chondrocyte density	
0	No decrease in cells
1	Focal decrease in cells
2	Multifocal decrease in cells
3	Multifocal confluent decrease in cells
4	Diffuse decrease in cells
Cluster formation	
0	Normal
1	< 4 clusters
2	≥ 4 but < 8 clusters
3	≥ 8 clusters
Safranin-O-Fast green staining	
0	Uniform staining throughout articular cartilage
1	Loss of staining in the superficial zone of hyaline cartilage
2	Loss of staining in the upper 2/3 of hyaline cartilage
3	Loss of staining in all of hyaline cartilage

Table 1: *Modified Mankin scoring system employed for articular cartilage assessment*

Statistical analysis

A Kolmogorov – Smirnoff Test of normality was used to evaluate the distribution of the data. Results of parametric data were displayed as mean ± standard deviation (SD) and results of nonparametric data were displayed as median (range). For the statistical analysis the ROIs 1, 7, and 13 were summarized into the horizontal dorsal cartilage zone, the ROIs 2, 8, 11, 14 and 17 into the horizontal central cartilage zone and the ROIs 3, 9, and 15 into the horizontal palmar cartilage zone. The ROIs 1, 2, 3, 7, 8, 9, 11 and 17 were grouped into the sagittal condylar zone and the ROIs 13, 14 and 15 were grouped in the sagittal intercondylar

zone. The inter observer agreement of the cartilage thickness measurements (histological and MRI) and the mean overall cartilage Mankin scores were analysed using intraclass correlation coefficients (ICC). Average measures were reported and ICCs > 0.7 were considered good, > 0.8 optimal and > 0.9 excellent. Associations between the mean histological cartilage thickness measurements (TC, HC and CC) and the MRI cartilage thickness measurements (dGEMRIC and T2) were investigated using Spearmans rho non-parametric correlations. Data analysis was performed using the SPSS 21.0 software[f].

A generalized linear mixed model approach was used to analyse the relationship between the dependent variable cartilage thickness measured on dGEMRIC and T2 maps (mm) and the independent variable bone (MP/DP), cartilage zones (sagittal condylar/intercondylar zones) and (dorsal/central/palmar) and cartilage disease (none/mild-moderate/severe). Independent variables with $P > 0.2$ were omitted from the final model. The significance level was set at $P < 0.05$. Random effects were the leg and replicate as measurements within a single leg and replicate measurements are likely to be correlated. Exploratory analysis indicated that the gamma distribution was the most appropriate model for the generalized linear mixed model (family=gamma, link=log). The analysis was undertaken in R[g]. The level of significance was set at $P < 0.05$.

6.1.4 *Results*

Nine cores were lost during the histopathological processing resulting in data of 123 ROIs being included in the study. The inter observer agreement of the MRI cartilage thickness measurements was excellent (ICC = 0.953) for dGEMRIC and optimal (ICC = 0.835) for the T2 maps.

MR cartilage thickness measurements

Normal cartilage was significantly thicker than severely diseased cartilage (Table 2). Cartilage in the dorsal zone was significantly thinner than cartilage in the central and in the palmar zone. In terms of significant differences in cartilage thickness it did not matter if the ROI was in the condylar groove or on the condyle or whether the ROI was on the MP or on the DP.

Independent parameters	Thickness in T1 (µm)	P-value
Intercept		**<0.001**
Normal cartilage	1253 (517-1791)	-
Mild – mod. cartilage disease	1179 (516-1974)	0.444
Severe cartilage disease	986 (519-2030)	**0.039**
Middle phalanx	1121 (521-1791)	0.189
Distal phalanx	1244 (346-2030)	-
Horizontal dorsal	950 (516-1791)	**-**
Horizontal central	1283 (346-2030)	**<0.001**
Horizontal palmar	1102 (532-1974)	**0.007**

Table 2: *Median and range of T1 relaxation times of the independent MR parameters in the generalized linear mixed models Significant P – values of the generalized linear mixed model are marked in bold. Sagittal cartilage zones (condylar/intercondylar) were omitted from the model due to P > 0.2. Abbreviations: mod. = moderate*

On T2 maps, cartilage located on the condyle was significantly thinner than cartilage located in the intercondylar groove (Table 3). Analogous to T1 maps cartilage located dorsally was thinner than cartilage located centrally. There was no difference between dorsally and palmar located cartilage. Whether the cartilage was located on the middle phalanx or the distal phalanx or whether cartilage was diseased did not affect mean cartilage thickness on T2 maps.

Independent parameters	Thickness in T2 (µm)	P-value
Intercept		**<0.001**
Horizontal dorsal	1078 (468-1670)	-
Horizontal central	1112 (311-2177)	**0.018**
Horizontal palmar	1088 (590-1796)	0.950
Sagittal condylar	1037 (311-2177)	-
Sagittal intercondylar	1162 (468-1944)	**<0.001**

Table 3: *Median and range of T2 relaxation times of the independent MR parameters in the generalized linear mixed models. Significant P – values of the generalized linear mixed model are marked in bold. Cartilage health*

(normal/mild to moderate cartilage disease/severe cartilage disease) and bone (middle phalanx/distal phalanx) were omitted from the final model due to P > 0.2.

Histological cartilage thickness measurements

The inter observer agreement of the cartilage thickness measurements in histology was excellent (ICC = 0.922) for the total cartilage, excellent (ICC = 0.939) for the hyaline cartilage and good (ICC = 0.712) for the calcified cartilage.

The cartilage of the MP was significantly thinner than the cartilage of the DP when TC and HC were measured. Analogous to T1 - and T2 maps cartilage located dorsally was thinner than cartilage located centrally in both TC and HC. There was no difference between dorsally and palmar located cartilage. Cartilage health and sagittal cartilage zones did not significantly affect the TC or the HC (Table 4 and Table 5).

Independent parameters	**Thickness in TC (µm)**	**P-value**
Intercept		**<0.001**
Middle phalanx	1662 (969-3263)	**<0.001**
Distal phalanx	2127 (885-3165)	-
Horizontal dorsal	1806 (1019-2590)	-
Horizontal central	2089 (885-3165)	**<0.001**
Horizontal palmar	1558 (969-3263)	0.495

Table 4: *Median and range of TC of the independent histological parameters in the generalized linear mixed model. Significant P – values of the generalized linear mixed model are marked in bold. Cartilage health (normal/mild to moderate cartilage disease/severe cartilage disease) and sagittal cartilage zone (condylar/intercondylar) were omitted from the final model due to P > 0.2. Abbreviations: TC = Total cartilage.*

Independent parameters	Thickness in HC (µm)	P-value
Intercept		**<0.001**
Middle phalanx	1477 (695-2961)	**<0.001**
Distal phalanx	1992 (767-3035)	-
Horizontal dorsal	1571 (876-2307)	-
Horizontal central	1952 (787-2807)	**<0.001**
Horizontal palmar	1391 (695-3035)	0.757

Table 5: *Median and range of HC of the independent histological parameters in the generalized linear mixed model. Significant P – values of the generalized linear mixed model are marked in bold. Cartilage health (normal/mild to moderate cartilage disease/severe cartilage disease) and sagittal cartilage zone (condylar/intercondylar) were omitted from the final model due to P > 0.2. Abbreviations: HC = hyaline cartilage.*

CC was thinner in the middle phalanx than the distal phalanx, significantly thinner in the dorsal cartilage zone compared to the central and the palmar zone and thinner on the condyle compared to the intercondylar space. Cartilage health had no effect on the CC (Table 6).

Independent parameters	Thickness in CC (µm)	P-value
Intercept		**<0.001**
Middle phalanx	196 (84-514)	**0.003**
Distal phalanx	199 (69-384)	-
Horizontal dorsal	174 (69-406)	-
Horizontal central	208 (77-514)	**<0.001**
Horizontal palmar	199 (84-352)	**0.042**
Sagittal condylar	196 (77-514)	-
Sagittal intercondylar	201 (69-384)	**0.009**

Table 6: *Median and range of CC of the independent histological parameters in the generalized linear mixed models. Significant P – values of the generalized linear mixed model are marked in bold. Cartilage health (normal/mild to moderate cartilage disease/severe cartilage disease was omitted from the final model due to P > 0.2.*

Abbreviations: CC = calcified cartilage

Correlations between histological and MRI data

There was a significant correlation between the T1 cartilage thickness measurements and the histological cartilage thickness measurements. The same was true for the T2 cartilage thickness measurements and the histological cartilage thickness measurements.
T1 cartilage thickness measurements correlated better with histological measurements (TC and HC) than T2 cartilage thickness measurements (TC and HC). For both T1 and T2 images the correlation coefficients were slightly higher for TC measurements than HC measurements (Table 7).

	Mean T1	**Mean T2**
Mean TC	r_s = 0.432; **p < 0.001**	r_s = 0.350; **p < 0.001**
Mean HC	r_s = 0.420; **p < 0.001**	r_s = 0.339; **p < 0.001**
Mean CC	r_s = 0.296; **p < 0.001**	r_s = 0.207; **p < 0.001**

Table 7: *Correlations between mean T1, mean T2 and mean TC, HC and CC. Significant P - values are marked in bold. Abbreviations: r_s = Spearman` s rho correlation coefficient value; TC = total cartilage, HC = hyaline cartilage, CC = calcified cartilage*

6.1.5 *Discussion*

T1 cartilage thickness measurements showed that joint health had a significant effect on cartilage thickness measurements. The severely diseased cartilage was thinner than normal cartilage. This was only detected on T1 maps. Cartilage thinning is one of the consequences of OA. Irrespective of the aetiological factor of OA, it finally leads to thinning of the articular cartilage, especially in areas of high load.

Cartilage was thinnest dorsally and thickest centrally. This corresponds to the results of Olive *et al.* who assessed DIPJ cartilage thickness using low-field MRI and found that the cartilage became progressively thinner centrodorsally and palmarly. [13] Histologically the proximal DP cartilage was thicker than distal MP cartilage. It is expected that the proximal

DP has more pressure to bear than the proximal MP during the different phases of motion. As a consequence the articular cartilage of the proximal DP may become thicker as an adaptation to these loads.

Whether a ROI was located on the condyle or in the intercondylar groove had a significant effect on the T2 cartilage thickness measurements, however not on the T1 or histological cartilage thickness measurements. T2 cartilage thickness was significantly thinner in the condylar compared to the intercondylar area. The difference was most pronounced when the cartilage was severely diseased. T2 maps are sensitive for determining the amount of collagen, its water content and its orientation within the cartilage. [7,8] We speculate that there is less collagen in the condylar versus the intercondylar areas and the joint margins, where there is less constant weight bearing.

Cartilage could be better identified on dGEMRIC rather than on T2 maps. On T1 maps the contrast between the bright articular cartilage and the dark synovial fluid and the subchondral bone was high, whereas on T2 maps the grey cartilage only had low contrast compared to the dark subchondral bone. On T2 maps the low signal cartilage was seen as a progressive continuum of the low signal subchondral bone. Olive *et al.* reported T1- and T2 weighted sequences to assess DIPJ cartilage. He found the T1 sequences to be superior in terms of contrast between the synovial fluid and the subchondral bone plate compared to the articular cartilage. [13] Olive *et al.* also reported that the cartilage plates of the distal MP and the proximal DP could not be clearly separated on T1 and T2 weighted sequences when the joint space was very narrow. This was most likely due to the use of a low-field magnet for the image acquisition, which resulted in poor image resolution. To separate the two opposing cartilage surfaces in the human knee, the use of traction was described to improve the evaluation. [14] This technique may also be considered in the future when evaluating opposing joint cartilages in the horse when using low-field systems under general anesthesia.

MRI measurement of cartilage is important in experimental and clinical OA. Our results demonstrate that cartilage thickness of the DIPJ can be measured with reasonable accuracy, although cartilage thickness was constantly underestimated on MR images (T1 and

T2 maps). We can only speculate why our MRI thickness measurements were smaller than the histological measurements. A reason could be the oblique orientation of the articular surfaces of the DP and the MP, causing volume averaging. [15] Differences in cartilage thickness measurements between histological and MRI data could also be caused by the used MR slice thickness. The lesser the slice thickness, the better the image resolution. [11] For the human knee a slice thickness of 1.5 mm with isotropic 0.3 mm in-plane resolution is recommended. [16] However this is not realistic in live equine patients that often require multiple imaging sequences of the affected joint and additional sequences of other regions. [11] In our study a 2.5 mm slice thickness was used in the T2 mapping sequence and a 3 mm slice thickness in dGEMRIC. These thicknesses were the same as in previous equine studies. [17]

It was encouraging that in our study the interobserver agreement of MRI measurements was excellent in T1 (ICC = 0.953) and optimal in T2 (ICC = 0.835). In the histology the agreement was good (CC: ICC = 0.712) to excellent (TC: ICC = 0.922; HC: ICC = 0.939). Because the width of the calcified cartilage is very thin compared to the hyaline and total cartilage and the tideline between the calcified and the hyaline cartilage is mostly wavy, the discrepancy of the measurements among the observers could be expected.

It has been shown that dGEMRIC and T2 cartilage mapping are accurate techniques for measuring equine cartilage thickness at the distal third metacarpal/metatarsal bone. [12] The normal cartilage of the distal distal third metacarpal/metatarsal bone is approximately 1 mm thick [12] versus the average thickness of the DIPJ cartilage of 2.1 – 3.1 mm [13] The metacarpophalangeal joint has a more rounded articular surface compared to the DIPJ, so direct comparisons cannot be made. A high-field MRI (≥ 1 tesla) is still regarded as the modality of choice to evaluate the articular cartilage of horses, because a more appropriate method does not exist yet. [18] A human study, comparing 3-tesla with 1.5-tesla images, reported superior cartilage thickness measurements when using the higher-field magnet strength. [19] The use of thinner slices for MRI scans in our study would have resulted in a lower signal to noise ratio however would have required more time. Findings in a study evaluating the human knee cartilage volume showed that there was only little difference in the human tibial cartilage volume when slice thicknesses were increased from 1.5 to 7.5

mm. [20] Because of the different curvature and thicknesses of the cartilage, the DIPJ cannot directly be compared with the human knee, but it can be assumed that our slice thicknesses (2.5 - 3 mm) will give reliable results.

In conclusion, findings of this study indicate that both, dGEMRIC and T2 maps correlated well with the histological cartilage thickness measurements in normal and degenerated cartilage in areas of opposing or non-opposing cartilage surfaces. There were regional differences in cartilage thickness depending on the cartilage site within the joint. The MP cartilage was thinner than the DP cartilage, cartilage in central areas was thicker than cartilage in dorsal areas and the cartilage of the condyles was thinner than the intercondylar cartilage.

Footnotes

a. Carstens, A., Delayed gadolinium enhanced magnetic resonance imaging and T2 mapping of cartilage of the cadaver distal metacarpus 3/metatarsus 3 of the normal Thoroughbred horse. PhD thesis, 2013, University of Pretoria, South Africa.

b. Phillips Health Care Ingenia, Phillips AG, Zuerich, Switzerland.

c. Magnevist gadopentate dimeglumine, Bayer Health Care Pharmaceuticals, Zuerich, Switzerland.

d. Osirix MD Version 7.5, Bernex, Switzerland

e. Leica Microsystems Ltd, Heerbrugg, Switzerland)

f. IBM SPSS, Armonk, NY, USA

g. R Core Team (2016). R: A language and environment for statistical computing. R Foundation for Statistical Computing, Vienna, Austria. URL https://www.R-project.org/. using the MASS, car and lme4 packages.

6.1.6 *References*

1. Dyson SJ. Lameness due to pain associated with the distal interphalangeal joint - 45 cases. *Equine Veterinary Journal* 1991;23:128-135.

2. McKnight AL, Posh J. Articular cartilage lesions seen with MRI at 0.25T in the distal equine limb. *Journal of Equine Veterinary Science* 2012;32:667-671.

3. Kristiansen KK, Kold SE. Multivariable analysis of factors influencing outcome of 2 treatment protocols in 128 cases of horses responding positively to intra-

articular analgesia of the distal interphalangeal joint. *Equine Veterinary Journal* 2007;39:150-156.

4. Frisbie DD. Synovial joint biology and pathobiology In: J. Auer JS, ed. *Equine Surgery*. 4 ed. St. Louis, Missouri: Elsevier, Saunders, 2012;1096-1114.

5. Goodrich LR, Nixon AJ. Medical treatment of osteoarthritis in the horse - A review. *Veterinary Journal* 2006;171:51-69.

6. Domayer SE, Welsch GH, Dorotka R, et al. MRI Monitoring of cartilage repair in the knee: a review. *Seminars in Musculoskeletal Radiology* 2008;12:302-317.

7. Goodwin DW. Visualization of the macroscopic structure of hyaline cartilage with MR imaging. *Seminars in Musculoskeletal Radiol*ogy 2001;5:305-312.

8. Xia Y, Moody JB, Alhadlaq H. Orientational dependence of T2 relaxation in articular cartilage: A microscopic MRI (microMRI) study. *Magnetic Resonance in Medicine* 2002;48:460-469.

9. Murray RC, Dyson, S. Image interpretation and artifacts. *Clinical Techniques in Equine Practice* 2007;6:16-25.

10. Taylor C, Carballido-Gamio J, Majumdar S, et al. Comparison of quantitative imaging of cartilage for osteoarthritis: T2, T1 rho, dGEMRIC and contrast-enhanced computed tomography. *Magnetic Resonance Imaging* 2009;27:779-784.

11. Olive J, D'Anjou MA, Girard C, et al. Fat-suppressed spoiled gradient-recalled imaging of equine metacarpophalangeal articular cartilage. *Veterinary Radiology & Ultrasound* 2010;51:107-115.

12. Carstens A, Kirberger RM, Dahlberg LE, et al. Validation of delayed gadolinium-enhanced magnetic resonance imaging of cartilage and T2 mapping for quantifying distal metacarpus/metatarsus cartilage thickness in Thoroughbred racehorses. *Veterinary Radiology & Ultrasound* 2013;54:139-148.

13. Olive J. Distal interphalangeal articular cartilage assessment using low-field magnetic resonance imaging. *Veterinary Radiology & Ultrasound* 2010;51:259-266.

14. Trattnig S, Mamisch TC, Pinker K, et al. Differentiating normal hyaline cartilage from post-surgical repair tissue using fast gradient echo imaging in delayed gadolinium-enhanced MRI (dGEMRIC) at 3 Tesla. *European Radiology* 2008;18:1251-1259.

15. Schramme M, Redding WR. Magnetic resonance imaging In: Baxter G, ed. *Adams and Stashak`s lameness in horses. 6th ed.* Wiley-Blackwell, 2011;416-459.

16. Eckstein F, Burstein D, Link TM. Quantitative MRI of cartilage and bone: degenerative changes in osteoarthritis. *NMR in Biomedicine* 2006;19:822-854.

17. Murray RC, Branch MV, Tranquille C, et al. Validation of magnetic resonance imaging for measurement of equine articular cartilage and subchondral bone thickness. *American Journal of Veterinary Research* 2005;66:1999-2005.

18. Pease A. Biochemical evaluation of equine articular cartilage through imaging. *Veterinary Clinics of North America-Equine Practice* 2012;28:637-646.

19. Eckstein F, Charles HC, Buck RJ, et al. Accuracy and precision of quantitative assessment of cartilage morphology by magnetic resonance imaging at 3.0T. *Arthritis & Rheumatism* 2005;52:3132-3136.

20. Cicuttini F, Morris KF, Glisson M, et al. Slice thickness in the assessment of medial and lateral tibial cartilage volume and accuracy for the measurement of change in a longitudinal study. *Journal of Rheumatology* 2004;31:2444-2448.

6.2 Chapter II:

Delayed gadolinium-enhanced magnetic resonance imaging of the normal and naturally occurred osteoarthritic equine distal interphalangeal joint cartilage in a 3 tesla magnet

Andrea S. Bischofberger, Dr. med. vet., DACVS, DECVS[1]; Anton E. Fürst, Prof., Dr. med. vet., DECVS[1]; Prof., Dr. med. vet., DECVS; Paul R. Torgerson, Prof., PhD, VetMB, DECVPH, DEVPC[2]; Ann Carstens BVSc, BVSc, MS, MMedVet (Large Animal Surgery), MMedVet (Diagnostic Imaging), PhD, DECVDI[3]; Monika Hilbe, Dr. med. vet., DECVP[4]; Patrick Kircher, Prof., Dr. med. vet., PhD, DECVDI[5].

From the [1]Equine Hospital, [2]Section of Veterinary Epidemiology [4]Institute of Veterinary Pathology, [5]Division of Diagnostic Imaging, Vetsuisse-Faculty, University of Zürich, Zürich, Switzerland; and the [3]Department of Companion Animal Clinical Studies, Faculty of Veterinary Science, University of Pretoria, Pretoria, South Africa.

The authors have no personal interests to declare. The study was funded by the Swiss Veterinary Association.

Contribution:

Study design, study execution, shared contribution to data collection, shared contribution to data analysis, data interpretation and manuscript writing, arrangement and formatting. Design of all figures and tables.

6.2.1 *Abstract*

Objective - To investigate dGEMRIC of the DIPJ in normal cartilage as well as different degrees of naturally occurring osteoarthritis, and to correlate the relaxation times with the cartilage`s GAG and water content.

Animals - 12 Warmblood cadaver forelimb DIPJs

Procedures - Mean T1 weighted relaxation times before (T1) and after ($T1_{Gd}$) intra articular gadolinium administration of predetermined sites of the DIPJ cartilage were obtained. Corresponding cartilage sites were examined macroscopically, histologically (Safranin-O-Fast green) and immunohistochemically (collagen type II). Cartilage health was graded macroscopically and histologically. The sites' GAG (µg/mg) and water content (%) were determined. The T1 and $T1_{Gd}$ values were correlated to the histological, macroscopic and biochemical data. Generalized linear models analysed the effects of cartilage sites, articular surface and cartilage health (histologic and macroscopic scores) on the relaxation times.

Results - 122 cartilage sites were analysed. The $T1_{Gd}$ value was lower than the T1 value in normal and diseased cartilage. Both T1 and $T1_{Gd}$ values correlated with the macroscopic and histologic cartilage health, whereby T1 increased and $T1_{Gd}$ decreased with advancing osteoarthritis. Within the DIPJ there was a topographical variation of T1 and $T1_{Gd}$. The GAG and water content correlated with the T1 value and the cartilage macroscopic and histologic findings, however not with the $T1_{Gd}$ value.

Conclusions and clinical relevance - Varying degrees of naturally occurring DIPJ osteoarthritis significantly affected dGEMRIC relaxation times, potentially having important consequences in early recognition of equine osteoarthritis.

6.2.2 *Introduction*

Naturally occurring OA is one of the principal causes of lameness and leads to early retirement of equine athletes. [1] OA is a degenerative disease characterized by proteolytic breakdown of the cartilage matrix, fibrillation and erosion of the cartilage surface and release of the breakdown products resulting in synovitis and associated subchondral bone and soft tissue changes. Although the features of naturally occurring OA in equine distal limbs were reported as early as 1973, [2] OA of the DIPJ is underreported in the veterinary literature. [3-5]

Diagnosis of DIPJ OA is made by clinical examination and peri neural and/or intra articular anaesthesia resulting in the localisation of lameness as well as diagnostic imaging modalities including radiography, ultrasonography, computed tomography and/or MRI. Since early hyaline cartilage lesions may not result in obvious clinical signs, [6,7] using imaging modalities that can identify these lesions timeously is essential to enable their management. Conventional MRI methods are based on imaging water content and have shown morphologic changes of the cartilage, which probably represent later stages of OA. [8] Such morphological changes are preceded by biochemical and structural changes in the extracellular cartilage matrix, which can be evaluated by cartilage imaging techniques such as dGEMRIC. [9] In humans such MR techniques have rapidly developed in recent years and have been used to identify early stages of OA. [10-15]

With degeneration, cartilage loses essential GAGs, which are negatively charged.[16] dGEMRIC uses an anionic, paramagnetic contrast agent Gd-DTPA^{2-}, either administered intravenously or intra articularly. With progressive GAG loss, as seen in OA, the negatively charged Gd-DTPA^{2-} penetrates the hyaline cartilage and adheres to the positively charged cartilage matrix in areas of lost GAGs. Parametric mapping of the cartilage can be performed by post processing dGEMRIC images creating color maps, which represent the cartilage relaxation times. [7,8]

To date the main interest of dGEMRIC in the equine industry is for the research field and only a handful of reports have been published in horses. In normal cadaver metacarpo/tarsophalangeal joints the feasibility of dGEMRIC has been reported using a 1.5

Tesla scanner.[17] The thin cartilage of the metacarpo/metatarsophalangeal joint however precluded optimal dGEMRIC evaluation. It has been established that dGEMRIC relaxation times were similar in fresh, chilled and frozen joints.[a] Further it was shown that dGEMRIC cartilage maps were accurate for measuring normal cadaver cartilage thickness at the distal aspect of the third metacarpal or metatarsal bone, when there was no contact with the proximal phalanx hyaline cartilage. In 5 ponies, dGEMRIC and T2 mapping were helpful to assess the serial healing of experimentally created femoral condyle lesions treated with bone morphogenic protein. [18] The premise that changes in hyaline cartilage glycosaminoglycan content may be accurately detected holds considerable promise and warrants investigation of this technique in horses.

This equine DIPJ cadaver study aimed at 1) investigating dGEMRIC in normal hyaline cartilage, 2) testing whether dGEMRIC can identify differing degrees of naturally occurring OA and 3) correlating relaxation times with the cartilage`s GAG concentration and water content, histological and macroscopic findings.

It was hypothesized that the technique would be feasible, would be accurate at identifying differing degrees of naturally occurring OA and would correlate with the cartilage GAG and water content.

6.2.3 *Materials and methods*

Horses

Either the right or left forelimb of 12 non-lame Warmblood horses aged 15.2 ± 9.2 (6 - 32 years) euthanized for reasons unrelated to the musculoskeletal apparatus was randomly dissected from the body at the middle carpal joint. The limbs were kept cool (4°C) until scanning.

MRI

The limbs were scanned within 24 hours of harvesting on different days over a 4-month period. A vitamin E capsule was taped to the lateral aspect of the hoof and each limb was positioned with the dorsal hoof wall facing downward and the toe facing towards the

gantry. A 16 - channel knee coil was used and the DIPJ of each forelimb was scanned at room temperature using a 3 Tesla MRI scanner.[b]

A transverse localizer was run on each DIPJ to identify the condylar and intercondylar sagittal slices. For each lateral and medial midcondylar sagittal slice and central intercondylar sagittal slice positioned in the middle of the distal aspect of the MP sagittal groove, pre contrast T1 relaxation time was measured using single slice inversion recovery spin echo sequences (TR 12 ms, TE 5.6 ms, field of view 100 x 100 mm, matrix 252 x 244, slice thickness 3 mm, receiver band width 131.6 kHz/pixel). Synoviocentesis of the DIPJ was performed using a 21 Gauge needle in the dorsal recess and as much synovial fluid as possible was aspirated. Gd-DTPA^{2-} [c] was injected into the DIPJ at 0.05 ml in 5 ml saline (0.025 mmol/joint). Following injection, the distal limb joints were manually flexed for 5 minutes to distribute the Gd-DTPA^{2-}. The limbs were scanned again 120 minutes following contrast injection using the same midcondylar and central intercondylar sagittal slices and the T1 post contrast relaxation time measurements were repeated.

Macroscopic cartilage assessment

The DIPJs were disarticulated and the cartilage surface of distal aspect of the MP and the proximal aspect of the DP were inspected and graded for macroscopic degenerative changes at specific preselected sites using a modified Outerbridge grading system (0 = normal; 1 = soft, discolored, swollen cartilage; 2 = partial thickness fissures, fragmentation or erosion; 3 = full thickness fissures, fragmentation or erosion). [19] A score was assigned to each ROI (see Figure 2, chapter I). The worst lesion present at the ROI determined the final cartilage score, if multiple lesions were present.

Tissue harvesting

Osteochondral cores (8 mm diameter) were cut from the distal aspect of the MP and the proximal aspect of the DP (see Figure 2, chapter I) using an OATS (osteochondral autograft transfer system) cutting tube.[d] A central 1000 µm thick osteochondral slice was cut from the core using a saw and further processed for histological sections. The cartilage was cut off the remaining subchondral bone core using a scalpel and was stored at -80°C until GAG and water analyses were to be performed.

MRI analysis

All ROIs (defined as shown in Figure 2, chapter I, Figure 1) were analysed for each midcondylar and the central intercondylar scan before and after contrast administration. Using commercially available software[e] ROIs (mean pixels: 198.5 ± 13.8) were drawn onto the hyaline cartilage using a free hand tool. Bulk T1 relaxation time measurements (ms) were obtained 3 times by two blinded observers (AB, AK, supervised by PK). $T1_{Gd}$ is the T1 relaxation time with the Gd-DTPA^{2-} and T1 is the relaxation time of the tissue without contrast agent. The mean relaxation time (ms) was calculated per ROI for each observer.

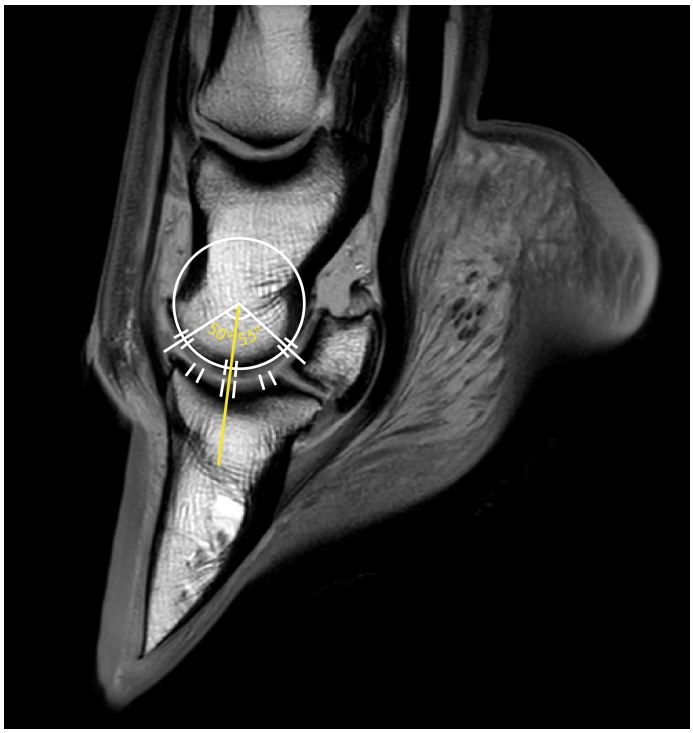

Figure 1: *Sagittal intercondylar magnetic resonance image (T2 turbo spin echo cal) of the distal interphalangeal joint (DIPJ) showing a translucent template illustrating a circle placed "at best fit" over the distal middle phalanx (MP) condyle and a yellow line drawn down the axis of the metaphysis of MP running through the center of rotation of the DIPJ. Dorsal regions of interest (ROIs) of distal MP (ROIs 1, 7 – Figure 2, chapter I) were defined using a 50° angle dorsal from the line drawn down the axis of the MP metaphysis and extending 5° dorsal and palmar. At these dorsal sites there was no contact between the distal MP and proximal distal phalanx (DP) hyaline cartilage, when the joint was in a neutral position. Central ROIs of distal MP (ROIs 2, 8 – Figure 2, chapter I) were defined as the distal aspect of the line drawn down the axis of the MP metaphysis and extending 5° dorsal and palmar. Palmar ROIs of distal MP (ROIs 3, 9 – Figure 2, chapter I) were defined using a*

55° angle palmar from the line drawn down the axis of the MP metaphysis and extending 5° dorsal and palmar. At these palmar sites there was contact between the distal MP and the navicular bone cartilage.
Dorsal ROI of proximal DP (ROI 13) was defined as the most dorsal extent of the hyaline cartilage extending 10° palmar. Central ROIs of proximal DP (ROIs 11, 14, 17 – Figure 2, chapter I) were defined as the distal aspect of the line drawn down the axis of the MP metaphysis extending 5° dorsal and palmar. Palmar ROI of proximal DP (ROI 15 - Figure 2, chapter I) was defined as the most palmar extent of the proximal DP cartilage articulating with distal MP extending 10° dorsally.

Histological and immunohistochemical sections

The osteochondral samples were fixed in 4% paraformaldehyde for 48 hours, decalcified in 25% EDTA for 4 weeks and embedded in paraffin. Sections were cut and stained with haematoxylin and eosin, Safranin-O-Fast green and toluidine blue.
For immunohistochemical staining of collagen type II, sections were dewaxed, incubated and digested with hyaluronidase, washed and incubated with a primary rabbit antibody (ab 34712)[f] and secondary biotinylated goat anti-rabbit secondary antibody.[g]

Histological and immunohistochemical analyses

Safranin-O-Fast green sections were assessed by three blinded observers (AB, RF, ABa supervised by MH), were scored for degenerative changes using a modified Mankin scoring system [20,21] (Table 1, chapter 1) and a mean score was calculated per section for each observer. According to the overall mean Mankin score three groups of cartilage health were made: normal cartilage: Mankin score = 0 - 1.9; minimal to moderate OA: Mankin score = 2.0 - 8.0; severe OA: Mankin score = 8.1 - 16.0.[h] Immunohistochemical sections of each ROI were described considering stain uptake, stain location and degree of staining (AB supervised by MH).

Biochemical cartilage analyses

Cartilage water content was determined using a modification of the method described by Brama *et al.* The cartilage samples were weighed before (wet weight) and after (dry weight) lyophilizing them using a speed vacuum machine for 4 hours. [22] The cartilage water content was expressed as percentage of wet weight.

Cartilage GAG concentration was determined using a modified method of the dimethylmethylene blue assay developed by Farndale *et al.* [23] with absorbance measured at

520 nm. Analyses were performed at TETEC© laboratory, Reutlingen, Germany. The cartilage GAG concentration was expressed as µg/mg cartilage normalized on wet weight.

Statistical analysis

The database was established in Microsoft Excel. The interobserver reliability was tested with an intra class correlation coefficient (ICC) for the histological scores (mean Mankin score) and the mean relaxation times (T1 and $T1_{Gd}$). Average measures were reported, whereby ICC > 0.7 = good, ICC > 0.8 = optimal, ICC > 0.9 = excellent. A Kolmogorov-Smirnoff test of normality was used to evaluate the distribution of the data. Results of parametric data were displayed as mean ± standard deviation. Results of nonparametric data were displayed as median (range). Of all observers an overall mean Mankin score and overall mean T1 and $T1_{Gd}$ relaxation times were calculated and included in the further analyses. The different ROIs were further grouped into cartilage zones depending on their location in the joint: condyle (ROIs 1, 2, 3, 7, 8, 9, 11 and 17) or condylar groove (ROIs 13, 14 and 15), and dorsal zone (ROIs 1, 7 and 13), central zone (ROIs 2, 8, 11, 14 and 17) or palmar zone (ROIs 3, 9 and 15). The analysis was performed using software SPSS 21.0.[i] The relationships between the T1 and $T1_{Gd}$ relaxation times, the cartilage GAG concentration, the cartilage water content, the cartilage macroscopic and histological scores were investigated using Spearman`s non-parametric correlations.

A generalized linear mixed model approach was used to analyse the relationship between the dependent variable T1 and $T1_{Gd}$ relaxation time (ms) and the independent variables Gd-$DPTA^{2-}$ (before/after administration) (only included in the T1 model), cartilage surface (MP/DP), cartilage zones ((condyle/condylar groove) and (dorsal/central/palmar)), macroscopic cartilage scores (0-3) and cartilage health (no/minimal-moderate/severe OA). Independent variables with P > 0.2 were omitted from the final model. The significance level was set at P < 0.05. Random effects were the leg and replicate as measurements within a single leg and replicate measurements are likely to be correlated. Exploratory analysis indicated that the gamma distribution was the most appropriate model for the generalized linear mixed model (family=gamma, link=log). The analysis was undertaken in R.[j]

6.2.4 *Results*

Ten cores were lost during the processing resulting in data of 122 ROIs being included in the study.

Macroscopic cartilage assessment

In 45 ROIs the cartilage was macroscopically normal, in 46 ROIs the cartilage was soft, discoloured and swollen, in 21 ROIs there were partial thickness fissures, fragmentation or erosions and in 10 ROIs there were full thickness fissures, fragmentation and erosions. Evidence of macroscopic degenerative cartilage changes had a significant effect on the T1 relaxation times ($P < 0.0001$) in the generalized linear mixed model. Cartilage with full thickness fissures, fragmentation or erosions (score 3) had significantly longer T1 relaxation times (ms) (705 [572 - 853]) compared to normal cartilage (score 0) (608 [476 - 747]), ($P < 0.0001$), also compared to soft, discolored, swollen cartilage (score 1) (608 [476 - 747]), ($P = 0.025$). However no significant difference was found between cartilage with full thickness fissures, fragmentation or erosions (score 3) and partial thickness fissures, fragmentation or erosions (score 2) (651 [527 - 779]), ($P = 0.181$). Cartilage macroscopic scores significantly correlated with the histological scores (mean overall Mankin score: $r_s = 0.71$, $P < 0.0001$; mean overall Mankin cartilage staining score: $r_s = 0.68$, $P < 0.0001$).

MRI analysis

A summary of the T1 and $T1_{Gd}$ relaxation times displaying median (ranges) is shown in Table 1. Figure 2 shows examples of pre and post contrast MR images of normal and diseased ROIs of the DIPJ cartilage and corresponding histological sections. There was a good to high level of inter observer agreement for the relaxation time values (T1 ICC = 0.78, $T1_{Gd}$ ICC = 0.94). In the generalized linear mixed model administration of intra articular contrast significantly decreased the relaxation times ($P < 0.0001$). There was a topographical variation of the relaxation times within the DIPJ, where by the T1 value (ms) of the DP articular surface 675 (476 -853) was higher than the T1 value of the MP articular surface 601 (454 - 767), ($P < 0.0001$). The T1 value (ms) dorsally 606 (463-739) was significantly less than palmarly 629 (434-797), ($P = 0.049$) and significantly less than in the middle of the DIPJ (662 [489-923]). The T1 values (ms) on the condyle (621[434-923]) or in the condylar groove (667 [476-853]) were not significantly different (this parameter was omitted from the final

generalized linear mixed model). The presence of OA had a significant effect on the T1 relaxation time ($P < 0.037$). The T1 relaxation time pre contrast of severely osteoarthritic cartilage (692) was increased compared to mild - moderately osteoarthritic cartilage (642) and compared to normal cartilage (607).

Following Gd-$DTPA^{2-}$ administration $T1_{Gd}$ of severely osteoarthritic cartilage was significantly shorter (199) compared to normal or moderately osteoarthritic cartilage (223) ($P = 0.03$). Macroscopic cartilage scores had a significant effect on $T1_{Gd}$ in the overall model ($P = 0.012$), however when comparing the $T1_{Gd}$ values between the different cartilage scores no significant difference was noted. In the generalized linear mixed model with $T1_{Gd}$ as dependent parameter no topographical variation of the $T1_{Gd}$ values was found. (Articular surface: $P = 0.21$, (omitted from the final model), cartilage zones (condyle/condylar groove): $P = 0.3$, (omitted from the final model) and cartilage zones (dorsal/central/palmar): $P = 0.17$ (not significant, but included in the final model)).

Parameters	**Normal cartilage (n=40)**	**Mild-moderate OA (n=68)**	**Severe OA (n=14)**
T1 value (ms)	607 (473 - 732)	642 (463 - 797)	692 (454 - 853)
$T1_{Gd}$ value (ms)	234 (182 - 330)	217 (116 -334)	210 (124 - 295)
Water (%)	71 (59 - 83)	73 (48 - 82)	77 (64 - 83)
GAG (µg/mg) ww	60 (21 - 104)	50 (18 - 106)	30 (15 - 73)

Table 1: *Showing a summary of the T1 and $T1_{Gd}$ relaxation times, the water content and the glycosaminoglycan (GAG) content displaying median (ranges) of the different degrees of osteoarthritis (OA). Abbreviations: ww = wet weight.*

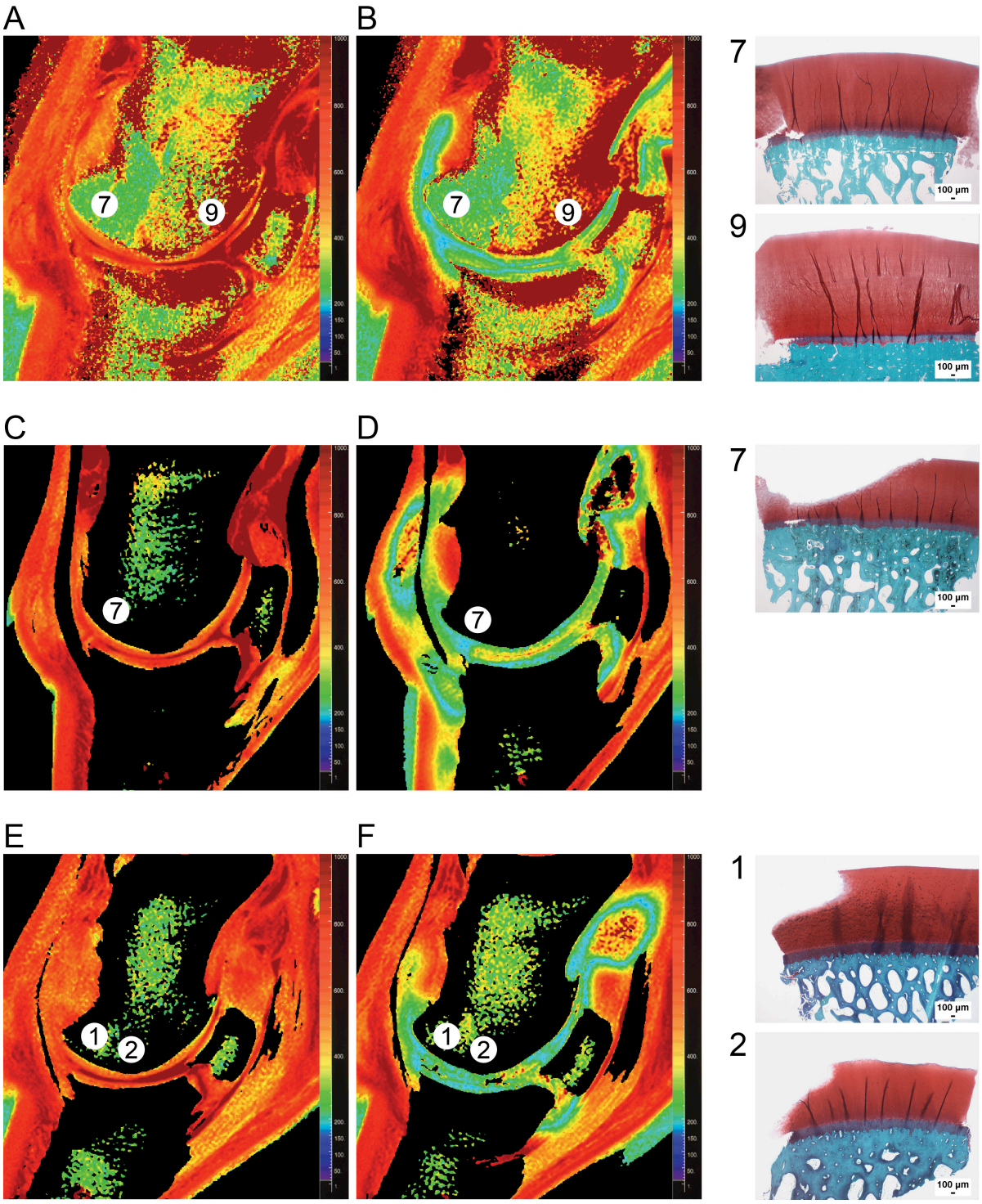

Figure 2: *T1 color-coded maps of: pre contrast delayed gadolinium enhanced MR imaging of cartilage of normal cartilage (A) and following intra articular gadolinium administration (B). On the right Safranin-O-Fast green specimens corresponding to selected region of interests (ROIs) (7, 9) are shown. The color bar on the right represents the T1 values using a continuous color translation of the T1 value from 1-1000 ms. Black relates to a T1 value of 1 ms, indicative of no glycosaminoglycans (GAGs) and dark red represents a T1 value of 1000 ms indicative of high amounts of GAGs present. The light green pixels of the articular cartilage indicate lower T1 values following contrast than those indicated by the red and yellow pixels on the pre contrast T1 maps. On the*

pre contrast T1 maps the T1 values decreased from the cartilage surface (red pixels) to the cartilage depth (yellow pixels). The post-contrast map shows a clearer delineation of the cartilage surface. On the-Safranin-O-Fast green specimens no abnormal lesion was noted at the corresponding ROIs (ROI 7 and 9).

Color-coded pre contrast T1 map (C) and post contrast T1 map (D) shows light to dark blue pixels within the normal green cartilage indicative of lower T1 values and GAG content at the ROI 7. The corresponding Safranin-O-Fast green section of the ROI 7 shows an erosion of 2/3 of the hyaline cartilage depth with accompanying loss of staining and superficial fibrillation.

Color-coded pre contrast (E) and post contrast T1 map (F) shows light to dark blue pixels within the normal green cartilage indicative of lower T1 values and GAG content at the ROI 1, 2, and 3. The corresponding Safranin-O-Fast green section of the ROI 1 shows an erosion of 1/3 of the hyaline cartilage depth with accompanying loss of staining and superficial fibrillation. The histological section of ROI 2 shows an erosion of 2/3 of the hyaline cartilage depth with accompanying loss of staining and superficial fibrillation.

Histological and immunohistochemical analyses

There was an optimal to excellent level of interobserver agreement of the histological scoring (Mankin score ICC = 0.98). Representative histological images (Safranin-O-Fast green and collagen type II immunohistochemistry) describing the typically seen cartilage lesions are provided in Figure 3.

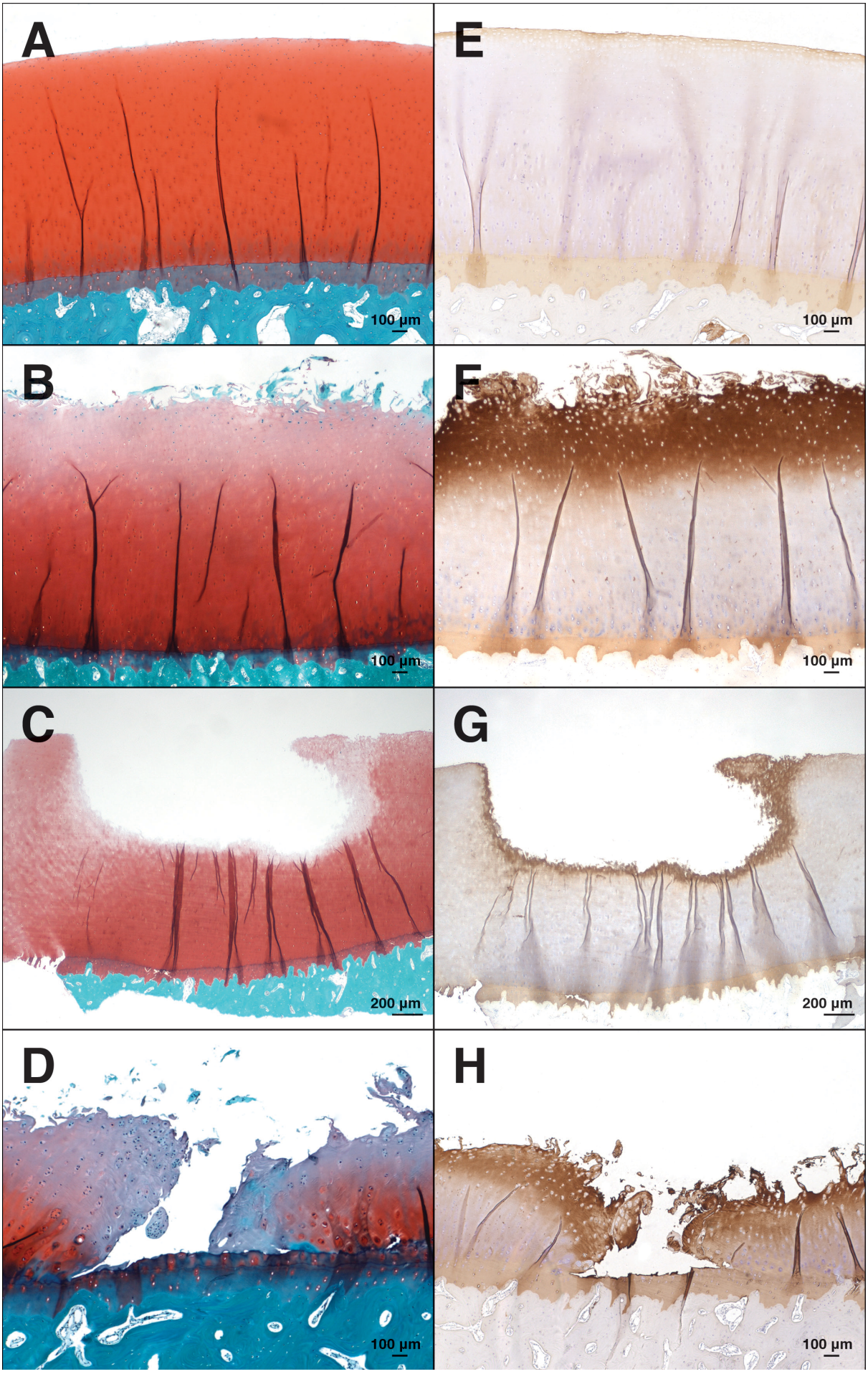
A
100 µm
E
100 µm
B
100 µm
F
100 µm
C
200 µm
G
200 µm
D
100 µm
H
100 µm

Figure 3: *Representative Safranin-O-Fast green histological (A - E) and collagen type II immunohistochemical sections (F - J) of specimens with different lesion severities. A: In normal hyaline cartilage there was a homogenous stain uptake throughout the extracellular matrix with a smooth cartilage surface and a regular subchondral bone. B: Marked fibrillations of the cartilage surface with loss of staining of the superficial hyaline cartilage zone and evidence of chondrocyte cluster formation. C: Erosion of the superficial 2/3 of hyaline cartilage with accompanying loss of staining of the upper 2/3 the hyaline cartilage. D: Full depth erosion of the hyaline cartilage with focal loss of staining in all the hyaline cartilage and marked chondrocyte cluster formation. Cracks in the calcified cartilage are present and there is a decreased amount and size of bone lacunae underneath the hyaline cartilage. Clefts and fissures are present with loss of staining of all the hyaline cartilage and possible calcification, with multifocal decrease in chondrocyte numbers and chondrocyte cluster formation. The calcified cartilage and underlying subchondral bone is collapsed, with cartilage islands within the subchondral bone. E: In normal hyaline cartilage there was minimal immunestaining of the superficial cartilage zone. Immunestaining increased in specimens with evidence of OA corresponding to loss of staining in Safranin-O-Fast green sections. When fibrillation, fissures (F) or partial (G) or full thickness erosions (H) were observed there was diffuse immunestaining of the superficial cartilage matrix at the lesion. With increasing OA severity the depth of staining of the extracellular matrix increased (J).*

Biochemical analysis

A summary of the GAG concentration and water content displaying median (range) is shown in Table 2. The mean overall GAG concentration correlated significantly negatively with the T1 value, the mean overall Mankin score and the macroscopic cartilage score, however no significant correlation was found between GAG concentrations and $T1_{Gd}$ values (Figure 4A - D). The cartilage water content significantly correlated with the T1 value, the mean overall Mankin score and macroscopic cartilage score, however not with the $T1_{Gd}$ value (Figure 4E - H).

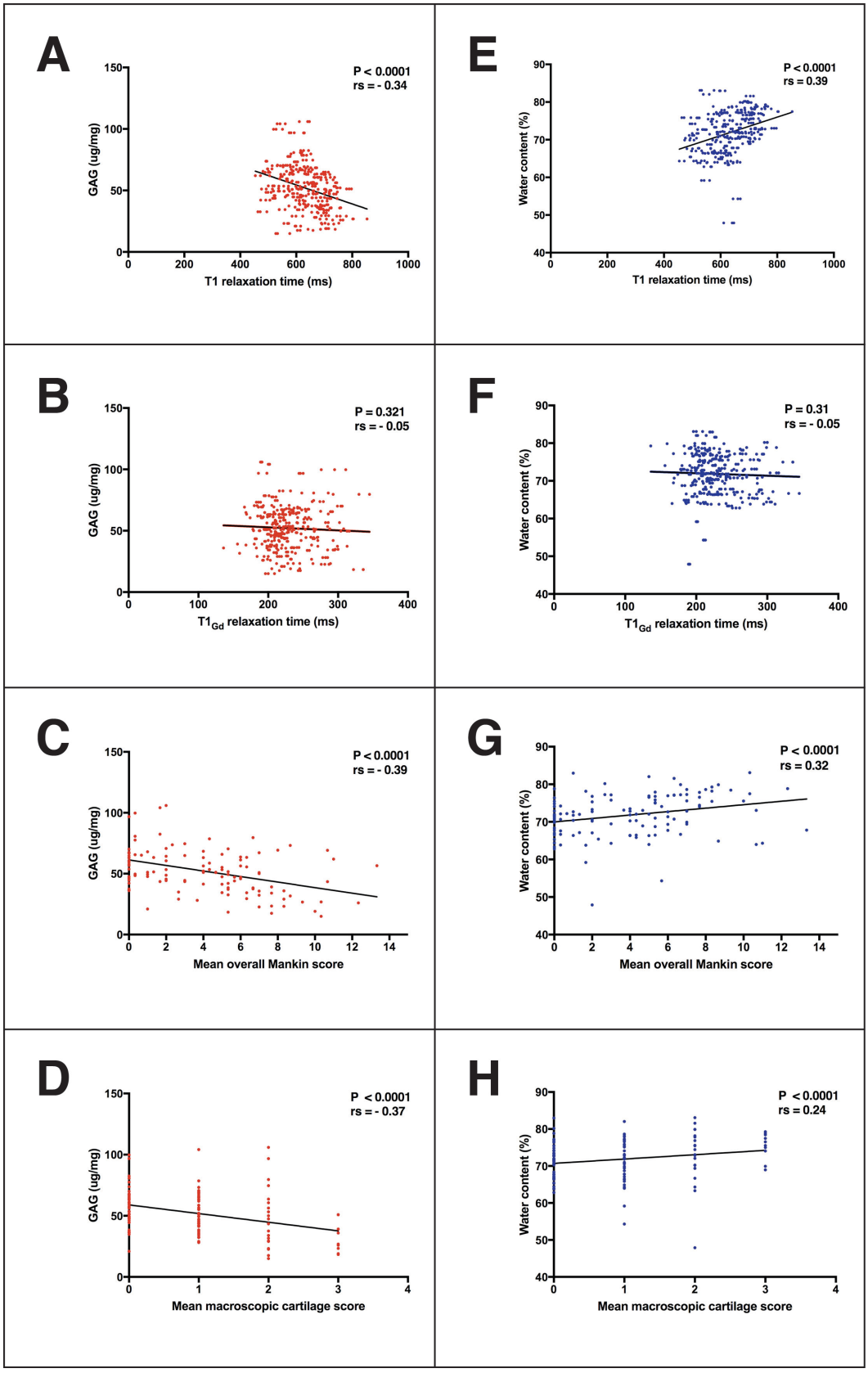

Figure 4: *Plots showing the Spearman`s correlations between the distal interphalangeal joint cartilage`s biochemical parameters (glycosaminoglycan (GAG) concentration (µg/mg) and water content (%)) and the magnetic resonance imaging data (T1 value (E) and $T1_{Gd}$ value (F)), the mean overall Mankin scores (G) and the mean macroscopic cartilage scores (H). (rs = Spearman`s rho correlation coefficient).*

6.2.5 *Discussion*

The objective of this cadaver study was to establish the dGEMRIC technique in DIPJ hyaline cartilage, to investigate whether dGEMRIC can identify different degrees of naturally occurring OA and correlate cartilage relaxation times with cartilage GAG concentration and water content. It was shown that T1 and $T1_{Gd}$ relaxation times in diseased equine DIPJ cartilage correlated with the macroscopic and histologic degree of naturally occurring cartilage OA. Moreover T1 relaxation times of normal and diseased DIPJs also correlated with the cartilage`s GAG concentration and water content.

Following intra articular contrast application T1 relaxation times significantly decreased to an overall obtained value of 234 ms (182 - 330) in normal cartilage. This was lower than in the previous study on cadaver fetlock joint cartilage[17], where post contrast values of 650 ms were obtained 120 min following intra articular contrast administration. This difference may be due to inherent cartilage differences between these joints or the differences in cartilage thickness. The distance from the cartilage surface to the bone cartilage interface of the distal aspect of the third metacarpal or metatarsal bone cartilage has been reported to be 0.79 - 0.99 mm thick on light microscopy. [24] Due to this, Carstens *et al.* had to analyse a combination of the thin opposing cartilage surfaces and a thin layer of synovial fluid at some sites in the fetlock joint. [24] In the DIPJ the mean cartilage thickness has been shown to range from 2.1 mm dorsally to 3.1 mm palmarly. [25] The thicker cartilage in this joint allowed only hyaline cartilage to be evaluated in the measured ROIs and may explain the discrepancies in post contrast T1 relaxation times between the studies. The Gd-$DTPA^{2-}$ dosage administered in the DIPJ was the same as was used in the previous study in the fetlock joint equalling 0.025mmol/5ml. [17] Due to the smaller size of the DIPJ this dosage may have been higher in comparison to the fetlock joint, thus maybe also resulting in the lower post contrast relaxation times. Following contrast administration acquisition of the post contrast T1 images was only done 120 minutes post injection. This was chosen by following the recommendations of a previous equine cadaver study, which observed a decreasing pattern of relaxation time over 120 minutes. [17]

In cases of cartilage degeneration there is a loss of proteoglycans and their side chains (GAGs), which diffuse out of the tissue. Due to this disruption in the cartilage matrix, the water content increases. This was also visible in our specimens, where the GAG concentration decreased with increasing histologic and macroscopic cartilage OA scores. dGEMRIC was developed for the indirect assessment of the hyaline cartilage GAG content. [15,26-28] Areas of low GAG content accumulate a higher concentration of Gd-DTPA^{2-} leading to shorter $T1_{Gd}$ relaxation times. This data illustrates this in the equine DIPJ cartilage. With advancing degree of cartilage degeneration, proteoglycans were lost and Gd-DTPA^{2-} penetrated into the hyaline cartilage leading to shorter $T1_{Gd}$ values in specimens with evidence of mild to severe OA. This is also reflected by the fact that the $T1_{Gd}$ values negatively correlated with the Safranin-O-Fast green staining loss observed histologically indicative of proteoglycan loss with advancing OA. The increase of water content in the progression of OA was also observed in our specimens. The $T1_{Gd}$ values became shorter when the water content increased, consistent with the advancing degree of OA. Overall the data showed that dGEMRIC correlated with equine cartilage degeneration supporting our hypothesis. The $T1_{Gd}$ values did not significantly correlate with the GAG concentrations or the water content, however we have no convincing evidence to explain this. Specimens may have been influenced by storage or by the laboratory technique employed, despite this being performed in an experienced and qualified laboratory, or the sample size may have been too small.

There were significant site dependent differences in T1 relaxation times noted within the DIPJ where the dorsal cartilage T1 value was shorter than the values in the joint middle or palmar aspect. The topographical variation of MRI parameters is well known in the human knee. [29] This variation is likely a reflection of the hyaline cartilages response to physiological loading and the relationship between the biomechanical and biochemical constitution of the tissue, resulting in different relaxation times. Brama *et al.* showed regional differences in the fetlock cartilage extracellular matrix components, where the GAG content was lowest in the dorsal regions. [22] To date the exact GAG and water profile of the normal equine DIPJ cartilage and its topographical variation have not been reported. However, inherent differences between the different types of joints could be true for the differences seen in the DIPJ. In the dorsal aspect of the joint there may be more intermittent loading leading to

less GAG production (hence lower T1 values) than in central or palmar regions where loading is more constant leading to more GAG production (hence higher T1 values).

T1 values of the MP articular surface were lower than the DP articular surface also likely reflecting the greater GAG content of the DP cartilage due to the continuous loading of this articular surface. The sale size of this study was too low to create a reliable complete topographical T1 relaxation time map of the normal DIPJ and this was not the study objective. However topographical differences shown here are important and should be taken into account when interpreting MRIs of the equine DIPJ cartilage.

The histological scoring system (modified Mankin scoring system) used in this study to score the lesion severity has previously been applied to naturally occurring OA in the equine carpal bones [20] and equine distal metacarpus. [30] It has been proven to be repeatable amongst observers and reliable in scoring the degree of cartilage degeneration in naturally occurring disease in previous studies, as well in this study. The focal nature of the cartilage lesions seen within a whole articular surface was striking and supports the findings from equine post traumatic carpal OA. [31] Areas of normal and diseased cartilage were found in close proximity in the same histologic specimen.

This study had a few unavoidable limitations. Despite using a template to match the MRI ROIs with the histological specimens obtained, small deviations may have occurred. A future study scanning the actual osteochondral cores and then histologically processing them is planned to preclude this limitation. In this study the authors however chose to scan the complete DIPJ to more closely imitate the clinical scenario. The cadaver DIPJs were from horses with varying ages. Thus we are likely to have a combination of pathologies originating from overload injuries as well as age related OA.

Until now dGEMRIC is not established enough for use in the equine clinical field and is more of interest for the research setting. The dGEMRIC image acquisition is time consuming and needs the administration of a contrast agent, which is a disadvantage in equine MRI. Horses are under general anaesthesia and repositioning the horse after intra articular contrast injection in the MRI scanner requires time. Standing MRI utilizes low

magnet strengths and the current resolution is not appropriate for accurate dGEMRIC of the equine cartilage, especially in thin cartilage areas. Future research should address the administration route of Gd-DTPA^{2-} (intra venous versus intra articular), effect of exercise on the Gd-DTPA^{2-} uptake into the hyaline cartilage and establish topographical variations of T1 and $T1_{Gd}$ relaxation times of normal hyaline cartilage.

This study is the first to describe the normal and osteoarthritic appearance of the DIPJ in dGEMRIC. The current data indicate that varying degrees of naturally occurring OA in the DIPJ have a significant effect on dGEMRIC values. Further research investigating the relationship between relaxation times and cartilage GAG content should be under taken. Nevertheless, this study lays a foundation for future studies investigating promising cartilage specific MRI sequences, having important consequences in early recognition of OA in a research and later potentially in a clinical setting.

Footnotes

a. Carstens, A., Delayed gadolinium enhanced magnetic resonance imaging and T2 mapping of cartilage of the cadaver distal metacarpus 3/metatarsus 3 of the normal Thoroughbred horse. PhD thesis, 2013, University of Pretoria, South Africa.

b. Phillips Health Care Ingenia, Phillips AG, Zurich, Switzerland.

c. Magnevist gadopentate dimeglumine, Bayer Health Care Pharmaceuticals, Zurich, Switzerland.

d. Arthrex Inc, Naples, FL, USA

e. Relaxation Maps Tool V 2.1.2., Koninklijke Philips Electronics N. V. 2013, Phillips AG, Zurich Switzerland.

f. Abcam Inc, Cambridge, MA, USA

g. Thermo Scientifics, Illinois, USA

h. IBM SPSS, Armonk, NY, USA

i. Stahl, A. Validierung neuer, knorpelsensitiver Sequenzen am Schafmodell im 3T-Hochfeld- MRT zur Erkennung von Frühveränderungen verursacht durch das Femoroacetabuläre impingement. Doctoral thesis, 2009, University of Zurich.

j. R Core Team (2016). R: A language and environment for statistical computing. R Foundation for Statistical Computing, Vienna, Austria. URL https://www.R-project.org/.) using the MASS, car and lme4 packages.

6.2.6 *References*

1. Jeffcott LB, Rossdale PD, Freestone J, et al. An asessment of wastage in Thoroughbred racing from conception to 4 years of age. *Equine Veterinary Journal* 1982;14:185-198.

2. Nilsson G, Olsson SE. Radiologic and patho-anatomic changes in the distal joints and the phalanges of the standardbred horse. *Acta Veterinaria Scandinavica Supplements* 1973;44:1-57.

3. Dyson SJ. Lameness due to pain associated with the distal interphalangeal joint - 45 cases. *Equine Veterinary Journal J* 1991;23:128-135.

4. McKnight AL, Posh, J. Articular cartilage lesions seen with MRI at 0.25T in the distal equine limb. *Journal of Equine Veterinary Sci*ence 2012;32:667-671.

5. Kristiansen KK, Kold SE. Multivariable analysis of factors influencing outcome of 2 treatment protocols in 128 cases of horses responding positively to intra-articular analgesia of the distal interphalangeal joint. *Equine Veterinary Journal* 2007;39:150-156.

6. Bekkers JEJ, Creemers LB, Dhert WJA, et al. Diagnostic modalities for diseased articular cartilage - From defect to degeneration: A review. *Cartilage* 2010;1:157-164.

7. Pease A. Biochemical evaluation of equine articular cartilage through imaging. *Veterinary Clinics of North America-Equine Practice* 2012;28:637-646.

8. Choi JA, Gold GE. MR imaging of articular cartilage physiology. *Magnetic Resonance Imaging Clinics of North America* 2011;19:249-82.

9. Domayer SE, Welsch GH, Dorotka R, et al. MRI monitoring of cartilage repair in the knee: a review. *Seminars in Musculolskeletal Radiol*ogy 2008;12:302-317.

10. Gold GE, Burstein D, Dardzinski B, et al. MRI of articular cartilage in OA: novel pulse sequences and coositional/functional markers. *Osteoarthritis and Cartilage* 2006;14:A76-A86.

11. Potter HG, Black BR, Chong LR. New techniques in articular cartilage imaging. *Clinics in Sports Medicine* 2009;28:77-94.

12. Trattnig S, Mamisch TC, Pinker K, et al. Differentiating normal hyaline cartilage from post-surgical repair tissue using fast gradient echo imaging in delayed gadolinium-enhanced MRI (dGEMRIC) at 3 Tesla. *European Radiology* 2008;18:1251-1259.

13. Trattnig S, Marlovits S, Gebetsroither S, et al. Three-dimensional delayed gadolinium-enhanced MRI of cartilage (dGEMRIC) for in vivo evaluation of reparative cartilage after matrix-associated autologous chondrocyte transplantation at 3.0T: Preliminary results. *Journal of Magnetic Resonance Imaging* 2007;26:974-982.

14. Bekkers JEJ, Bartels LW, Benink RJ, et al. Delayed gadolinium enhanced MRI of cartilage (dGEMRIC) can be effectively applied for longitudinal cohort evaluation of articular cartilage regeneration. *Osteoarthritis and Cartilage* 2013;21:943-949.

15. Trattnig S, Mlynarik V, Breitenseher M, et al. MRI visualization of proteoglycan depletion in articular cartilage via intravenous administration of Gd-DTPA. *Magnetic Resonance Imaging* 1999;17:577-583.

16. Frisbie DD. Synovial joint biology and pathobiology. In: Auer J, Stick J, eds. *Equine Surgery.* 4th ed. St. Louis, Missouri: Elsevier, Saunders, 2012;1096-1114.

17. Carstens A, Kirberger RM, Velleman M, et al. Feasibility for mapping cartilage T1 relaxation times in the distal metacarpus3/metatarsus3 of Thoroughbred racehorses using delayed gadolinium-enhanced magnetic resonance imaging of cartilage (dgemric): normal cadaver study. *Veterinary Radiology & Ultrasound* 2013;54:365-372.

18. Menendez MI, Clark DJ, Carlton M, et al. Direct delayed human adenoviral B-2 or B-6 gene therapy for bone and cartilage regeneration in a pony osteochondral model. *Osteoarthritis and Cartilage* 2011;19:1066-1075.

19. Outerbridge RE. The etiology of chondromalacia of the patella. *Journal of Bone and Joint Surgery-British Vol*ume 1961;43:613-613.

20. Lacourt M, Gao C, Li A, et al. Relationship between cartilage and subchondral bone lesions in repetitive iact trauma-induced equine osteoarthritis. *Osteoarthritis and Cartilage* 2012;20:572-583.

21. Mankin HJ, Dorfman H, Lippiell L, et al. Biochemical and metabolic abnormalities in articular cartilage from osteo-arthritic human hips .2. correlation of morphology with biochemical and metabolic data. *Journal of Bone and Joint Surgery-American Volume* 1971;A 53:523-37.

22. Brama PAJ, Tekoppele JM, Bank RA, et al. Topographical mapping of biochemical properties of articular cartilage in the equine fetlock joint. *Equine Veterinary Journal* 2000;32:19-26.

23. Farndale RW, Buttle DJ, Barrett AJ. Iroved quantitation and discrimination of sulfated glycosaminoglycans by use of Dimethylmethylene blue. *Biochimica Et Biophysica Acta* 1986;883:173-177.

24. Carstens A, Kirberger RM, Dahlberg LE, et al. Validation of delayed gadolinium-enhanced magnetic resonance imaging of cartilage and T2 mapping for quantifying distal metacarpus/metatarsus cartilage thickness in Thoroughbred racehorses. *Veterinary Radiology & Ultrasound* 2013;54:139-148.

25. Olive J. Distal interphalangeal articular cartilage assessment using low-field magnetic resonance imaging. *Veterinary Radiology & Ultrasound* 2010;51:259-266.

26. Bashir A, Gray ML, Hartke J et al. Nondestructive imaging of human cartilage glycosaminoglycan concentration by MRI. *Magnetic Resonance in Medicine* 1999;41:857-865.

27. Laurent D, Wasvary J, Rudin M, et al. In vivo assessment of macromolecular content in articular cartilage of the goat knee. *Magnetic Resonance in Medicine* 2003;49:1037-1046.

28. Mlynarik V, Trattnig S, Huber M, et al. The role of relaxation times in monitoring proteoglycan depletion in articular cartilage. *Journal of Magnetic Resonance Imaging* 1999;10:497-502.

29. Kurkijarvi JE, Nissi MJ, Kiviranta I, et al. Delayed gadolinium-enhanced MRI of cartilage (dGEMRIC) and T-2 characteristics of human knee articular cartilage: topographical variation and relationships to mechanical properties. *Magnetic Resonance in Medicine* 2004;52:41-46.

30. Vinardell T, Dejica V, Poole AR, et al. Evidence to suggest that cathepsin K degrades articular cartilage in naturally occurring equine osteoarthritis. *Osteoarthritis and Cartilage* 2009;17:375-383.

31. Bertuglia A, Lacourt M, Girard C, et al. Osteoclasts are recruited to the subchondral bone in naturally occurring post-traumatic equine carpal osteoarthritis and may contribute to cartilage degradation. *Osteoarthritis and Cartilage* 2016;24:555-66.

6.3 Chapter III:

T2 mapping of the normal and naturally occurring osteoarthritic equine cadaver distal interphalangeal joint cartilage in a 3 tesla magnet

Andrea S. Bischofberger, Dr. med. vet., DACVS, DECVS[1]; Anton E. Fürst, Prof., Dr. med. vet., DECVS[1]; Prof., Dr. med. vet., DECVS; Paul R. Torgerson, Prof., PhD, VetMB, DECVPH, DEVPC[2]; Ann Carstens BVSc, BVSc, MS, MMedVet (Large Animal Surgery), MMedVet (Diagnostic Imaging), PhD, DECVDI[3]; Monika Hilbe, Dr. med. vet., DECVP[4]; Patrick Kircher, Prof., Dr. med. vet., PhD, DECVDI[5].

From the [1]Equine Hospital, [2]Section of Veterinary Epidemiology [4]Institute of Veterinary Pathology, [5]Division of Diagnostic Imaging, Vetsuisse-Faculty, University of Zürich, Zürich, Switzerland; and the [3]Department of Companion Animal Clinical Studies, Faculty of Veterinary Science, University of Pretoria, Pretoria, South Africa.

The authors have no personal interests to declare. The study was funded by the Swiss Veterinary Association.

Contribution:

Study design, study execution, shared contribution to data collection, shared contribution to data analysis, data interpretation and manuscript writing, arrangement and formatting. Design of all figures and tables.

6.3.1 *Abstract*

Objective - To investigate T2 mapping of the DIPJ normal cartilage as well as cartilage with different degrees of naturally occurring OA, and to correlate the T2 relaxation times with the cartilage`s GAG concentration, water content and collagen structure.

Animals - 12 Warmblood cadaver DIPJs

Procedures - Mean T2 weighted relaxation times of predetermined sites of the DIPJ were obtained. Corresponding cartilage sites were examined macroscopically, histologically (Safranin-O-Fast green, picrosirius red) and immunohistochemically (collagen type II). Cartilage health was graded macroscopically and histologically. The site`s GAG (µg/mg) and water contents were determined. The T2 values were correlated to the histologic and macroscopic and biochemical data. Generalized linear mixed models analysed the effects of cartilage sites, articular surface and cartilage health (histological score) on the relaxation times.

Results - 122 cartilage sites were analysed. Median (range) of T2 weighted relaxation times (ms) found were: normal cartilage: 32 (22-47), mild to moderate OA: 32 (19-62) and severe OA: 35.5 (22-47). There was a topographical variation of the T2 values within the joint. The T2 value was higher dorsal than palmar in the joint. The center of the joint had the lowest T2 value. Cartilage health did not have a significant effect on the T2 values in the generalized linear mixed model. The T2 values negatively correlated with the water content, however not with the collagen structure (picrosirius red, collagen type II immunohistochemistry) or the GAG content.

Conclusions and clinical relevance - T2 mapping of the DIPJ was established and topical variation of T2 values were shown, however T2 maps were not sensitive enough to depict the varying degrees of osteoarthritis in this cadaver study, needing follow-up investigation.

6.3.2 *Introduction*

One of the most robust techniques to assess the articular cartilage in vivo is MRI. Conventional MRI methods are based on imaging water content and have shown morphologic changes of the cartilage, representing already progressed stages of OA. [1] Biochemical and structural changes in the extracellular cartilage matrix precede morphological changes. These changes can be evaluated by relaxation time-coded colour-maps. Different mapping techniques have been described in T2, T2*, T1rho and delayed gadolinium enhanced MRI of cartilage. [1,2]

The primary type of collagen in the articular cartilage is type II (90 - 95% of dry weight). [3] The collagen fibers are organised in a three-dimensional framework, accounting for the resistance of the articular cartilage to tensile and shear forces. [4] Loss of the collagen organisation and an increase in its hydration are hallmark features of OA. [5] Quantitative T2 mapping has been reported as a reliable technique to visualize cartilage hydration, collagen integrity and orientation. [6] In vitro studies have shown that increased T2 values correlated with histologically present degeneration. [7-12]

In humans in vivo T2 mapping studies have been conducted in the human knee joint, [13-17] the human hip joint, [18,19] the human ankle, [20] and the human proximal interphalangeal joint of the hands. [21]

Different T2 values for deep and superficial cartilage layers [22] and region dependent changes in T2 values have been shown in the human knee. [23,24] Superficial cartilage was found to have significantly longer T2 values compared to the deeper cartilage layer. [6,15] T2 values have also been reported to be age dependent, and have been reported to become longer with advanced age in the superficial layer of the patellar cartilage. [6] No clear sex dependent changes of T2 values have been reported. [24]

In horses T2 mapping has exclusively been used for research purposes. It was shown that quantitative T2 values were similar in fresh, chilled and frozen equine

metacarpo/metatarsophalangeal joints.[a] Further it was shown that T2 maps were accurate to measure normal cadaver cartilage thickness at the distal third metacarpal/metatarsal bone, when there was no contact between opposing cartilage surfaces. [25] T2 mapping of the articular cartilage of equine stifle specimens helped differentiate reparative fibrocartilage following arthroscopic osteochondral autograft transplantation and microfracture arthroplasty from normal hyaline cartilage. [26] T2 mapping in addition to histopathology was used to compare the repair of full thickness cartilage defects on the lateral trochlear ridge of the femur undergoing microfracturing or treatment with bone marrow aspirate. [27] In five ponies, T2 mapping was used to assess the serial healing of experimentally created femoral condyle lesions treated with bone morphogenic protein. [28]

This equine DIPJ cadaver study aimed at 1) investigating T2 mapping techniques in normal hyaline cartilage, 2) testing whether T2 mapping can identify different degrees of naturally occurring OA and 3) correlating T2 relaxation times with the cartilage`s GAG, water content and collagen structure described on picrosirirus red sections and collagen type II immunohistochemistry.

It was hypothesized that the technique would be feasible, would be accurate at identifying differing degrees of naturally occurring OA and would correlate with the cartilage GAG and water content and collagen type II structure.

6.3.3 *Material and methods*

Horses

Of twelve Warmblood horses aged 15.2 ± 9.2 (6 - 32 years) euthanized for reasons unrelated to the musculoskeletal apparatus either a right or left forelimb was randomly dissected from the body at the middle carpal joint. (Same study population as in chapters I and II) The limbs were kept cool (4°C) until scanning.

MRI

The limbs were scanned within 24 hours of harvesting on different days over a 4-month period. A vitamin E capsule was taped to the lateral aspect of the hoof and each limb was positioned with the dorsal hoof wall facing downward and the toe facing towards the

gantry. A 16 - channel knee coil was used and the DIPJ of each forelimb was scanned at room temperature using a 3 tesla MRI scanner[b]. T2 mapping images were obtained using multi-slice multi-echo spin-echo sequences (TR 2000 ms, TE 6 x 13 ms, field of view 160 x 160 mm, matrix 380 x 311, slice thickness 2.5 mm, receiver band width 291.1 Hz/pixel).

Macroscopic assessment of the cartilage surface

The DIPJs were disarticulated and the cartilage surface of the distal MP and the proximal DP was inspected and graded for macroscopic degenerative changes using a modified Outerbridge grading system (0 = normal; 1 = soft, discolored, swollen cartilage; 2 = partial thickness fissures, fragmentation or erosion; 3 = full thickness fissures, fragmentation or erosion). [29] A score was assigned to each ROI (see Figure 2, chapter I and Figure 1, chapter II). The worst lesion present at the ROI determined the final cartilage score, if multiple lesions were present.

Tissue harvesting

Osteochondral cores (8 mm in diameter) were cut from the distal MP and the proximal DP using an OATS (osteochondral autograft transfer system) cutting tube[c]. A central 1000 µm thick osteochondral slice was cut from the core using a saw and processed for histological sections. Cartilage was cut off the remaining subchondral bone core using a scalpel and was stored at -80°C for the GAG and water analyses.

MR image analysis

Three ROIs were analysed for the each midcondylar and central intercondylar scan. ROIs were defined (see Figure 1, chapter II). Using commercially available software[d] T2 bulk average relaxation times were measured three times and the mean relaxation time (ms) calculated for each ROI.

Histological and immunohistochemical sections

The osteochondral samples were fixed in 4% paraformaldehyde for 48 hours, decalcified in 25% EDTA for 4 weeks, embedded in paraffin and sections were cut and stained with haematoxylin and eosin, Safranin-O-Fast green, picrosirius red and toluidine blue.

For immunohistochemical staining of collagen type II sections were dewaxed, incubated and digested with hyaluronidase, washed and incubated with a primary rabbit antibody (ab 34712)[e] and secondary biotinylated goat anti-rabbit secondary antibody[f].

Histological and immunohistochemical analyses

Safranin-O-Fast green stains were assessed by three blinded observers (AB, RF and AB supervised by MH), were scored for degenerative changes using a modified Mankin scoring system [30,31] (see Table 1, chapter I) and a mean score was calculated for every section and each observer. According to the mean overall Mankin score 3 groups of cartilage health were made: normal cartilage: 0-1.9 Mankin score; minimal to moderate OA: 2.0-8.0 Mankin score; severe OA: 8.1-16.0 Mankin score[g].

Picrosirius red stains were graded by two blinded observers and scored for degenerative changes using polarised light microscopy[h] to assess collagen structure [32] (0 = normal; 1 = loss of integrity of 1/3 of cartilage thickness; 2 = loss of integrity of 2/3 of cartilage thickness; 3 = loss of integrity of 3/3 of cartilage thickness) and a mean overall score was calculated per section for each observer. A loss of integrity was defined as a loss of the collagen architecture in comparison to normal articular cartilage. All sections were assessed at the angle, which resulted in the maximum birefringence of the articular surface. [33] Order of collagen and fibril thickness determines the polarization color of the red stained type II collagen. Briefly highly ordered thick collagen fibers are bright yellowish-orange color (highly birefringent), thin fibers are green-yellowish color (mildly birefringent) and non-ordered collagen (non-birefringent) is dark. [33]

Immunohistochemical sections were graded by two blinded observers and scored according to the criteria shown in Table 1. For each section a mean overall immunohistochemical score was calculated for each observer.

Stain uptake	
No staining	0
Focal staining	1
Multifocal staining	2
Multifocal confluent staining	3
Diffuse staining	4
Stain location	
No staining	0
Staining in upper 1/3 of hyaline cartilage	1
Staining in upper 2/3 of hyaline cartilage	2
Staining in all the hyaline cartilage	3
Stain degree	
No staining	0
Light staining	1
Intermediate staining	2
Dark staining	3

Table 1: *Scoring system used to assess the type II collagen following immunohistochemistry*

Biochemical cartilage analyses

Cartilage water content was determined using a modification of the method described by Brama *et al.* The cartilage samples were weighed before (wet weight) and after (dry weight) lyophilizing them using a speed vacuum machine for four hours. [34] The cartilage water content was expressed as % of wet weight.

Cartilage GAG concentration was determined following a modified method of the dimethylmethylene blue assay developed by Farndale *et al.* [35] with absorbance measured at 520 nm. Analyses were performed at TETEC© laboratory, Reutlingen, Germany. The cartilage GAG concentration was expressed as µg/mg cartilage normalized on wet weight.

Statistical analysis

The database was established in Microsoft Excel. The interobserver reliability was tested with an ICC for the histological scores (mean Mankin score, mean picrosirius red scores, mean immunohistochemical scores) and the mean T2 relaxation times. Average measures were reported, whereby ICC > 0.7 = good, ICC > 0.8 = optimal, ICC > 0.9 = excellent. A Kolmogorov-Smirnoff test of normality was used to evaluate the distribution of the data. Results of parametric data were displayed as mean ± standard deviation. Results of nonparametric data were displayed as median (range). Of all observers an overall mean Mankin score, overall mean picrosirius red score and overall mean immunohistochemical score was calculated and included in the further analyses. The different ROIs were further grouped into cartilage zones depending on their location in the joint: condyle (ROIs 1, 2, 3, 7, 8, 9, 11 and 17) or condylar groove (ROIs 13, 14 and 15), and dorsal zone (ROIs 1, 7 and 13), central zone (ROIs 2, 8, 11, 14 and 17) or palmar zone (ROIs 3, 9 and 15). The relationships between the T2 relaxation times, the cartilage GAG concentration, the cartilage water content, the cartilage macroscopic and histological scores were investigated using Spearman`s non-parametric correlations. The analysis was performed using software SPSS 21.0[I]

A generalized linear mixed model approach was used to analyse the relationship between the dependent variable T2 relaxation time (ms) and the independent variables cartilage surface (MP/DP), cartilage zones ([condyle/condylar groove] and [dorsal/central/palmar]), macroscopic cartilage scores (0-3) and cartilage health (no/mild-moderate/severe OA). Independent variables with P > 0.2 were omitted from the final model. The significance level was set at P < 0.05. Random effects were the leg and replicate as measurements within a single leg and replicate measurements are likely to be correlated. Exploratory analysis indicated that the gamma distribution was the most appropriate model for the generalized linear mixed model (family=gamma, link=log). The analysis was undertaken in R[j].

6.3.4 *Results*

Ten cores were lost during the processing resulting in data of 122 ROIs being included in the study.

Macroscopic assessment of the cartilage surface

In 45 ROIs the cartilage was macroscopically normal, in 46 ROIs the cartilage was soft, discoloured and swollen, in 21 ROIs there were partial thickness fissures, fragmentation or erosions and in 10 ROIs there were full thickness fissures, fragmentation and erosions. The following T2 relaxation times (ms) were found: Normal cartilage: 31 (19 - 47); soft, discolored, swollen cartilage (score 1): 30 (21 - 55); cartilage with partial thickness fissures, fragmentation or erosion (score 2): 35 (22 – 62) and cartilage with full thickness fissures, fragmentation or erosions (score 3): 38 (24 - 54). Evidence of macroscopic degenerative cartilage changes did not have a significant effect ($P > 0.2$) on the T2 relaxation times in the generalized linear mixed model. Cartilage macroscopic scores significantly correlated with the histological scores (mean overall Mankin score: $r_s = 0.71$, $P < 0.0001$; mean overall picrosirius red score: $r_s = 0.34$, $P < 0.0001$; mean overall immunohistochemistry score: $r_s = 0.24$, $P < 0.0001$).

MRI image analysis

Figure 1 shows examples of T2 maps of normal and diseased ROIs of the DIPJ cartilage.

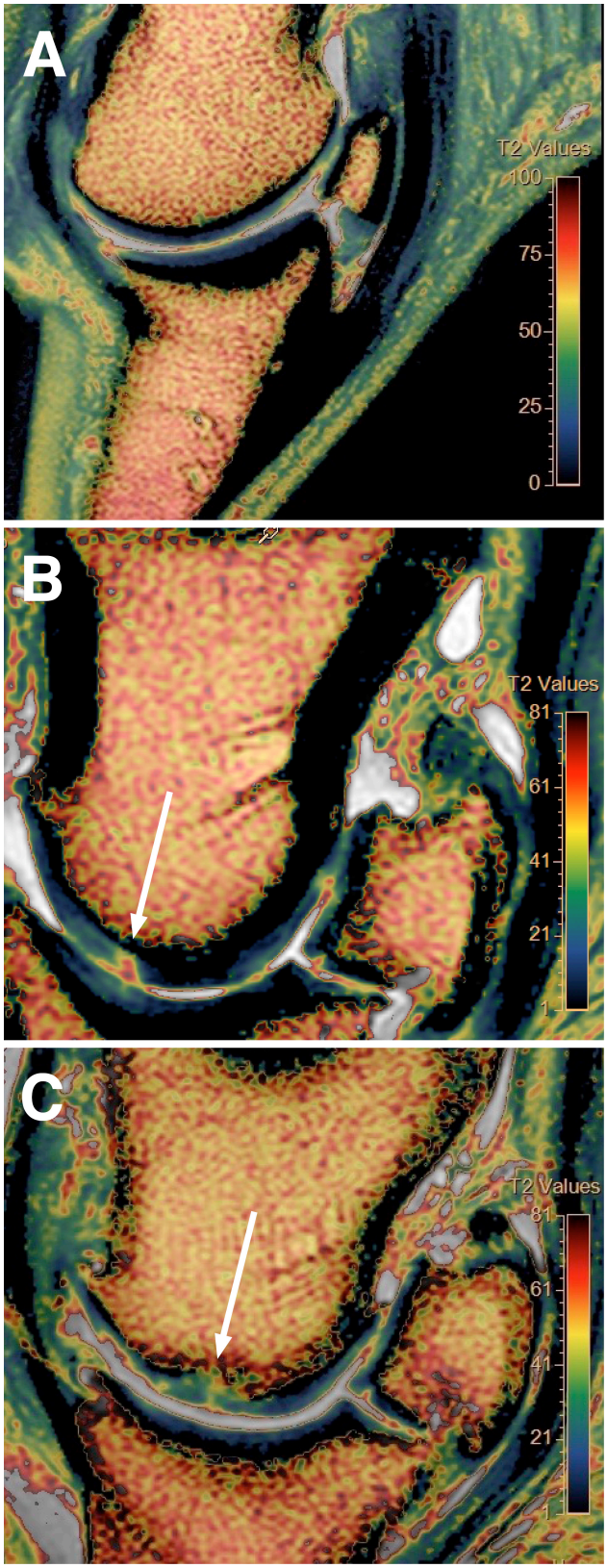

Figure 1: *Color coded T2 maps of a normal (A) and of osteoarthritic (B, C) distal interphalangeal joints (DIPJs). The bar on the right represents the T2 values using a continuous color transition of the T2 values from 0 - 100 ms. Black relates to a T2 value of 1 ms and dark red represents a T2 value of 100 ms. A: Normal articular cartilage has a laminar appearance on T2 maps. The T2 values of normal articular cartilage are higher in the*

superficial cartilage layers zones (red, yellow pixels) and decrease in the deeper cartilage layers (blue pixels). B: There is evidence of red and yellow pixels within the normal blue cartilage indicative of higher T2 values and a partial-thickness cartilage erosion at the center of the distal middle phalanx cartilage (white arrow). C: There is evidence of green and yellow pixels through the whole normal blue cartilage. The demarcation of the subchondral bone (black) is also destroyed indicative of a full-thickness cartilage erosion and collapse of the subchondral bone at the center of the distal middle phalanx cartilage (white arrow).

A summary of the T2 relaxation times showing median (ranges) of the independent factors analysed in the generalized linear mixed model is shown in Table 2.

Independent parameters	**T2 relaxation time (ms)**	
	Median (range)	*95% CI*
Normal cartilage	32.0 (22-47)	31.9-34.2
Mild to mod. cartilage disease	32.0 (19-62)	32.4-34.8
Severe cartilage disease	35.5 (22-47)	32.4-37.2
Dorsal cartilage zone	36.0 (22-62)	35.5-38.5
Middle cartilage zone	30.0 (19-52)	29.7-31.6
Palmar cartilage zone	34.0 (21-55)	33.0-36.5
Condyles	34.0 (19-62)	33.6-35.6
Intercondylar groove	29.0 (21-54)	29.5-32.3
Distal phalanx	35.0 (21-62)	31.3-34.5
Middle phalanx	30.0 (19-54)	31.4-34.6

Table 2: *Median (range) and 95% confidence intervals (CI) of T2 relaxation times of the independent parameters included in the generalized linear mixed model. Abbreviation: mod. = moderate.*

There was an excellent level of interobserver agreement for the MRI T2 relaxation time measurements (ICC = 0.9).

There was a topographical variation of the T2 relaxation times within the DIPJ. In the generalized linear mixed model the cartilage situated dorsally (36[22-62]) had a significantly higher T2 value (ms) compared to the cartilage situated palmarly (34[21-55]) ($P = 0.005$). The cartilage in the joint center had the lowest T2 value (30[19-52]) ($P < 0.001$). Cartilage on the condyle had a significantly higher T2 value (34[19-62]) than cartilage in the condylar groove

(29 [21-54]) (P < 0.001). Whether cartilage was situated on the articular surface of the proximal DP or the distal MP (P > 0.2), or which the cartilage health status was (P > 0.2), did not significantly affect the T2 values in the generalized linear mixed model. Both independent factors were omitted from the final model due to P > 0.2.

In terms of the collagen type II structure the T2 values did not correlate with the pirosirius red scores (r_s: 0.032, P = 0.547) or the immunohistochemical scores (r_s: 0.103, P = 0.056).

Histological and immunohistochemical analyses

There was an optimal to excellent level of interobserver agreement of the histological scoring (Mankin score ICC = 0.98, picrosirius red score ICC = 0.81, immunohistochemistry score ICC = 0.97). Representative histological images (Safranin-O-Fast green, collagen type II immunohistochemistry and picrosirius red) describing the typically seen cartilage lesions are provided in Figure 2.

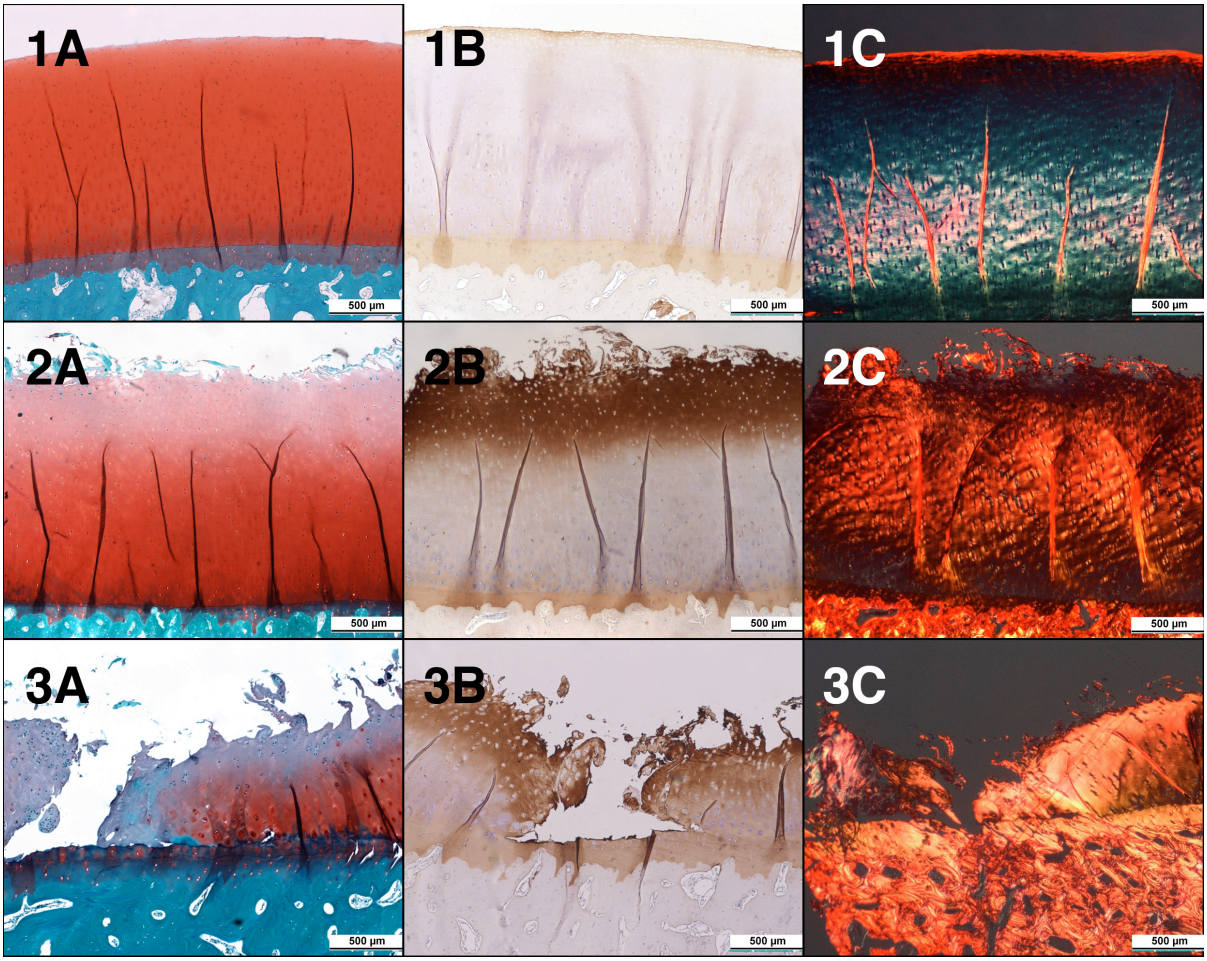

Figure 2: *Representative Safranin-O-Fast green histological (1-3A, also shown in chapter II, Fig. 3D) and collagen type II immunohistochemical (1-3B, also shown in chapter II, Fig. 3H) and picrosirius red (1-3C) histological sections of specimens with different lesion severities. 1A: In normal hyaline cartilage there was a homogenous stain uptake throughout the extracellular matrix with a smooth cartilage surface and a regular subchondral bone. Immunohistochemically there was minimal immunestaining of the superficial cartilage zone (1B). Immunestaining increased in specimens with evidence of OA corresponding to loss of staining in Safranin-O-Fast green sections. 1C: When cartilage was normal there was a maximal degree of bifringence on the intact cartilage surface. Dense packed collagen type II fibers of the articular cartilage surface polarized in an orange color. 2A: Marked fibrillations of the cartilage surface with loss of staining of the superficial hyaline cartilage zone and evidence of chondrocyte cluster formation. When fibrillation (2B) or full thickness erosions (3B) were observed there was diffuse immunestaining of the superficial cartilage matrix at the lesion and with increasing OA severity the depth of staining of the extracellular matrix increased. 2C: The cartilage surface with evidence of fibrillations showing loss of birefringence appears black. 3A: Full depth erosion of the hyaline cartilage with focal loss of staining in all the hyaline cartilage and marked chondrocyte cluster formation. Cracks in the calcified cartilage are present and there is a decreased amount and size of bone lacunae underneath the hyaline cartilage. Clefts and fissures are present with loss of staining of all the hyaline cartilage and possible calcification, with multifocal decrease in chondrocyte numbers and chondrocyte cluster formation. 3C: Sample*

with full-thickness erosion and fibrillation of the superficial zone and a fissure. The surface shows a black color because of the loss of birefringence. Other regions shows a yellow stain.

Biochemical analysis

In normal articular cartilage the overall GAG concentration was 60.0 µg/mg (21.0-104.2) and the water content was 71.0 % (59.2-83.0). When cartilage had evidence of mild to moderate OA the GAG concentration was 49.7 µg/mg and the water content was 73.0% (47.9-82.0). In articular cartilage with a severe OA the GAG concentration was 30.4 µg/mg (15.0-73.2) and the water content was 76.5% (64.0-83.1). The cartilage water content was significantly negatively correlated with the mean T2 values (r_s: - 0.15, P = 0.006), positively correlated with the mean Mankin score (r_s: 0.34, P < 0.001) and the mean picrosirius red score (r_s: 0.44, P = 0.008), however did not correlate with the mean immunohistochemical score (r_s: 0.09, P = 0.077). The cartilage GAG concentration was positively correlated with the mean Mankin score (r_s: 0.39, P < 0.001), the mean picrosirius red score (r_s: 0.21, P < 0.001), the mean immunohistochemistry score (r_s: 0.17, P = 0.002) and negatively correlated with the water content (r_s: -0.77, P < 0.001). However the cartilage GAG concentration was not correlated with the mean T2 values (r_s: - 0.05, P = 0.36).

6.3.5 *Discussion*

The objective of this DIPJ cadaver study was to establish the T2 mapping technique in DIPJ hyaline cartilage, to investigate whether T2 mapping can identify different degrees of naturally occurred OA and to correlate cartilage relaxation times with cartilage water, GAG content and collagen type II structure described on picrosirirus red sections and collagen type II immunohistochemistry. It was shown that the T2 mapping technique is feasible, that cartilage health did not significantly affect the T2 values and that the T2 values of normal and diseased DIPJs correlated with the cartilages water content, however not the with GAG concentration of the collagen type II structure.

T2 mapping of cadaver DIPJ cartilage was established for the first time in horses.
We had expected that T2 relaxation times would be significantly influenced by the state of cartilage health. Against our hypothesis this was not the case in the generalized linear mixed model. Thus we need to assume that T2 mapping was not sensitive enough to depict the

differing degrees of OA in our cadaver DIPJs. It is unclear why this happened. Possibly the histological gradation gap between the normal cartilage and the diseased cartilage was not extreme enough. Other explanations may be sample size and sample distribution: we had 40 normal cartilage samples, 68 mild to moderately diseased cartilage samples and 14 severely diseased cartilage samples. So there were maybe too few severely diseased samples in comparison to the other two cartilage health groups. Also that fact that cadavers were used needs to be kept in mind, despite there having been investigations showing that dGEMRIC T1 and T2 relaxation times were similar in fresh, chilled and frozen cadaver limbs [a]. The transverse relaxation time T2 is sensitive to slow-moving protons and is a function of the water content, the collagen content and orientation of the highly anisotropic ordered collagen fibrils in the extracellular matrix. [1] (Also supported by the fact that water content negatively correlated with T2 values in this study). The water content and motion may be different in fresh cadaver cartilage compared to cartilage of live horses. Limb temperature may have also influenced T2 values. Limbs were cooled at 4°C over night and scanned within 24 hours at room temperature, the exact limb temperature at the limb of scanning was not determined, so maybe temperature differences influenced the T2- values.

There were significant site-dependent differences in T2 relaxation times noted within the DIPJ. T2 relaxation times were longer in the dorsal zone compared to the palmar zone of the joint and lowest in the central zone of the joint. T2 relaxation times were longer in the condyles compared to the intercondylar grooves. The topographical variation of MRI parameters is well known in the human knee. [23] This variation is likely a reflection of the articular cartilages response to physiological loading and the relationship between the biomechanical and biochemical constitution of the tissue, resulting in different relaxation times. The topographical differences shown here are important and should be taken into account when interpreting MRIs of the equine DIPJ cartilage.

In human articular cartilage the sensitivity of T2 values to the collagen architecture has been confirmed by comparison with polarized microscopy. [36,37] The scoring system used to describe the structural grade in the picrosirius red sections has previously been used in equine arthritic fetlock joint cartilage [32] to successfully identify differences between healthy and OA cartilage. The authors cannot find any convincing explanation why the T2 values did

not correlate with the picrosirius red scores. Neither do we have any explanation why there was no correlation with the immunohistochemical scores. It may be possible that the scoring systems are too crude in comparison to the more sensitive T2 values.

Collagen type II fibers were assessed qualitatively with a polarizing microscope. Polarization color depends on the thickness of the fibers. Studies have shown that thin fibers appear yellow to green, while thicker fibers polarize in a longer wavelength, showing an orange to red appearance. However not only fiber thickness but also fiber organization and package plays an important role. Dense packed and well-aligned collagen fibers also polarize in a longer wavelength (orange to red). Collagen type II fibers of the superficial zones are highly ordered and polarized in an orange color. In areas with integrity loss the fibers have a dark appearance because non-ordered collagen type II fibers do not behave birefringent. Healthy cartilage sections showed a relative homogenous staining while staining became more irregular in secions with higher grades of OA. Sections with OA only had loss of birefringence in the areas of the lesion, while the other zones of the secion, which had a regular surface polarized in an orange color. An advantage of this method is, that also the structure of cartilage can be examined. Beside the polarization of the collagen fibers, fibrillation, fissures and erosions are also visible, providing additional information about cartilage health. Despite noting the differences in bifringence of the collagen fibers in our specimens, there was a tendency that the sections were predominated by the picrosirius red stain. This is probably attributed to the staining protocol used or more likely to a technical error, because the protocol has been used previously [32] and has not caused these types of artefacts.

In our study the surface of a healthy articular cartilage always had a light brown staining on immunohistochemical sections. This could be the consequence of the normal wear and tear in the articular cartilage metabolism. One would expect a homogenous staining throughout normal cartilage. Possibly the antibody could penetrate more when cartilage was degraded compared to normal cartilage leading to the inhomogenous staining. Because the cartilage surface was smooth and constant and showed no signs of early stages of OA like fibrillation or fissures these sections were considered normal despite the light brown staining at the surface. In this study the amount of staining increased with a higher

content of cleavage products and this increased with the increasing severity of OA in the cartilage specimens. This presumption was confirmed by the fact that the immunohistochemistry score significantly correlated with the mean overall Mankin score. An advantage of using immunohistochemistry to describe collagen type II is that other signs of articular cartilage pathologies like fibrillation, fissures, and erosions are visible. A disadvantage of this method is, that there is no exact quantification of the collagen type II content, and we have no infomation about the number of crosslinks between the collagen type II fibers.

This study had a few unavoidable limitations. Despite using a template to match the MRI ROIs with the histological specimens obtained, small deviations may have occurred. A future study scanning the actual osteochondral cores and then histologically processing them is planed to overcome this limitation. In this study the authors however chose to scan the complete DIPJ to more closely imitate the clinical scenario. The cadaver DIPJs were from horses with varying ages. Thus we are likely to have a combination of pathologies originating from over load injuries as well as age related OA. According to various studies, regional variations of cartilage T2 values are also affected by age, because ageing affects the collagen matrix changes and reorganization. [38] The effect of age on T2 relaxation times was not taken into the equation in this study, however should be considered when evaluating further hyaline cartilage using T2-mapping. We did not consider that T2 values have shown a spatial variation within the actual joint cartilage. In the human knee shorter T2 values were found in the deep cartilage layer compared to the superficial ones. [15] This finding may also be present in equine cartilage and should be kept in mind and may be subject to further cartilage segmentation studies.

T2 mapping is a convenient sequence to be used in equine MR because there is no need to use a contrast agent and the image acquisition is fast. This may be advantageous when horses are under general anaesthesia for the MR image acquisition.

The current data indicate that there is a topical variation of T2 values in the equine DIPJ. Where higher T2 values can be expected dorsally in the joint and low T2 values can be found in the joint center. T2 values negatively correlated with the cartilage water content,

however not with the collagen structure or the GAG concentration. However against our hypothesis T2 mapping was not sensitive enough to detect varying degrees of naturally occurring OA in the DIPJ. A follow up study with more samples of severely diseased cartilage should be performed to test the sensitivity of the imaging sequence in equine hyaline cartilage before the technique can be reliably used in an equine research setting or in the future in a clinical setting.

Footnotes

a. Carstens, A., Delayed gadolinium enhanced magnetic resonance imaging and T2 mapping of cartilage of the cadaver distal metacarpus 3/metatarsus 3 of the normal Thoroughbred horse. PhD thesis, 2013, University of Pretoria, South Africa.

b. Phillips Health Care Ingenia, Phillips AG, Zuerich, Switzerland.

c. Arthrex Inc, Naples, FL, USA

d. Relaxation Maps Tool V 2.1.2., Koninklijke Philips Electronics N. V. 2013, Phillips AG, Zuerich Switzerland.

e. Abcam Inc, Cambridge, MA, USA

f. Thermo Scientifics, Illinois, USA

g. Stahl, A. Validierung neuer, knorpelsensitiver Sequenzen am Schafmodell im 3T-Hochfeld-MRT zur Erkennung von Frühveränderungen verursacht durch das Femoroacetabuläre Impingement. Doctoral thesis, 2009, University of Zürich

h. Leica Microsystems (Schweiz) AG, Glattbrugg, Switzerland

i. IBM SPSS, Armonk, NY, USA

i. R Core Team (2016). R: A language and environment for statistical computing. R Foundation for Statistical Computing, Vienna, Austria. URL https://www.R-project.org/.) using the MASS, car and lme4 packages.

6.3.6 *References*

1. Choi JA, Gold GE. MR Imaging of Articular Cartilage Physiology. *Magnetic Resonance Imaging Clinics of North America* 2011;19:249-282.

2. Taylor C, Carballido-Gamio J, Majumdar S, et al. Comparison of quantitative imaging of cartilage for osteoarthritis: T2, T1 rho, dGEMRIC and contrast-enhanced computed tomography. *Magnetic Resonance Imaging* 2009;27:779-784.

3. Frisbie DD. Synovial joint biology and pathobiology In: J. Auer JS, ed. *Equine Surgery*. 4 ed. St. Louis, Missouri: Elsevier, Saunders, 2012;1096-1114.

4. Kuettner KE. Biochemistry of articular cartilage in health and disease. *Clinics of Biochemistry* 1992;25:155-163.

5. Goodrich LR, Nixon AJ. Medical treatment of osteoarthritis in the horse - A review. *Veterinary Journal* 2006;171:51-69.

6. Mosher TJ, Dardzinski BJ. Cartilage MRI T2 relaxation time mapping: Overview and applications. *Seminars in Musculoskeletal Radiology* 2004;8:355-368.

7. Mlynarik V, Trattnig S, Huber M, et al. The role of relaxation times in monitoring proteoglycan depletion in articular cartilage. *Journal of Magnetic Resonance Imaging* 1999;10:497-502.

8. Nissi MJ, Toyras J, Laasanen MS, et al. Proteoglycan and collagen sensitive MRI evaluation of normal and degenerated articular cartilage. *Journal of Orthopaedic Research* 2004;22:557-564.

9. Watrin-Pinzano A, Ruaud JP, Cheli Y, et al. Evaluation of cartilage repair tissue after biomaterial implantation in rat patella by using T2 mapping. *Magnetic Resonance Materials in Physics Biology and Medicine* 2004;17:219-228.

10. Watrin-Pinzano A, Ruaud JP, Cheli Y, et al. T2 mapping: an efficient MR quantitative technique to evaluate spontaneous cartilage repair in rat patella. *Osteoarthritis and Cartilage* 2004;12:191-200.

11. Spandonis Y, Heese FP, Hall LD. High resolution MRI relaxation measurements of water in the articular cartilage of the meniscectomized rat knee at 4.7 T. *Magnetic Resonance Imaging* 2004;22:943-951.

12. Gahunia HK, Babyn P, Lemaire C, et al. Osteoarthritis Staging - Comparison between magnetic-resonance-imaging, gross pathology and histopathology in the rhesus macaque. *Osteoarthritis and Cartilage* 1995;3:169-180.

13. Van Breuseghem I, Bosmans HT, Elst LV, et al. T2 mapping of human femorotibial cartilage with turbo mixed MR imaging at 1.5 T: feasibility. *Radiology* 2004;233:609-614.

14. Mosher TJ, Smith HE, Smith MB. In vivo spatial variation in cartilage MRI-T2-values of the knee. *Arthritis and Rheumatism* 2000;43:S220-S220.

15. Wirth W, Maschek S, F WR, et al. Layer-specific femorotibial cartilage T2 relaxation time in knees with and without early knee osteoarthritis: Data from the Osteoarthritis Initiative (OAI). *Scientific Reports* 2016;6:34202.

16. Dardzinski BJ, Laor T, Schmithorst VJ, et al. Mapping T2 relaxation time in the pediatric knee: Feasibility with a clinical 1.5-T MR imaging system. *Radiology* 2002;225:233-239.

17. Mosher TJ, Smith H, Dardzinski BJ, et al. MR Imaging and T2 mapping of femoral cartilage: In vivo determination of the magic angle efect. *American Journal of Roentgenology* 2001;177:665-669.

18. Watanabe A, Boesch C, Anderson SE, et al. Ability of dGEMRIC and T2 mapping to evaluate cartilage repair after microfracture: a goat study. *Osteoarthritis and Cartilage* 2009;17:1341-1349.

19. Nishii T, Tanaka H, Sugano N, et al. Evaluation of cartilage matrix disorders by T2 relaxation time in patients with hip dysplasia. *Osteoarthritis and Cartilage* 2008;16:227-233.

20. Welsch GH, Mamisch TC, Weber M, et al. High-resolution morphological and biochemical imaging of articular cartilage of the ankle joint at 3.0 T using a new dedicated phased array coil: in vivo reproducibility study. *Skeletal Radiology* 2008;37:519-526.

21. Lazovic-Stojkovic J, Mosher TJ, Smith HE, et al. Interphalangeal joint cartilage: High-spatial-resolution in vivo MR T2 mapping - A feasibility study. *Radiology* 2004;233:292-296.

22. Wirth W, Maschek S, Roemer FW, et al. Layer-specific femorotibial cartilage T2 relaxation time in knees with and without early knee osteoarthritis: Data from the Osteoarthritis Initiative (OAI). *Scientific Reports* 2016;6:34202.

23. Kurkijarvi JE, Nissi MJ, Kiviranta I, et al. Delayed gadolinium-enhanced MRI of cartilage (dGEMRIC) and T-2 characteristics of human knee articular cartilage: topographical variation and relationships to mechanical properties. *Magnetic Resonance in Medicine* 2004;52:41-46.

24. Wirth W, Maschek S, Eckstein F. Sex- and age-dependence of region- and layer-specific knee cartilage composition (spin-spin-relaxation time) in healthy reference subjects. *Annals of Anatomy* 2017;210:1-8.

25. Carstens A, Kirberger RM, Dahlberg LE, et al. Validation of delayed gadolinium-enhanced magnetic resonance imaging of cartilage and T2 mapping for quantifying distal metacarpus/metatarsus cartilage thickness in Thoroughbred racehorses. *Veterinary Radiology & Ultrasound* 2013;54:139-148.

26. White LM, Sussman MS, Hurtig M, et al. Cartilage T2 assessment: Differentiation of normal hyaline cartilage and reparative tissue after arthroscopic cartilage repair in equine subjects. *Radiology* 2006;241:407-414.

27. Fortier LA, Potter HG, Rickey EJ, et al. Concentrated bone marrow aspirate improves full-thickness cartilage repair compared with microfracture in the equine model. *Journal of Bone and Joint Surgery-American Voulme* 2010;92:1927-1937.

28. Menendez MI, Clark DJ, Carlton M, et al. Direct delayed human adenoviral BMP-2 or BMP-6 gene therapy for bone and cartilage regeneration in a pony osteochondral model. *Osteoarthritis and Cartilage* 2011;19:1066-1075.

29. Outerbridge RE. The etiology of chondromalacia of the patella. *Journal of Bone and Joint Surgery-British Volume* 1961;43:613-613.

30. Lacourt M, Gao C, Li A, et al. Relationship between cartilage and subchondral bone lesions in repetitive impact trauma-induced equine osteoarthritis. *Osteoarthritis Cartilage* 2012;20:572-583.

31. Mankin HJ, Dorfman H, Lippiell.L, et al. Biochemical and metabolic abnormalities in articular cartilage from osteoarthritic human hips .2. Correlation of morphology with biochemical and metabolic Data. *Journal of Bone and Joint Surgery-American Volume* 1971;A 53:523-37.

32. Vinardell T, Dejica V, Poole AR, et al. Evidence to suggest that cathepsin K degrades articular cartilage in naturally occurring equine osteoarthritis. *Osteoarthritis and Cartilage* 2009;17:375-383.

33. Hughes LC, Archer CW, Gwynn I. The ultrastructure of mouse articular cartilage: collagen orientation and implications for tissue functionality. A polarised light and scanning electron microscope study and review. *European Cells and Materials* 2005;9:68-84.

34. Brama PAJ, Tekoppele JM, Bank RA, et al. Topographical mapping of biochemical properties of articular cartilage in the equine fetlock joint. *Equine Veterinary Journal* 2000;32:19-26.

35. Farndale RW, Buttle DJ, Barrett AJ. Improved quantitation and discrimination of sulfated glycosaminoglycans by use of Dimethylmethylene Blue. *Biochimica Et Biophysica Acta* 1986;883:173-177.

36. Nieminen MT, Rieppo J, Toyras J, et al. T2 relaxation reveals spatial collagen architecture in articular cartilage: a comparative quantitative MRI and polarized light microscopic study. *Magnetic Resonance in Medicine* 2001;46:487-493.

37. Grunder W, Wagner M, Werner A. MR-microscopic visualization of anisotropic internal cartilage structures using the magic angle technique. *Magnetic Resonance in Medicine* 1998;39:376-382.

38. Mosher TJ, Liu Y, Yang QX, et al. Age dependency of cartilage magnetic resonance imaging T2 relaxation times in asymptomatic women. *Arthritis and Rheumatism*2004;50:2820-2828.

7 Overall discussion

As shown in the present thesis, both dGEMRIC and T2 mapping may be performed in the DIPJ of the horse cadaver limb.

An initial study was performed to in fact determine whether the cartilage, which was visualised on dGEMRIC and T2 maps was representative of the true DIPJ cartilage. It was determined whether the cartilage thickness measured on dGEMRIC images, T2 maps and histologic sections were similar. It was shown that this was to be so, validating the mapping techniques as truly representing the distal MP and proximal DP cartilage. In a study comparing the distal thickness established histomorphometrically and on MR images (dGEMRIC and T2 maps) cartilage thickness was only similar in locations where the cartilage was not in close approximation to opposing adjacent cartilage in the third metacarpal/metatarsal bone. [54] This was not noted as an issue in the DIPJ. Better image resolution by using a three tesla magnet as well as the thicker cartilage of the DIPJ (about twice the thickness) compared to the metacarpo/metatarsophalangeal joint are possible reasons.

Topographical variations in cartilage thickness were found. Thinner areas of cartilage in the DIPJ were found on the proximal DP and in the dorsal joint area. Topical variations of cartilage thickness in the DIPJ have been shown previously and correspond to the results found in this study. [10] These physiologic changes in cartilage thickness should not be confused with partial thickness erosions and should be kept in mind when evaluating DIPJ cartilage on MRI. The changes in cartilage thickness within the joint are likely attributed to the different pressures the individual areas have to bear during loading and their adaptation to these loads.

Once true cartilage visibility was established the dGEMRIC and T2 mapping techniques were investigated. First it was determined that the T1 relaxation time decreased significantly following intraarticular gadolinium administration. The T1 values of normal cadaver cartilage ranged from 473 -732 ms and $T1_{Gd}$ values ranged from 182-330 ms.

Second it was investigated whether varying degrees of naturally occured OA had a significant effect on the dGEMRIC and T2 values. For the dGEMRIC technique this could be proven, however for the T2 technique this was not the case. The dGEMRIC data shown in Chapter II nicely shows that with advancing degree of cartilage degeneration, proteoglycans were lost and contrast media penetrated into the hyaline cartilage leading to shorter $T1_{Gd}$ values in specimens with evidence of mild to severe OA.

Cartilage OA had no significant effect on the T2 values. We can only speculate why T2 mapping was not sensitive enough to depict OA in our cadaver limbs. The median T2 values obtained for normal cartilage (32 ms) mildly to moderately diseased cartilage (32 ms) and severely diseased cartilage (35 ms) were similar to the T2 values obtained in human knees ranging from about 35 to 45 ms for the deep and superficial cartilage layers, respectively. T2 mapping has also previously been found to be less sensitive in detecting early cartilage degeneration, in comparison to other cartilage MR imaging methods. [60] Nevertheless T2 mapping is sensitive to changes in the collagen matrix and changes in water content and water motion. [60] Thus an effect of cartilage health on the T2 values was expected. Possibly the degrees of OA in the cartilage health group were too similar and there was not a large enough gradation in disease severity between the cartilage health groups to account for a difference in T2 values between them.

As biochemical parameters of the cartilage we selected water, GAG and collagen type II because they are the main components responsible for changes in the T1 or T2 relaxation time in cases of cartilage degeneration. Collagen type II was not absolutely quantified using an ELISA. We opted to assess the collagen type II content via immunohistochemistry to have a semi quantification and an idea of the spatial distribution of the collagen type II fibers. We opted to assess the collagen architecture using polarized microscopy and picrosirius red staining. Generally collagen type II is produced to repair cartilage lesions, when these lesions cannot be repaired the collagen type II is split and into a COL 2 3/4C short fragment and into a COL 2 3/4 M fragment. These degradation fragments can also be identified immunohistochemically, however this was not performed.

Despite being very sensitive the dGEMRIC image acquisition is time consuming and needs the administration of a contrast agent, which is a major disadvantage in equine MRI. Horses are scanned under general anaesthesia and repositioning the horse after intraarticular contrast injection in the MRI scanner is a laborious and time consuming. A standing high field magnet would be ideal to solve these problems in the future, however the low image resolution of the current low field standing technologies preclude performing dGEMRIC studies in the standing horse at the moment. On the other hand, if proven sensitive enough, T2 mapping would be a convenient sequence to use in live horses because scanning times are fast and there is no need for contrast application. However also this technique is not suitable for the low resolution of the standing low field units of today.

The common limitation for all parts of these studies was the relatively low number of cadaver limbs used, which relates to the decision making of cost effectiveness between tissue sampling and power of experiments. I am quite confident that the number of tissue ROI (n = 122) studied in this investigation gives sufficient evidence to say that both mapping techniques have been reliably established in the equine DIPJ. A further common limitation ist the fact that despite using a template small deviations may have occurred when matching ROIs measured on MRI and osteochondral samples obtained.

This work lays a foundation for future studies investigating cartilage specific MRI sequences. Today these sequences are probably still mostly employed in a research setting however ultimately infomation of the cartilage health state will be invaluable in the early diagnosis and also the management of OA in the DIPJ, in clinical patients providing guidance in terms of the appropriate treatment and monitoring disease state and repsonse to treatment.

8 Outlook and perspectives

The next logical step investigating the dGEMRIC technique would be to confirm the technique in the live horse, and once reference values for the live horse have been established to compare them to the values found in cadaver limbs. Future research should also address the administration route of Gd-DTPA^{2-}. Using an intravenous route in alive horses would be much easier than using the intraarticular approach.

A preliminary project has been performed with the goal to evaluate dGEMRIC in clinical patients with intravenous contrast agent injection and to compare the T1 values with the previously obtained T1 values following intraarticular contrast administration (data from chapter II). Only data of five clinical patients were available. Using the normal scanning protocol used in our clinic we could not achieve a significant reduction (P = 0.392) of the T1 relaxation time following contrast media administration. The mean T1 value was 717.1 ± 28.4 ms and the mean $T1_{Gd}$ value 678.4 ± 34.5 ms following intravenous administration of 40ml of contrast media. We have to assume that not enough contrast media was taken-up by the cartilage, or by the time the scan was performed (after a median of 50 minutes) the contrast media was already washed out of the cartilage. For the use of intravenous contrast media the ideal time point of scanning first needs to be determined. In human medicine patients typically exercise lightly for 15 minutes following contrast administration and images are obtained 45 to 90 minutes after intravenous contrast administration. [109] Horses need to be under general anaesthesia to generate dGEMRIC images. Hence the contrast agent is administered intravenously whilst the horse is under general anaesthesia, and the joint cannot be flexed due to the positioning in the gantry nor can the horse be exercised. General anaesthesia may also influences the contrast agent uptake in the cartilage, because it is may change the blood circulation of the articular structures. Maybe if there is peripheral vasoconstriction during the anaesthesia, the concentration of contrast agent near the joint and the diffusion into the cartilage may be lower than in an awake or for sure lower than in an exercising horse. A specific scanning protocol for dGEMRIC images using intravenous contrast administration needs to be developed for the horse. We cannot extrapolate the data from humans. The effect of exercise pre or post contrast administration also needs to be investigated and kept in mind when developping an intravenous scanning protocol for dGEMRIC in live horses.

There was also a significant difference in the T1 values comparing cadaver and live horse cartilage relaxation times. Five cases are not enough to draw any definitive conclusions, but we can assume that the metabolism of the cartilage, despite being slow, is different in cadaver specimens compared to live horses having an effect on the T1 relaxation times.

In terms of T2 mapping a follow up cadaver study should be performed with more extreme grades of OA to establish whether T2 maps can be used to identify more severe OA than analysed in the present study. Scanning actual osteochondral biopsies before histologically processing them instead of measuring ROIs within a whole joint and obtaining biopsies at the ROIs following a template may definitely prove or disprove which degree of OA in equine cadaver cartilage T2-maps can detect.

Different T2 values for deep and superficial cartilage layers have been shown in the human knee. [70,94,110] Superficial cartilage was found to have significantly longer T2 values compared to the deeper cartilage layer. [70,63] In our study (chapter III) "bulk" T2 average values throughout the full depth of normal and diseased articular cartilage were established. Future studies should aim at differentiating superficial and deep cartilage layers. We have attempted to do this in a preliminary study of 6 of the normal DIPJs, where we could show that the T2 value of the superficial cartilage was twice as long (66.9 ± 24.6 ms (47.9-104.4)) than the T2 value of the deep cartilage (35.7 ± 7.6 ms (28.0-45.9)) following manual segmentation of the normal DIPJ. Further research needs to attempt to differentiate between the two cartilage layers in diseased limbs. We know from humans that the superficial cartilage zone is more sensitive to the presence of cartilage lesions than the deep cartilage layer, and thus potentially more sensitive in detecting compositional differences of the cartilage in the early stages of knee OA.

In human knee cartilage T1 values also show spatial variations (low values at the surface and higher values in deep tissue). [94] The same stratification can be expected in equine cartilage for the T1 values and should be subject of future studies.

Finally dGEMRIC and T2 mapping needs to be performed on horse DIPJs with differing degrees of OA and a known degree of lameness in order to relate joint degeneration noted on MR images to the clinical symptoms.

Footnotes

a. Carstens A. Delayed gadolinium enhanced magnetic resonance imaging and T2 mapping of the cadaver distal metacarpus3/metatarsus3 of the normal Thoroughbred horse. *Faculty of Veterinary Science*. Pretoria: University of Pretoria, 2013.

9 References

1. Clegg P, Booth T. Drugs used to treat osteoarthritis in the horse. *In Practice* 2000;22:594-603.

2. Oke SL, McIlwraith WC. Review of the economic impact of osteoarthritis and oral joint-health supplements in horses. *Proc of* the *American Association of Equine Practitioners* 2010;56:12-16.

3. de Grauw JC. Molecular monitoring of equine joint homeostasis. *Veterinary Quarterly* 2011;31:77-86.

4. Bailey CJ, Reid SWJ, Hodgson DR, et al. Flat, hurdle and steeple racing: risk factors for musculoskeletal injury. *Equine Veterinary Journal* 1998;30:498-503.

5. Wilsher S, Allen WR, Wood JLN. Factors associated with failure of Thoroughbred horses to train and race. *Pferdeheilkunde* 2006;22:503-504.

6. Rossdale PD, Hopes R, Digby NJW. Epidemiological-study of wastage among racehorses 1982 and 1983. *Veterinary Record* 1985;116:66-69.

7. Dyson SJ. Lameness due to pain associated with the distal interphalangeal joint - 45 cases. *Equine Veterinary Journal* 1991;23:128-135.

8. Dippel M, Ruczizka U, Valentin S, et al. Influence of increased intraarticular pressure on the angular displacement of the isolated equine distal interphalangeal joint. *Journal of Equine Veterinary Science* 2016;38:54-63.

9. Olive J, Lambert N, Bubeck KA, et al. Comparison between palpation and ultrasonography for evaluation of experimentally induced effusion in the distal interphalangeal joint of horses. *American Journal of Veterinary Research* 2014;75:34-40.

10. Olive J. Distal interphalangeal articular cartilage assessment using low-field magnetic resonance imaging. *Veterinary Radiology & Ultrasound* 2010;51:259-266.

11. McGill SL, Gutierrez-Nibeyro SD, Schaeffer DJ, et al. Saline arthrography of the distal interphalangeal joint for low-field magnetic resonance imaging of the equine podotrochlear bursa: Feasibility study. *Veterinary Radiology & Ultrasound* 2015;56:417-424.

12. Dyson SJ. The distal phalanx and the distal interphalangeal joint In: Ross M, Dyson, S.J., , ed. *Diagnosis and management of lameness in the horse*. 2nd ed. Pennsylvania: Elsevier Health Sciences, 2010;349-355.

13. Viitanen MJ, Wilson AM, McGuigan HP, et al. Effect of foot balance on the intra-articular pressure in the distal interphalangeal joint in vitro. *Equine Veterinary Journal* 2003;35:184-189.

14. Frisbie DD. Synovial joint biology and pathobiology In: J. Auer JS, ed. *Equine Surgery*. 4 ed. St. Louis, Missouri: Elsevier, Saunders, 2012;1096-1114.

15. Poole AR, Kojima T, Yasuda T, et al. Composition and structure of articular c artilage: a template for tissue repair. *Clinical Orthopedic Related Research* 2001:S26-33.

16. Clyne M. Pathogenesis of degenerative joint disease. *Equine Veterinary Journal* 1987;19:15-18.

17. Martel-Pelletier J, Boileau C, Pelletier J-P, et al. Cartilage in normal and osteoarthritis conditions. *Best Practice & Research Clinical Rheumatology* 2008;22:351-384.

18. Kuettner KE. Biochemistry of articular cartilage in health and disease. *Clinical Biochemistry* 1992;25:155-163.

19. McIlwraith WC. Erkrankungen der Gelenke, Sehnen, Bänder sowie ihrer Hilfseinrichtungen. In: Stashak TS, ed. *Adams' Lahmheit bei Pferden. 4th ed.* Verlag M. & H. Schaper, 2008;339-485.

20. Frisbie DD. Synovial joint biology and pathobiology In: J. Auer JS, ed. *Equine Surgery*. 4 ed. St. Louis, Missouri: Elsevier, Saunders, 2012;1096-1114.

21. Goodrich LR, Nixon AJ. Medical treatment of osteoarthritis in the horse - A review. *Veterinary Journal* 2006;171:51-69.

22. Kawcak CE, McIlwraith CW, Norrdin RW, et al. The role of subchondral bone in joint disease: a review. *Equine Veterinary Journal* 2001;33:120-126.

23. Kidd J, Fuller C, Barr A. Osteoarthritis in the horse. *Equine Veterinary Education* 2001;13:160-168.

24. Buckwalter J, Mankin H. Articular cartilage: degeneration and osteoarthritis, repair, regeneration, and transplantation. *Instructional course lectures* 1997;47:487-504.

25. Arokoski J, Jurvelin J, Väätäinen U, et al. Normal and pathological adaptations of articular cartilage to joint loading. *Scandinavian Journal of Medicine & Science in Sports* 2000;10:186-198.

26. Kawcak CE, Frisbie DD, Werpy NM, et al. Effects of exercise vs experimental osteoarthritis on imaging outcomes. *Osteoarthritis and Cartilage* 2008;16:1519-1525.

27. McIlwraith CW, Frisbie DD, Kawcak CE, et al. The OARSI histopathology initiative - recommendations for histological assessments of osteoarthritis in the horse. *Osteoarthritis and Cartilage* 2010;18:S93-S105.

28. van Harreveld PD, Lillich JD, Kawcak CE, et al. Effects of immobilization followed by remobilization on mineral density, histomorphometric features, and formation of the bones of the metacarpophalangeal joint in horses. *American Journal of Veterinary Research* 2002;63:276-281.

29. Neundorf RH, Lowerison MB, Cruz AM, et al. Determination of the prevalence and severity of metacarpophalangeal joint osteoarthritis in Thoroughbred racehorses via quantitative macroscopic evaluation. *American Journal of Veterinary Research* 2010;71:1284-1293.

30. Outerbridge RE. The etiology of chondromalacia patellae. 1961. *Clinical Orthopedic Related Research* 2001:5-8.

31. Cruz AM, Hurtig MB. Multiple pathways to osteoarthritis and articular fractures: is subchondral bone the culprit? *Veterinary Clinics of North America - Equine Pract* 2008;24:101-116.

32. Brommer H, van Weeren PR, Brama PA. New approach for quantitative assessment of articular cartilage degeneration in horses with osteoarthritis. *American Journal of Veterinary Research* 2003;64:83-87.

33. Bolam CJ, Hurtig MB, Cruz A, et al. Characterization of experimentally induced post-traumatic osteoarthritis in the medial femorotibial joint of horses. *American Journal of Veterinary Research* 2006;67:433-447.

34. Lacourt M, Gao C, Li A, et al. Relationship between cartilage and subchondral bone lesions in repetitive impact trauma-induced equine osteoarthritis. *Osteoarthritis and Cartilage* 2012;20:572-583.

35. Mankin HJ, Dorfman H, Lippiell.L, et al. Biochemical and metabolic abnormalities in articular cartilage from osteoarthritic human hips .2. Correlation of morphology with biochemical and metabolic data. *Journal of Bone and Joint Surgery-American Volume* 1971;A 53:523-37.

36. Butler J, Colles, C., Dyson, S., Kold, S., Poulos, P. Foot, Pastern and Fetlock. *Clinical radiology of the horse*. 3 ed. Oxford: John Wiley & Sons, 2012;253-293.

37. Sage AM, Turner TA. Ultrasonography of the soft tissue structures of the equine foot. *Equine Veterinary Education* 2002;14:221-224.

38. McIlwraight C, Nixon, A, Wright, I. Arthroscopic surgery of the distal and proximal interphalangeal joints In: McIlwraight C, Nixon, A, Wright, I, ed. *Diagnostic and surgical arthroscopy in the horse*. 4th ed. Philadelphia: Mosby Elsevier, 2015;316-343.

39. Dunn TC, Lu Y, Jin H, et al. T2 relaxation time of cartilage at MR imaging: Comparison with severity of knee osteoarthritis. *Radiology* 2004;232:592-598.

40. Broderick LS, Turner DA, Renfrew DL, et al. Severity of articular-cartilage abnormality in patients with osteoarthritis - Evaluation with fast spin-echo Mr Vs arthroscopy. *American Journal of Roentgenology* 1994;162:99-103.

41. Peterfy CG. Imaging of the disease process. *Current Opinion in Rheumatology* 2002;14:590-596.

42. Watrin-Pinzano A, Ruaud JP, Olivier P, et al. Effect of proteoglycan depletion on T2 mapping in rat patellar cartilage. *Radiology* 2005;234:162-170.

43. Berberat JE, Nissi MJ, Jurvelin JS, et al. Assessment of interstitial water content of articular cartilage with T-1 relaxation. *Magnetic Resonance Imaging* 2009;27:727-732.

44. Jacobs MA, Ibrahim TS, Ouwerkerk R. AAPM/RSNA physics tutorial for residents - MR imaging: Brief overview and emerging applications. *Radiographics* 2007;27:1213-U1265.

45. Porter EG, Werpy NM. New concepts in standing advanced diagnostic equine imaging. *Veterinary Clinics of North America-Equine Practice* 2014;30:239-268.

46. Rutt BK, Lee DH. The impact of field strength on image quality in MRI. *Journal of Magnetic Resonance Imaging* 1996;6:57-62.

47. Dyson S, Murray R, Schramme M, et al. Magnetic resonance imaging of the equine foot: 15 horses. *Equine Veterinary Journal* 2003;35:18-26.

48. Olive J, D'Anjou MA, Girard C, et al. Fat-suppressed spoiled gradient-recalled imaging of equine metacarpophalangeal articular cartilage. *Veterinary Radiology & Ultrasound* 2010;51:107-115.

49. Smith MA, Dyson SJ, Murray RC. Reliability of high- and low-field magnetic resonance imaging systems for detection of cartilage and bone lesions in the equine cadaver fetlock. *Equine Veterinary Journal* 2012;44:684-691.

50. Crema MD, Roemer FW, Guermazi A. Magnetic resonance imaging in knee osteoarthritis research: Semiquantitative and compositional assessment. *Magnetic Resonance Imaging Clinics of North America* 2011;19:295-321.

51. Raynauld JP, Martel-Pelletier J, Abram F, et al. Analysis of the precision and sensitivity to change of different approaches to assess cartilage loss by

quantitative MRI in a longitudinal multicentre clinical trial in patients with knee osteoarthritis. *Arthritis Research & Therapy* 2008;10.

52. Carstens A, Kirberger RM, Dahlberg LE, et al. Validation of delayed gadolinium-enhanced magnetic resonance imaging of cartilage and T2 mapping for quantifying distal metacarpus/metatarsus cartilage thickness in Thoroughbred racehorses. *Veterinary Radiology & Ultrasound* 2013;54:139-148.

53. Murray RC, Branch MV, Tranquille C, et al. Validation of magnetic resonance imaging for measurement of equine articular cartilage and subchondral bone thickness. *American Journal of Veterinary Research* 2005;66:1999-2005.

54. Eckstein F, Sittek H, Milz S, et al. The potential of magnetic resonance imaging (MRI) for quantifying articular cartilage thickness - A methodological study. *Clinical Biomechanics* 1995;10:434-440.

55. Pease A. Biochemical Evaluation of Equine Articular Cartilage Through Imaging. *Veterinary Clinics of North America-Equine Practice* 2012;28:637-646.

56. Link TM, Stahl R, Woertler K. Cartilage imaging: motivation, techniques, current and future significance. *European Radiology* 2007;17:1135-1146.

57. Yoshioka H, Stevens K, Genovese M, et al. Articular cartilage of knee: normal patterns at MR imaging that mimic disease in healthy subjects and patients with osteoarthritis. *Radiology* 2004;231:31-38.

58. Choi JA, Gold GE. MR Imaging of Articular Cartilage Physiology. *Magnetic Resonance Imaging Clinics of North America* 2011;19:249-282.

59. Taylor C, Carballido-Gamio J, Majumdar S, et al. Comparison of quantitative imaging of cartilage for osteoarthritis: T2, T1 rho, dGEMRIC and contrast-

enhanced computed tomography. *Magnetic Resonance Imaging* 2009;27:779-784.

60. Mosher TJ, Dardzinski BJ. Cartilage MRI T2 relaxation time mapping: overview and applications. *Seminars in Musculoskeletal Radiology* 2004;8:355-368.

61. Mlynarik V, Trattnig S, Huber M, et al. The role of relaxation times in monitoring proteoglycan depletion in articular cartilage. *Journal of Magnetic Resonance Imaging* 1999;10:497-502.

62. Nissi MJ, Toyras J, Laasanen MS, et al. Proteoglycan and collagen sensitive MRI evaluation of normal and degenerated articular cartilage. *Journal of Orthopaedic Research* 2004;22:557-564.

63. Watrin-Pinzano A, Ruaud JP, Cheli Y, et al. Evaluation of cartilage repair tissue after biomaterial implantation in rat patella by using T2 mapping. *Magnetic Resonance Materials in Physics Biology and Medicine* 2004;17:219-228.

64. Watrin-Pinzano A, Ruaud JP, Cheli Y, et al. T2 mapping: an efficient MR quantitative technique to evaluate spontaneous cartilage repair in rat patella. *Osteoarthritis and Cartilage* 2004;12:191-200.

65. Spandonis Y, Heese FP, Hall LD. High resolution MRI relaxation measurements of water in the articular cartilage of the meniscectomized rat knee at 4.7 T. *Magnetic Resonance Imaging* 2004;22:943-951.

66. Gahunia HK, Babyn P, Lemaire C, et al. Osteoarthritis staging - Comparison between magnetic-resonance-imaging, gross pathology and histopathology in the rhesus macaque. *Osteoarthritis and Cartilage* 1995;3:169-180.

67. Smith HE, Mosher TJ, Dardzinski BJ, et al. Spatial variation in cartilage T2 of the knee. *Journal of Magnetic Resonance Imaging* 2001;14:50-55.

68. Van Breuseghem I, Bosmans HT, Elst LV, et al. T2 mapping of human femorotibial cartilage with turbo mixed MR imaging at 1.5 T: feasibility. *Radiology* 2004;233:609-614.

69. Mosher TJ, Smith HE, Smith MB. In vivo spatial variation in cartilage MRI-T2-values of the knee. *Arthritis and Rheumatism* 2000;43:S220-S220.

70. Wirth W, Maschek S, F WR, et al. Layer-specific femorotibial cartilage T2 relaxation time in knees with and without early knee osteoarthritis: Data from the Osteoarthritis Initiative (OAI). *Scientific Reports* 2016;6:34202.

71. Dardzinski BJ, Laor T, Schmithorst VJ, et al. Mapping T2 relaxation time in the pediatric knee: Feasibility with a clinical 1.5-T MR imaging system. *Radiology* 2002;225:233-239.

72. Mosher TJ, Smith H, Dardzinski BJ, et al. MR Imaging and T2 mapping of femoral cartilage: In vivo determination of the magic angle effect. *American Journal of Roentgenology* 2001;177:665-669.

73. Watanabe A, Boesch C, Anderson SE, et al. Ability of dGEMRIC and T2 mapping to evaluate cartilage repair after microfracture: a goat study. *Osteoarthritis and Cartilage* 2009;17:1341-1349.

74. Nishii T, Tanaka H, Sugano N, et al. Evaluation of cartilage matrix disorders by T2 relaxation time in patients with hip dysplasia. *Osteoarthritis and Cartilage* 2008;16:227-233.

75. Welsch GH, Mamisch TC, Weber M, et al. High-resolution morphological and biochemical imaging of articular cartilage of the ankle joint at 3.0 T using a new dedicated phased array coil: in vivo reproducibility study. *Skeletal Radiology* 2008;37:519-526.

76. Lazovic-Stojkovic J, Mosher TJ, Smith HE, et al. Interphalangeal joint cartilage: High-spatial-resolution in vivo MR T2 mapping - A feasibility study. *Radiology* 2004;233:292-296.

77. Singh J, Schooler J, Kumar D, et al. Evaluation of t1 rho relaxation times in meniscal tears during static loading. *Osteoarthritis and Cartilage* 2013;21:S186-S186.

78. Grunder W, Kanowski M, Wagner M, et al. Visualization of pressure distribution within loaded joint cartilage by application of angle-sensitive NMR microscopy. *Magnetic Resonance in Medicine* 2000;43:884-891.

79. Alhadlaq HA, Xia Y. Modifications of orientational dependence of microscopic magnetic resonance imaging T(2) anisotropy in compressed articular cartilage. *Journal of Magnetic Resonance Imaging* 2005;22:665-673.

80. Nag D, Liney GP, Gillespie P, et al. Quantification of T-2 relaxation changes in articular cartilage with in situ mechanical loading of the knee. *Journal of Magnetic Resonance Imaging* 2004;19:317-322.

81. Mosher TJ, Liu Y, Torok CM. Functional cartilage MRI T2 mapping: evaluating the effect of age and training on knee cartilage response to running. *Osteoarthritis and Cartilage* 2010;18:358-364.

82. Mosher TJ, Smith HE, Collins C, et al. Change in knee cartilage T2 at MR imaging after running: A feasibility study. *Radiology* 2005;234:245-249.

83. Domayer SE, Welsch GH, Nehrer S, et al. T2 mapping and dGEMRIC after autologous chondrocyte implantation with a fibrin-based scaffold in the knee: Preliminary results. *European Journal of Radiology* 2010;73:636-642.

84. Welsch GH, Trattnig S, Hughes T, et al. T2 and T2*mapping in patients after matrix-associated autologous chondrocyte transplantation: initial results on clinical use with 3.0-Tesla MRI. *European Radiology* 2010;20:1515-1523.

85. Bashir A, Gray ML, Hartke J, et al. Nondestructive imaging of human cartilage glycosaminoglycan concentration by MRI. *Magnetic Resonance in Medicine* 1999;41:857-865.

86. Burstein D, Gray ML, Hartman AL, et al. Diffusion of small solutes in cartilage as measured by nuclear-magnetic-resonance (Nmr) spectroscopy and imaging. *Journal of Orthopaedic Research* 1993;11:465-478.

87. Trattnig S, Mlynarik V, Breitenseher M, et al. MRI visualization of proteoglycan depletion in articular cartilage via intravenous administration of Gd-DTPA. *Magnetic Resonance Imaging* 1999;17:577-583.

88. Nieminen MT, Rieppo J, Silvennoinen J, et al. Spatial assessment of articular cartilage proteoglycans with Gd-DTPA-Enhanced T1 imaging. *Magnetic Resonance in Medicine* 2002;48:640-648.

89. Kwack KS, Cho JH, Kim MS, et al. Comparison study of intraarticular and intravenous gadolinium-enhanced magnetic resonance imaging of cartilage in a canine model. *Acta Radiologica* 2008;49:65-74.

90. Trattnig S, Mamisch TC, Pinker K, et al. Differentiating normal hyaline cartilage from post-surgical repair tissue using fast gradient echo imaging in delayed gadolinium-enhanced MRI (dGEMRIC) at 3 Tesla. *European Radiology* 2008;18:1251-1259.

91. Trattnig S, Marlovits S, Gebetsroither S, et al. Three-dimensional delayed gadolinium-enhanced MRI of cartilage (dGEMRIC) for in vivo evaluation of reparative cartilage after matrix-associated autologous chondrocyte

transplantation at 3.0T: Preliminary results. *Journal of Magnetic Resonance Imaging* 2007;26:974-982.

92. Trattnig S, Millington SA, Szomolanyi P, et al. MR imaging of osteochondral grafts and autologous chondrocyte implantation. *European Radiology* 2007;17:103-118.

93. Bekkers JEJ, Bartels LW, Benink RJ, et al. Delayed gadolinium enhanced MRI of cartilage (dGEMRIC) can be effectively applied for longitudinal cohort evaluation of articular cartilage regeneration. *Osteoarthritis and Cartilage* 2013;21:943-949.

94. Kurkijarvi JE, Nissi MJ, Kiviranta I, et al. Delayed gadolinium-enhanced MRI of cartilage (dGEMRIC) and T-2 characteristics of human knee articular cartilage: topographical variation and relationships to mechanical properties. *Magnetic Resonance in Medicine* 2004;52:41-46.

95. Baldassarri M, Goodwin JSL, Farley ML, et al. Relationship between cartilage stiffness and dGEMRIC index: Correlation and prediction. *Journal of Orthopaedic Research* 2007;25:904-912.

96. Samosky JT, Burstein D, Grimson WE, et al. Spatially-localized correlation of dGEMRIC-measured GAG distribution and mechanical stiffness in the human tibial plateau. *Journal of Orthopaedic Research* 2005;23:93-101.

97. Van Breuseghem I. Ultrastructural MR imaging techniques of the knee articular cartilage: problems for routine clinical application. *Eur Radiol* 2004;14:184-192.

98. Burstein D, Velyvis J, Scott KT, et al. Protocol issues for delayed Gd(DTPA)(2-)-enhanced MRI: (dGEMRIC) for clinical evaluation of articular cartilage. *Magnetic Resonance in Medicine* 2001;45:36-41.

99. Boesen M, Jensen K, Qvistgaard E, et al. Delayed gadolinium-enhanced magnetic resonance imaging (DGEMRIC) of hip joint cartilage - Better cartilage delineation after intraarticular than intravenous gadolinium injection. *Annals of the Rheumatic Diseases* 2006;65:579-579.

100. Gold GE, Burstein D, Dardzinski B, et al. MRI of articular cartilage in OA: novel pulse sequences and compositional/functional markers. *Osteoarthritis and Cartilage* 2006;14:A76-A86.

101. Potter HG, Black BR, Chong LR. New techniques in articular cartilage imaging. *Clinics in Sports Medicine* 2009;28:77-94.

102. Carstens A, Kirberger RM, Velleman M, et al. Feasibility for mapping cartilage T1 relaxation times in the distal metacarpus3/metatarsus3 of Thoroughbred racehorses using delayed gadolinium-enhanced magnetic resonance imaging of cartilage (Dgemric): normal cadaver study. *Veterinary Radiology & Ultrasound* 2013;54:365-372.

103. Menendez MI, Clark DJ, Carlton M, et al. Direct delayed human adenoviral BMP-2 or BMP-6 gene therapy for bone and cartilage regeneration in a pony osteochondral model. *Osteoarthritis and Cartilage* 2011;19:1066-1075.

104. Fortier LA, Potter HG, Rickey EJ, et al. Concentrated bone marrow aspirate improves full-thickness cartilage repair compared with microfracture in the equine model. *Journal of Bone and Joint Surgery-American Volume* 2010;92:1927-1937.

105. White LM, Sussman MS, Hurtig M, et al. Cartilage T2 assessment: Differentiation of normal hyaline cartilage and reparative tissue after arthroscopic cartilage repair in equine subjects. *Radiology* 2006;241:407-414.

106. Bolen G, Haye D, Dondelinger R, et al. Magnetic resonance signal changes during time in equine limbs refrigerated at 4 degrees C. *Veterinary Radiology & Ultrasound* 2010;51:19-24.

107. Bolen GE, Haye D, Dondelinger RE, et al. Impact of successive freezing-thawing cycles on 3-T magnetic resonance images of the digits of isolated equine limbs. *American Journal of Veterinary Research* 2011;72:780-790.

108. Widmer WR, Buckwalter KA, Hill MA, et al. A technique for magnetic resonance imaging of equine cadaver specimens. *Veterinary Radiology & Ultrasound* 1999;40:10-14.

109. Gold SL, Burge AJ, Potter HG. MRI of hip cartilage: joint morphology, structure, and composition. *Clin Orthop Relat Res* 2012;470:3321-3331.

110. Wirth W, Maschek S, Eckstein F. Sex- and age-dependence of region- and layer-specific knee cartilage composition (spin-spin-relaxation time) in healthy reference subjects. *Annals of Anatomy* 2017;210:1-8.

10 Curriculum Vitae

Personal data

Name	**Andrea Simone Bischofberger**
Academic degrees	Dr. med. vet. Dipl. ACVS / ECVS
Home address	Heubergstrasse 13, 8185 Winkel, CH
Date of birth	April 26, 1979, from Heiden AR, CH
Current position	Senior Clinical Lecturer (Oberärztin) Clinic for Equine Surgery, Equine Hospital Vetsuisse-Faculty, University of Zürich Winterthurerstrasse 260, 8057 Zürich, CH
Work phone	+41 44 635 84 70
Work email	abischofberger@vetclinics.uzh.ch

10.1 Education and degrees/certificates

Date	Institution	Degree/certificate
2. 2014	Diplomate of the European College of Veterinary Surgeons	ECVS - accredited
2. 2013	Diplomate of the American College of Veterinary Surgeons - Large Animal	ACVS - board certified
2008 - 2012	UVTHC, University of Sydney, Australia	Resident certificate
2007 - 2008	CVEH, Chino Hills, CA, USA	Internship certificate
2006 - 2007	ISME, Vetsuisse-Faculty, University of Bern, CH	Internship certificate
2004 - 2006	Vetsuisse-Faculty, University of Zürich, CH	Dr. med. vet.
1999 - 2004	Vetsuisse-Faculty, University of Zürich, CH	Med. vet.
1996 - 1997	High school exchange program, Vitré, France	
1995 - 1999	High school/college, Aarau, CH	Diploma (Maturität)
1998 - 1999	Elementary school, Frick, CH	
1994 - 1998	Elementary school, Manchester, GB	

10.2 Professional positions

Date	Institution
Since 2014	**PhD Student,** Graduate School for Cellular and Biomedical Sciences, University of Bern, CH
Since 2012	**Senior Clinical Lecturer in Equine Surgery (Oberärztin),** Equine Hospital, Vetsuisse-Faculty, University of Zürich, CH
2012 - 2013	**Equine Emergency Surgeon,** Vetsuisse-Faculty, University of Bern, CH
2008 - 2012	**Equine Surgery Resident,** UVTHC, University of Sydney, Australia
2007 - 2008	**Equine Surgery Intern and Clinical Instructor,** CVEH, Chino Hills, CA, USA
2006 - 2007	**Rotating Equine Intern,** ISME, Vetsuisse-Faculty, University of Bern, CH
2005 - 2006	**Doctoral Student,** Vetsuisse-Faculty, University of Zürich, CH

Acquired funding

Date	Funding agency	Project title	Amount awarded
2015	Tierärztliche Verrechnungsstelle, CH	Delayed gadolinium enhanced magnetic resonance imaging and T2 mapping of cartilage to depict early degenerative cartilaginous change in horses **Primary investigator**	45 000 CHF
2015	National Research Foundation South Africa	Cartilage segmentation on T2 maps of the equine distal interphalangeal joint in horses **Co-investigator**	1500 CHF

Awards

2011	Science Week. Australian College of Veterinary Scientists, Gold Coast, Australia	Best oral presentation in residents forum	1000 AUS $

Language skills

German Native language
English Fluent spoken and written, 2011 IELTS (academic) overall band score 8
French Good spoken and written
Italian Basic knowledge

10.3 Teaching experience

- **Lectureship in equine surgery - University of Zürich, CH**

Date	Level	Lecture Title *(Original title in German)*	Hours/ semester	Type
2015 *Fall*	Years 3-5	Career choice, going overseas	0.14	Lecture
Since 2015	-	Q-exam: professional exam question reviewing	-	-
Since 2015 *Spring*	Year 5	Advanced studies: equine emphasis *(Schwerpunkt Pferd)*	0.29	Lectures, practical exercises
Since 2015 *Spring*	Year 4	Cardinal symptoms: lameness and ataxia *(Leitsymptom: Lahmheit und Ataxie*)	0.07	Lectures, tutorials, practical exercises, case presentations
Since 2014 *Fall*	Year 2	Organ-centered module: Musculoskeletal apparatus *(Organblock Bewegungsapparat)*	0.14	Lecture
Since 2014 *Fall*	Graduate level	Continuing education seminar equine	1	
Since 2014 *Fall*	Graduate level	Book club equine surgery	1	
Since 2014 *Spring, Fall*	Graduate level	Journal club equine surgery	0.5	
Since 2014 *Spring, Fall*	Year 5	Clinical rotation equine track	2.94	Case based teaching in clinics

Since 2014 *Spring, Fall*	Year 5	Clinical rotation general track	2.94	Case based teaching in clinics
Since 2014	Year 5	Swiss DVM licensing exam *(Staatsexamen)*		Examinator practical and oral exam
Since 2014	Year 4	Cardinal symptoms exam *(Leitsymptomprüfung)*		Examinator oral exam

- **Lectureship in veterinary science, basic education of farm and animal professionals - Strickhof, Winterthur, CH**

Date	**Level**	**Lecture Title** ***(Original title in German)***	**Hours/ semester**	**Type**
2014 - 2015	Years 1, 2	Horse health in the basic education of equine professionals *(Pferdegesundheit im Berufskundeunterricht der Grundbildung zum Pferdefachmann)*	30	Lectures

- **Teaching responsibilities (Resident) - University of Sydney 2008 – 2012**

Practical training of students in daytime and afterhours surgical service
Distal limb dissection and surgical anatomy - practical exercises
Daily student teaching rounds

- **Teaching responsibilities (Intern/Clinical Instructor) Chino Valley Equine Hospital, 2008 - 2007**

Practical training of students on out rotations in daytime service

Supervision of veterinarians in advanced clinical training

Date	**Training program**	**Trainee**
Since 2014	ECVS (Primary supervisor)	Muriel Federici
2014 - 2016	FVH	Sibylle Staubli

Supervision of research students

Date	Degree	Name	Project
Since 2016	Master	T. Stäubli	Complete SDFT ruptures
Since 2016	Dr. med. vet.	R. Joos	Orbita fractures in horses
Since 2015	ECVDI	J. Suarez	CTA and MRA to detect cartilage defects
Since 2015	Dr. med. vet.	A. Bachmann	Biochemical cartilage map of the coffin joint
Since 2015	Dr. med. vet.	R. Fürst	Cartilage thickness on T1 and T2 maps
Since 2014	ECVS	M. Federici	Luxations of the SDFT from the calcaneus
2014 - 2016	Dr. med. vet.	S. Frei	Fixation of supraglenoid tubercle fractures
2014 - 2016	FVH	B. Schwenk	Traffic accident-related injuries in horses
2014 - 2015	Master	R. Joos	Basal proximal sesamoid bone fractures
2013 - 2015	Master	N. Butz	Coronation injuries in horses
2011	Summer student	L. Lambertini	Efficacy of fucoidan and omeprazole in preventing and treating gastric ulceration
2010 - 2011	Honors thesis	A. Tsang	Effect of protein C on equine wound healing
2010	Summer student	I. Hadidane	Effect of laryngeal prostheses on the rima glottidis area

Recent and current international research partners

Name	Institution	Project
A. Carstens	University of Pretoria, South Africa	Delayed gadolinium enhanced magnetic resonance imaging and T2 mapping of cartilage to depict early degenerative cartilaginous change in horses
A. Dart	Research and Clinical Training Unit, University of Sydney, Australia	Second intention wound healing in equine distal limbs, multiple wound healing projects
C. Little	Raymond Purves Bone and Joint Research Laboratories, Kolling Institute of Medical Research, University of Sydney Australia	The effect of manuka honey gel on the TGF β1 and β3 concentration, bacterial counts and histomophology of contaminated full thickness skin wounds in equine distal limbs

C. Jackson	Sutton Arthritis Research Laboratories, Kolling Institute of Medical Research, University of Sydney, Australia	Role of protein C in wound healing

Continuing education on didactic learning

2016	Forschungsnahes Lernen und Lehren- Didactica, ETH, Zürich, CH
2014	Supervising students - dealing with roles and relationships, Didactica, ETH, Zürich, CH
2014	Meine Powerpoint Folien mit einfachen Mitteln verbessern, Didactica, ETH, Zürich, CH
2013	Rhetorical skills in the classroom and lecture hall, Didactica, ETH, Zürich, CH

Reviewer activity

2016	The Veterinary Journal
2015	Equine Veterinary Science
Since 2014	Veterinary Surgery
	Equine Veterinary Journal
	Equine Veterinary Education

Academic service

Since 2015	Responsible for implementation of the new equine hospital information system in the equine surgery clinic, University of Zürich, CH
Since 2014	Member of the educational committee of the Swiss Veterinary Association (GST)
2015 - 2016	Member of the search committee for the assistant professorship for experimental surgery, University of Zürich, CH
2002 - 2004	Member of the student body association (Fachverein), University of Zürich, CH

Professional associations - memberships

Fédération Equestre Internationale (FEI)	Official treating veterinarian
American College of Veterinary Surgeons (ACVS)	Diplomate, by examination
European College of Veterinary Surgeons (ECVS)	Diplomate, accredited
Swiss Equine Veterinary Association (SVPM)	Association member
Swiss Veterinary Association (GST)	Association member and educational committee member

Professional development courses

2016	**Business tools: Business foundation compact**, ETH, Zürich, CH
2016	**Business tools: Business plan, business model canvas and co. professionally made,** ETH, Zürich, CH
2015	**Scientific Integrity Lecture,** Graduate School for Cellular und Biomedical Sciences, University of Bern, CH
2015	**Molecular Biological Methods in Clinical Research**, University of Bern, Switzerland (2.0 ECTS by written examination)
2015	**Successful Fund Acquisition for Researchers**, University of Zürich, CH
2015	**Introduction into Epidemiology and Biostatistics Parts I and II,** University of Bern, CH (4.0 ECTS by oral examination)
2015	**LTK Module 1: Introductory Course in Laboratory Animal Science,** University of Zürich, CH
2013	**Emergency Training BLS-AED nach SRC,** (Resuscitation and defibrillation), University of Zürich, CH

Attended courses and conferences

2016

25th Annual Scientific Meeting ECVS, Lisbon, Portugal

Minimally invasive buccotomy workshop, Dr. M. Stoll, University of Zürich, CH

CT of the equine oral and nasal cavities. Continuing education seminar, University of Bern, CH

11th Netzwerktagung Pferdeforschung Schweiz, Annual Scientific Meeting, Avenches, CH

2015

Intensive tooth extraction workshop in horses, University of Utrecht, Netherlands

Orthopedic day. Continuing education seminar, University Zürich, CH

2014

Wound management and use of antibiotics in horses. Continuing education seminar, University of Zürich, CH

23rd Annual Scientific Meeting ECVS, Copenhagen, Denmark

Ultrasonography of the back workshop, Copenhagen, Denmark

Instructional symposium on equine laparoscopy, Michigan State University, USA

Orthopedic problems in foals. Continuing education seminar, University of Zürich, CH

Vaccinations in horses. Continuing education seminar, University of Zürich, CH

2013

The sport horse veterinarian. Continuing education seminar, Zürich, CH

Emergency medicine 19th Continuing education seminar, Bern, CH

2012

New therapeutic strategies in the horse. Continuing education seminar, Zürich, CH

21st Annual Scientific Meeting ECVS, Barcelona, Spain

2011

ACVS Veterinary Symposium, Chicago, USA

20th Annual Scientific Meeting ECVS, Ghent, Belgium

Science week, Australian College of Veterinary Scientists, Gold Coast, Australia

Equine Veterinary Association, NSW State Meeting, Sydney, Australia

Resident Training Weekend, Randwick Equine Hopsital, Australia

Australian Veterinary Association Annual Conference, Adelaide, Australia

Training Weekend, Australian College of Veterinary Scientists, Melbourne, Australia

Equine Veterinary Association, NSW State Meeting, Sydney, Australia

Resident Training Weekend, Camden, NSW, Australia

10.4 Publication list

Original articles in peer reviewed journals

Published

21. Sacks M, Ringer SK, ***Bischofberger AS,*** Berchtold SM, Bettschart-Wolfensberger R. *Vet. Anaesth. Analg.* 2017;44(5):1128-1138. **Clinical comparison of dexmedetomidine and medetomidine for isoflurane balanced anaesthesia in horses.**

20. Frei S, Geyer H, Fürst A, Hoey S, ***Bischofberger AS.*** *Vet. Comp. Ortho. Trauma*. 2017;30(2):99-106. **Evaluation of the optimal plate position for the fixation of supraglenoid tubercle fractures in Warmbloods.**

19. Federici M, Fürst A, Hoey S, ***Bischofberger AS.*** *Eq. Vet. Educ*. 2017. Epub **Outcome of conservative and surgical treatment and outcome of luxations of the superficial digital flexor tendon from the calcaneal tuber.**

18. Frei S, Geyer H, Fürst A, Hoey S, ***Bischofberger AS.*** *Vet. Comp. Ortho. Trauma*. 2017;30(2):99-106. **Evaluation of the optimal plate position for the fixation of supraglenoid tubercle fractures in Warmbloods.**

17. Butz N, Dreyfus A, Fürst A, ***Bischofberger AS.*** *Eq. Vet. Educ***.** 2016;29(1):38-44. **Wounds to the dorsal aspect of the carpus (coronation injury) in horses: Treatment, complications and survival.**

16. Schwenk B, Fürst A, ***Bischofberger AS.*** *Pferdeheilkunde***.** 2016;3:192-199. **Traffic accident-related injuries in horses.**

15. ***Bischofberger AS*****,** Horadagoda N, Dart CM, Perkins N, Little C, Jeffcott L, Dart. *Aust. Vet. J.* 2016;94:27-34. **The effect of manuka honey gel on the transforming growth factor β1 and β3 concentration, bacterial counts and histomorphology of contaminated full thickness skin wounds in equine distal limbs.**

14. ***Bischofberger AS*****,** Tsang A, Horadagoda N, Dart CM, Perkins N, Jeffcott L, Jackson CJ, Dart A. *Aust. Vet. J.* 2015;93:361-366. **Effect of activated protein C in second intention healing of equine distal limb wounds: a preliminary study.**

13. ***Bischofberger AS*****,** Washk M, Dart AJ. *Pratique Vét. Éq.* 2015;185:26-35. **Les sutures en fil d`acier pour la fermeture de l`abdomen lors de relaparotomie compliquée.** *(*The use of stainless steel wire in a horizontal mattress pattern for secondary closure of the equine linea alba).

12. ***Bischofberger AS****,* Wehrli Eser M, Jackson M, Fürst A. *Der praktische Tierarzt.* 2014;95:620-627. **Die Laryngoplastik: Intraoperative und post-operative Komplikationen.** (Laryngoplasty: Intraoperative and postoperative complications).

11. ***Bischofberger AS*****,** Hadidane I, Werezska M, Perkins N, Jeffcott L, Dart AJ. *Vet. Surg.* 2013;42:286-290. **Effect of age and prostheses location on rima glottidis area in equine**

cadaveric larynges.

10. ***Bischofberger AS,*** Werezska M, Hadidane I, Perkins N, Jeffcott L, Dart AJ. *Vet. Surg.* 2013;42:280-285. **Optimal tension, position and number prostheses required for maximum rima glottidis area after laryngoplasty.**

9. ***Bischofberger AS,*** Dart CM, Perkins N, Kelly A, Jeffcott L, Dart AJ. *Vet. Surg.* 2013;42:154-60. **The effect of short and longer term treatment with manuka honey on second intention healing of contaminated and non-contaminated wounds on the distal aspect of the forelimbs in horses.**

8. ***Bischofberger AS,*** Dart A. *Pratique Vét. Éq.* 2012;44:1-4. **Le miel de manuka dans le traitement des plaies distales des membres chez le cheval.** (Use of Manuka honey in wound healing of equine distal limb wounds).

7. Kwan C, Bell R, Koenig T, ***Bischofberger AS,*** Horodagoda N, Perkins N, Jeffcott L, Dart AJ. *Aust. Vet. J.* 2012, 90:315-320. **Effects of intra-articular sodium pentosan polysulphate and glucosamine in horses on the cytology and viscosity of synovial fluid.**

6. ***Bischofberger AS,*** Dart CM, Perkins N, Dart AJ. *Vet. Surg.* 2011;40:898-902. **A preliminary study on the effect of manuka honey on second intention healing of contaminated wounds on the distal aspect of the forelimbs of horses.**

5. ***Bischofberger AS,*** Brauer T, Gugelchuck G, Klohnen A. *Eq. Vet. J.* 2010;42:304-9. **Difference in incisional complications following exploratory celiotomies using antibacterial-coated suture material for subcutaneous closure: Prospective randomised study in 100 horses.**

4. ***Bischofberger AS,*** Fürst A, Auer J, Lischer CJ. *Eq. Vet. J.* 2009;41:465-473. **Surgical management of complete diaphyseal third metacarpal and metatarsal bone fractures: Clinical outcome in 10 mature horses and 11 foals.**

3. ***Bischofberger AS,*** Ringer SK, Geyer H, Imboden I, Ueltschi G, Lischer CJ. *Am. J. Vet. Res.* 2006;67:577-82. **Histomorphologic evaluation of extracorporeal shock wave therapy of the fourth metatarsal bone and the origin of the suspensory ligament in horses without lameness.**

2. ***Bischofberger AS,*** Konar M, Ohlerth S, Geyer H, Lang J, Ueltschi G, Lischer CJ. *Eq. Vet. J.* 2006;38:508-516. **Magnetic resonance imaging, ultrasonography and histology of the origin of the suspensory ligament: A comparative study of the normal anatomy in fore- and hindlimbs of 4-13 year old warmblood horses.**

1. Lischer CJ, ***Bischofberger AS,*** Fürst A, Lang J, Ueltschi G. *Schweiz. Arch. Tierheilk.* 2006;148:86-97. **Disorders of the origin of the suspensory ligament: A diagnostic challenge.**

<u>Accepted / In print</u>

2. ***Bischofberger AS,*** Fürst A, Torgerson P, Hilbe M, Carstens A, Kircher P. *Am. J. Vet. Res.* 2018. **Delayed gadolinium enhanced magnetic resonance imaging of the normal and naturally occurred osetoarthrithis equine distal interphalangeal joint cartilage in a 3 tesla magnet.**

1. Suarez J, Kühn K, ***Bischofberger AS,*** Richter H, Kircher P, Hoey S. Vet. Radiol. Ultrasound 2018 **Comparison between magnetic resonance imaging, computed tomography and arthrography to identify cartilage defects of the equine carpal joints.**

Submitted / Under revision / In preparation

5. **Bischofberger AS,** Fürst A, Torgerson P, Carstens A, Hilbe M, Kircher P. **T2 mapping of the normal and naturally occurring osteoarthritic equine cadaver distal interphalangeal joint cartilage in a 3 tesla magnet.**

4. Joos R, Ohlerth S, Baschnagel F, Fürst A, ***Bischofberger AS*****. Configuration of orbita fractures in horse.**

3. Fürst R, Fürst A, Bachmann A, Federici M, Torgerson P, Kircher P, ***Bischofberger AS.*** **Validation of delayed gadolinium-enhanced magnetic resonance imaging of cartilage and T2 mapping for quantifying normal and naturally occurring osteoarthritic distal interphalangeal joint cartilage thickness in Warmblood horses.**

2. Weber S, Ohlerth S, Mosing M, Torgerson P, Fürst A, ***Bischofberger AS*****. Evaluation of the distribution of mepivacain 2% following local infiltration of the infraorbital nerve via the infraorbital foramen**.

1. Schoster A, Altermatt N, ***Bischofberger AS.*** **Retrospective analysis of outcome and complications after large intestinal trocharisation in horses (2004-2015).**

Case reports / Case series in peer reviewed journals

4. Frei S, Fürst A, Sacks M, ***Bischofberger AS.*** *Vet. Comp. Ortho. Trauma****.*** 2016;3:246-252. **Fixation of supraglenoid tubercle fractures using distal femoral locking plates in three Warmblood horses.**

3. Federici M, Del Chica F, Rütten M, Fürst A, ***Bischofberger AS*****.** *Eq. Vet. Educ.* 2015;27:585-591. **Peripheral nerve sheath tumor in the maxillary sinus of a mare.**

2. ***Bischofberger AS,*** Dart CM, Dart AJ. *Aust. Vet. J.* 2010;88:283-85. **Surgical treatment of osteomyelitis and sequestration of the ilium by a cranial partial hemipelvectomy in an alpaca cria.**

1. ***Bischofberger AS****,* Posthaus H, Konar M, Pekarkova M, Grzybowski M, Brehm W. *Eq. Vet. Educ.* 2008;20:340-347. **Ocular angiosarcoma in a pony - MRI and histopathologic**

appearance.

Review articles in peer reviewed journals

1. Dart AJ, ***Bischofberger AS,*** Dart CM, Jeffcott L. *Eq. Vet. Educ.* 2015;27:658-664. **A review of research into second intention equine wound healing using manuka honey: Current recommendations and future applications.**

Clinical commentaries in peer reviewed journals

2. Dart AJ, ***Bischofberger AS.*** *Eq. Vet. Educ.* 2011;23:294-95. **Clinical Commentary: Peritonitis in the horse: A treatment dilemma.**

1. Dart AJ, ***Bischofberger AS.*** *Eq. Vet. Educ.* 2010;22:73-76. **Clinical Commentary: Shockwave therapy-Is there an application to enhance wound healing in horses?**

Book chapters

4. ***Bischofberger AS,*** Theiss F. (2017) **EOTRH Syndrome.** In: Blackwell`s Five-*Minute Veterinary Consult,* 3rd edn. Ed: J.-P. Lavoie, K. Hinchcliff, Wiley-Blackwell Publishing, London, UK.

3. ***Bischofberger AS,*** Theiss F. (2017) **Periodontal Disease.** In: Blackwell`s Five-*Minute Veterinary Consult,* 3rd edn., Ed: J.-P. Lavoie, K. Hinchcliff, Wiley-Blackwell Publishing, London UK.

2. Theiss F, ***Bischofberger AS.*** (2017) **Retained Deciduous Teeth.** In: Blackwell`s Five-*Minute Veterinary Consult,* 3rd edn., Ed: J.-P. Lavoie, K. Hinchcliff, Wiley-Blackwell Publishing, London UK.

1. Theoret C, Lepage O, Dart AJ, ***Bischofberger AS,*** *Koenig J.* (2016) **Innovative adjunctive approaches to wound management.** In: *Equine Wound Management*, 3rd edn., Ed: T. Stashak, C. Theoret, Wiley-Blackwell Publishing, London, UK.

In press

2. ***Bischofberger AS.*** (2018) **Drains, bandages and external coaptation.** In: *Equine Surgery*, 5th edn., Ed: J. Auer, J. Stick, Elsevier Saunders, St. Louis, USA.

1. ***Bischofberger AS,*** Auer J. (2018) **Angular limb deformities.** In: *Equine Surgery*, 5th edn., Ed: J. Auer, J. Stick, Elsevier Saunders, St. Louis, USA.

Theses

1. Dr. med. vet thesis: ***Bischofberger AS:*** **The effect of extracorporeal shock wave treatment at the origin of the suspensory ligament and fourth metatarsal bone in sound horses – a histomorphologic and scintigraphic study.** 2006 University of Zürich, CH.

Abstracts in peer reviewed conference proceedings

23. Carstens A, Fürst A, Hilbe, M, Kircher, P, ***Bischofberger AS.*** In Proc of the European veterinary diagnostic imaging congress 2017, Verona, Italy. **Delayed gadolinium-enhanced magnetic resonance imaging of the normal and naturally degenerated equine distal interphalangeal joint.**

22. Suarez J, Kühn K, ***Bischofberger AS,*** Richter H, Kircher P, Hoey S. In Proc of the European veterinary diagnostic imaging congress 2017, Verona, Italy. **Comparison between magnetic resonance imaging, computed tomography and arthrography to identify cartilage defects of the equine carpal joints.**

21. Federici M, Fürst A, Hoey s, ***Bischofberger AS.*** In Proc of the 2nd International Congress of the German Equine Veterinary Association, Berlin, Germany. 2016. **Treatment and outcome of luxations of the superficial digital flexor tendon from the calcaneal tuber.**

20. Frei S, Geyer H, Fürst A, Hoey S, ***Bischofberger AS.*** In Proc of 11th Netzwerktagung Pferdeforschung Schweiz, Avenches, Schweiz. Arch. Tierheilk. 2016;158:269-284. **Fixation von Frakturen des Tuberculum supraglenoidale am Schulterblatt bei drei Warmblutpferden mittels einer distalen Femurplatte: Morphologische und morphometrische Studie der Scapula zur Bestimmung der optimalen Plattenposition.**

19. Butz N, Dreyfus A, Fürst A, ***Bischofberger AS.*** In Proc of 11th Netwerktagung Pferdeforschung Schweiz, Avenches, Schweiz. Arch. Tierheilk. 2016;158:269-284. **Couronnement beim Pferd: Behandlung, Komplikationen und Prognose.**

18. Federici M, Fürst A, Hoey s, ***Bischofberger AS.*** In Proc of 25th Annual Scientific Meeting of ECVS 2016, Lisbon, Portugal. *Vet. Surg.* 2016. **Treatment and outcome of luxations of the superficial digital flexor tendon from the calcaneal tuber.**

17. Sacks M, Ringer SK, ***Bischofberger AS,*** Bettschart-Wolfensberger R. In Proc of World Congress of Veterinary Anesthesia, Kyoto, Japan, 2015. **Sedation, cardiovascular function and recovery of medetomidine versus dexmedetomidine isoflurane balanced anaesthesia in horses – preliminary study results.**

16. ***Bischofberger AS,*** Tsang A, Waschk M, Dart C, Perkins N, Jackson C, Jeffcott L. Dart AJ. In Proc of 37th Bain Fallon Lectures, Hunter Valley, 2015. **The effect of activated protein C on second intention healing in standardised, surgically created, full thickness wounds in**

the distal limb of horses.

15. ***Bischofberger AS,*** Horadagoda N, Dart C, Perkins N, Little C, Jeffcott L, Dart AJ. In Proc of 37th Bain Fallon Lectures, Hunter Valley, 2015. **The effect of manuka honey gel on transforming growth factor β1 and β3 concentration, bacterial counts and histomorphology of contaminated full thickness wounds in equine distal limbs.**

14. ***Bischofberger AS,*** Dart CM, Bell RB, Jeffcott LB, Perkins N, Jeffcott L Dart AJ. In Proc of 37th Bain Fallon Lectures, Hunter Valley, 2015. **The effect of manuka honey and 66% manuka honey gel on second intention healing of contaminated and non-contaminated distal limb wounds in the horses.**

13. ***Bischofberger AS,*** Tsang A, Horadagoda N, Perkins N, Jeffcott L, Dart A. In Proc of 21st Annual Scientific Meeting of ECVS 2012, Barcelona, Spain. *Vet. Surg.* 2012. **The effect of activated Protein C on second intention healing in standardized, surgically created full thickness skin wounds in the distal limbs of horses.**

12. ***Bischofberger AS,*** Horadagoda N, Dart CM, Perkins N, Little C, Jeffcott L, Dart A. In Proc of 21st Annual Scientific Meeting of ECVS 2012, Barcelona, Spain. *Vet. Surg.* 2012. **The effect of Manuka honey gel on transforming growth factor β1 and β3 concentration, bacterial counts and histomorphology of contaminated full thickness skin wounds.**

11. ***Bischofberger AS,*** Kelly A, Dart CM, Perkins N, Jeffcott, Dart A. In Proc of ACVS Symposium 2011, Chicago, USA. *Vet. Surg.* 2011;40:781-907, E20. **The effect of short and longer-term treatment with manuka honey gel on second intention healing of wounds contaminated with feces and non-contaminated wounds on the distal aspect of equine forelimbs.**

10. ***Bischofberger AS,*** Wereszka M, Hadidane I, Perkins N, Jeffcott L, Dart A. In Proc of ACVS Symposium 2011, Chicago, USA. *Vet. Surg.* 2011;40:781-907, E21. **The effect of prosthesis tension, position and number on the area of the rima glottidis in normal equine laryngeal specimens.**

9. ***Bischofberger AS,*** Wereszka M, Hadidane I, Perkins N, Jeffcott L, Dart A. In Proc of 20th Annual Scientific Meeting ECVS 2011, Ghent, Belgium. *Vet. Surg.* 2011;40:515-645, E9. **The effect of horse age, prosthesis tension, position and number on the area of the rima glottidis in equine laryngeal specimens.**

8. ***Bischofberger AS.*** In Proc of Australian Veterinary Association Annual Conference 2011, Adelaide, SA, Australia. 2011;D3.6b. **The effect of Manuka honey on second intention healing of contaminated and uncontaminated wounds in equine distal limbs.**

7. ***Bischofberger AS****.* In Proc of Australian Veterinary Association Annual Conference 2011, Adelaide, SA, Australia. 2011;D3.6c. **The effect of horse age, prosthesis tension, position and number on the area of the rima glottidis in equine laryngeal specimens.**

6. ***Bischofberger AS,*** Dart C, Perkins N, Jeffcott L, Dart A. In Proc of Bain Fallon Memorial Lectures 2010, Equine Veterinary Association, Hunter Valley, NSW, Australia. *Aust. Eq.*

Vet. 2010;29:80. **The effect of manuka honey gel on second intention healing of contaminated and uncontaminated equine distal limb wounds in horses.**

5. ***Bischofberger AS,*** Brauer T, Fischer AT, Klohnen A. In Proc of 17th Annual Scientific Meeting ECVS 2008, Basel, Switzerland. *Vet. Surg.* 2008;37:311-411, E9. **Incisional complications following exploratory celiotomies: does antimicrobial (triclosan) coated suture material decrease the likelihood of incisional infection?**

4. Klohnen A, Brauer T, ***Bischofberger AS*****.** In Proc of ACVS Symposium 2008, San Diego, CA, USA. *Vet. Surg.* 2008;37:501-601, E18. **Incisional complications following exploratory celiotomies: does antimicrobial (triclosan) coated suture material decrease the likelihood of incisional infection?**

3. Klohnen A, Sonis J, Raffetto J, ***Bischofberger AS.*** In Proc of ACVS Symposium 2008, San Diego, CA, USA. *Vet. Surg.* 2008;37:501-601, E18. **Adhesion formation rate after exploratory celiotomies in horses with and without intra-abdominal use sodium carboxymethylcellulose: a 4 year study.**

2. ***Bischofberger AS,*** Konar M, Ohlerth S, Geyer H, Lang J, Ueltschi G, Lischer CJ In Proc of 15th Annual Scientific Meeting ECVS 2006, Sevilla, Spain. *Vet. Surg.* 2006;35:E1-20. **MRI, ultrasonography and histology of the origin of the suspensory ligament: A comparative study of the normal equine anatomy.**

1. ***Bischofberger AS,*** Ringer SK, Geyer H, Imboden I, Ueltschi G, Lischer CJ.In Proc of 15th Annual Scientific Meeting ECVS 2006, Sevilla, Spain. *Vet. Surg.* 2006;35:E1-20. **Histomorphologic and scintigraphic evaluation of extracorporeal shock wave therapy of the origin of the suspensory ligament and fourth metatarsal bone in sound horses.**

Non-peer reviewed publication

4. ***Bischofberger AS,*** *The Horse.com.* 2016. **New surgical technique for fixing equine shoulder fractures.**

3. ***Bischofberger AS,*** Dart A. *The Horse Magazine.* 2012. **The role of manuka honey in wound healing.**

2. ***Bischofberger AS,*** Dart A. *The Veterinarian.* 2011. **Second intention wound healing in distal limb wounds in horses: A role for manuka honey.**

1. ***Bischofberger AS,*** Dart A. Media release of the University of Sydney. 2011. **Honey helps heal horses wounds.**

Oral presentations at scientific conferences

12. ***Bischofberger AS***, Fürst A, Bachmann A, Fürst R, Carstens A, Hilbe, M, Kircher P. Conference of the Graduate School for Cellular and Biomedical Sciences, 2017, Bern, CH.

Delayed gadolinium-enhanced magnetic resonance imaging of the normal and naturally degenerated equine distal interphalangeal joint cartilage.

11. Carstens A, Fürst A, Hilbe, M, Kircher, P, ***Bischofberger AS.*** European Veterinary Diagnostic imaging congress 2017, Verona, Italy. **Delayed gadolinium-enhanced magnetic resonance imaging of the normal and naturally degenerated equine distal interphalangeal joint.**

10. Suarez J, Kühn K, ***Bischofberger AS,*** Richter H, Kircher P, Hoey S. European Veterinary Diagnostic imaging congress 2017, Verona, Italy. **Comparison between magnetic resonance imaging, computed tomography and arthrography to identify cartilage defects of the equine carpal joints.**

9. ***Bischofberger AS,*** Horadagoda N, Dart CM, Perkins N, Little C, Jeffcott L, Dart A. Scientific abstract, 21st Annual Scientific Meeting of ECVS 2012, Barcelona, Spain. **The effect of Manuka honey gel on transforming growth factor β1 and β3 concentration, bacterial counts and histomorphology of contaminated full thickness skin wounds.**

8. ***Bischofberger AS,*** Wereszka M, Hadidane I, Perkins N, Jeffcott L, Dart A.Scientific abstract, Resident forum, ACVS Symposium 2011, Chicago, IL, USA. **The effect of prosthesis tension, position and number on the area of the rima glottidis in normal equine laryngeal specimens.**

7. ***Bischofberger AS,*** Kelly A, Dart C, Perkins N, Jeffcott, Dart A. Scientific abstract, ACVS Symposium 2011, Chicago, IL, USA. **The effect of short and longer-term treatment with manuka honey gel on second intention healing of wounds contaminated with feces and non-contaminated wounds on the distal aspect of equine forelimbs.**

6. ***Bischofberger AS,*** Wereszka M, Hadidane I, Perkins N, Jeffcott L, Dart A. Scientific abstract, 20th Annual Scientific Meeting ECVS 2011, Ghent, Belgium. **Effect of horse age, prosthesis position and tension on the rima glottidis area in laryngeal specimens.**

5. ***Bischofberger AS,*** Wereszka M, Hadidane I, Perkins N, Jeffcott L, Dart A. Resident forum, Science Week 2011. Australian College of Veterinary Scientists, Gold Coast, QL, Australia. **Effect of horse age, prosthesis position and tension on the rima glottidis area in laryngeal specimens.**

4. ***Bischofberger AS,*** Scientific abstract resident forum, Science Week 2011. Australian College of Veterinary Scientists, Gold Coast, QL, Australia. **Effect of Manuka honey on second intention healing of contaminated equine distal limb wounds.**

3. **Bischofberger AS,** Wereszka M, Hadidane I, Perkins N, Jeffcott L, Dart A. Scientific abstract, Australian Veterinary Association Annual Conference 2011. Adelaide, SA, Australia. **Effect of horse age, prosthesis position and tension on the rima glottidis area in laryngeal specimens.**

2. ***Bischofberger AS,*** Dart A. Scientific abstract, Australian Veterinary Association Annual Conference 2011. Adelaide, SA, Australia. **The effect of Manuka honey on second intention**

healing of contaminated equine distal limb wounds.

1. ***Bischofberger AS,*** Konar M, Ohlerth S, Geyer H, Lang J, Ueltschi G, Lischer CJ. Scientific abstract, resident forum, 15th Annual Scientific Meeting ECVS 2006. Sevilla, Spain. **MRI, ultrasonography and histology of the origin of the suspensory ligament: A comparative study of the normal equine anatomy.**

Oral presentations for veterinary societies, at continuing education meetings

14. ***Bischofberger AS.*** Graubündtner Tierärzte Tagung, Chur. Continuing education for veterinarians, 2017. **Intraoperative findings during emergency laparotomy.**

13. ***Bischofberger AS.*** Continuing education for veterinarians, 2017. **Emergency management and transport of colic patients.**

12. ***Bischofberger AS.*** National horse centre (NPZ), Bern. Continuing education for veterinarians, 2017. **Emergency management and transport of equine fracture patients.**

11. ***Bischofberger AS.*** Vetsuisse-Faculty, University of Zürich, Continuing education for veterinarians, Boehringer seminar, 2017. **Angular and flexural limb deformities in foals.**

10. ***Bischofberger AS.*** Vetsuisse-Faculty, University of Zürich, Continuing education for veterinarians, Boehringer seminar, 2017. **MRI of the equine hyaline cartilage.**

9. ***Bischofberger AS.*** Vetsuisse-Faculty, University of Zürich, Continuing education for nursing and technical staff, 2016. **Role of honey in equine wound healing.**

8. ***Bischofberger AS.*** Vetsuisse-Faculty, University of Zürich, Continuing education for farriers, 2016. **Flexural limb deformities in foals.**

7. ***Bischofberger AS.*** Vetsuisse-Faculty, University of Zürich, Continuing education for farriers, 2016. **Angular limb deformities in foals.**

6. ***Bischofberger AS.*** Vetsuisse-Faculty, University of Zürich, Continuing education for veterinarians, Boehringer seminar, 2014. **Equine Wound management - Use of antibiotics, antiseptics or honey.**

5. ***Bischofberger AS.*** Vetsuisse-Faculty, University of Zürich, Continuing education for veterinarians, Boehringer seminar, 2014. **Use of NSAIDs in foals.**

4. ***Bischofberger AS.*** Vetsuisse-Faculty, University of Zürich, Continuing education for farriers, 2014. **Angular limb deformities in foals.**

3. ***Bischofberger AS.*** Vetsuisse-Faculty, University of Zürich, Continuing education for farriers, 2014. **Flexural limb deformities in foals.**

2. ***Bischofberger AS.*** Australian College of Veterinary Scientists- Resident training weekend 2011. Melbourne, VIC, Australia. **Subchondral cystic lesions - Treatment options.**

1. ***Bischofberger AS.*** Australian Veterinary Association, Branch Meeting 2010, Camden, NSW Australia. **Role of honey in second intention wound healing in horses.**

Webinars, Podcasts

2. ***Bischofberger AS.*** *Podcast Equine Vet. Educ.* 2015. **A review of research into second intention equine wound healing using manuka honey: Current recommendations and future applications.**

1. ***Bischofberger AS.*** *Vet webinar.com.* 2015. **Wundbehandlung beim Pferd - Desinfektionsmittel, Antibiotika oder einfach nur Honig.**

Poster presentations

9. ***Bischofberger AS,*** Fürst A, Kircher P. Conference of the Graduate School for Cellular and Biomedical Sciences, University of Bern, CH, 2016. **Validation of T2-mapping and delayed gadolinium enhanced magnetic resonance imaging of cartilage (dGEMRIC) in the distal interphalangeal joints of Warmblood horse cadavers.**

8. Frei S, Geyer H, Fürst A, Hoey S, ***Bischofberger AS.*** 11th Netzwerktagung Pferdeforschung Schweiz, Avenches, CH. 2016. **Fixation von Frakturen des Tuberculum supraglenoidale am Schulterblatt bei drei Warmblutpferden mittels einer distalen Femurplatte: Morphologisch und morphometrische Studie der Scapula zur Bestimmung der optimalen Plattenposition.**

7. ***Bischofberger AS,*** Tsang A, Waschk M, Dart C, Perkins N, Jackson C, Jeffcott L. Dart AJ. 37th Bain Fallon Lectures, Hunter Valley, 2015. **The effect of activated protein C on second intention healing in standardised, surgically created, full thickness wounds in the distal limb of horses.**

6. ***Bischofberger AS,*** Horadagoda N, Dart C, Perkins N, Little C, Jeffcott L, Dart AJ. 37th Bain Fallon Lectures, Hunter Valley, 2015. **The effect of manuka honey gel on transforming growth factor β1 and β3 concentration, bacterial counts and histomorphology of contaminated full thickness wounds in equine distal limbs.**

5. ***Bischofberger AS,*** Dart CM, Bell RB, Jeffcott LB, Perkins N, Jeffcott L Dart AJ. 37th Bain Fallon Lectures, Hunter Valley, 2015. **The effect of manuka honey and 66% manuka honey gel on second intention healing of contaminated and non-contaminated distal limb wounds in the horses.**

4. ***Bischofberger AS,*** Tsang A, Horadagoda N, Perkins N, Jeffcott L, Dart A. 21st Annual Scientific Meeting of ECVS 2012, Barcelona, Spain. 2012. **The effect of activated Protein C**

on second intention healing in standardised, surgically created full thickness skin wounds in the distal limbs of horses.

3. ***Bischofberger AS,*** Dart A. Bain Fallon Conference 2010. Equine Veterinary Association, Hunter Valley, NSW, Australia. **Effect of Manuka honey gel on second intention healing of contaminated and uncontaminated distal limb wounds in horses.**

2. ***Bischofberger AS,*** Brauer T, Fischer AT, Klohnen A. 9th International Equine Colic Research Symposium 2008**.** Liverpool, UK. **Incisional complications following exploratory celiotomy: Does antibacterial coated suture material decrease the likelihood of incisional complications?**

1. ***Bischofberger AS,*** Ringer SK, Geyer H, Imboden I, Ueltschi G, Lischer CJ. 15th Annual Scientific Meeting ECVS 2006. Sevilla, Spain. **Histomorphologic and scintigraphic evaluation of extracorporeal shock wave therapy of the origin of the suspensory ligament and fourth metatarsal bone in sound horses.**

10.5 Research projects

Ongoing research projects

10. Seidler A, Ohlerth S, ***Bischofberger AS.*** Tenosynovitis of the equine digital flexor tendon sheath: Comparison of ultrasound, tenovaginoscopy and tenography findings.
    2017 – 2018 University of Zürich, CH
    Clinical study – Supervisor of master thesis

9. Stäubli T, Bryner M, ***Bischofberger AS.*** **Complete rupture of the SDFT in horses.**
    2016 - 2017 University of Zürich, CH
    Clinical study - Supervisor of master thesis

8. Schoster A, Altermatt N, ***Bischofberger AS.*** **Retrospective analysis of outcome and complications after large intestinal trocharisation in horses (2004-2015).**
    2015 - 2017 University of Zürich, CH
    Clinical study - Co-investigator of master thesis

7. Suarez J, Kühn K, ***Bischofberger AS,*** Richter H, Kircher P, Hoey S. **Comparison between magnetic resonance imaging, computed tomography and arthrography to identify cartilage defects of the equine carpal joints.**
    2015 - 2017 University of Zürich, CH
    Experimental study - Co-investigator of resident project

6. Schön S, Ohlerth S, Mosing M, Fürst A, ***Bischofberger AS*****. Evaluation of the distribution of mepivacain 2% following local infiltration of the infraorbital nerve via the infraorbital foramen**.
    2015 - 2017 University of Zürich, CH
    Experimental study - Supervisor of resident project

5. Joos R, Ohlerth S, Baschnagel F, Fürst A, ***Bischofberger AS*****. Configuration of orbita fractures in horse**. 2014 - 2017 University of Zürich, CH
    Experimental study - Scientific supervisor of Dr. med vet thesis

4. ***Bischofberger AS,*** Fürst A, Kircher P**. Delayed gadolinium enhanced magnetic resonance imaging and T2 mapping of cartilage to depict early degenerative cartilaginous change in horses.**
    2014 - 2017 University of Zürich, CH
    Experimental study - DVM,PhD thesis

3. Bachmann A, Fürst R, Fürst A, ***Bischofberger AS.*** **Mapping of the biochemical properties of the articular cartilage of normal and diseased distal interphalangeal joints.**
    2015 – 2017 University of Zürich, CH
    Experimental study - Scientific supervisor of Dr. med vet thesis

2. Fürst R, Fürst A, ***Bischofberger AS.*** **Validation of dGEMRIC and T2 mapping for quantifying distal interphalangeal joint cartilage thickness in Warmbloods.**
    2015 - 2017 University of Zürich, CH
    Experimental study - Scientific supervisor of Dr. med vet thesis

1. Federici M, Hoey S, Fürst A, ***Bischofberger AS*. Surgical and conservative management of luxations of the superficial digital flexor tendon from the calcaneus in horses.**
2014 - 2017 University of Zürich, CH
Retrospective clinical study - Supervisor of resident project

Completed research projects

20. Kirchmeier A, ***Bischofberger AS.*** **Delayed gadolinium enhanced magnetic resonance imaging following IV contrast administration in distal interphalangeal joints.**
2015 - 2016 University of Zürich, CH
Clinical study - Supervisor of master thesis

19. Frei S, Fürst A, ***Bischofberger AS.*** **Anatomical considerations for the fixation of supraglenoid tubercle fractures in horses.**
2014 - 2016 University of Zürich, CH
Experimental study - Scientific supervisor of Dr. med vet thesis

18. Schwenk B, Fürst A, ***Bischofberger AS.*** **Traffic accident-related injuries in horses.**
2014 - 2016 University of Zürich, CH
Retrospective clinical study - Supervisor FVH research project

17. Joos R, Federici M, ***Bischofberger AS.*** **Descriptions of the fracture configuration of basal proximal sesamoid bone fractures in non-race horses**.
2014 - 2015 University of Zürich, CH
Clinical retrospective study - Supervisor of master thesis

16. Studer N, ***Bischofberger AS.*** **Depression fractures of the equine skull.**
2013 - 2015, University of Zürich, CH
Clinical retrospective study - Supervisor of master thesis

15. Butz N, Dreyfus A, Fürst A, ***Bischofberger AS.*** **Couronnement beim Pferd**
2013 – 2015, University of Zürich, CH
Clinical retrospective study - Supervisor of master thesis

14. ***Bischofberger AS,*** Lambertini L, Perkins N, Dart A. **In a preliminary study Fucoidan and Omeprazole were equally efficient in preventing and treating experimentally induced gastric ulceration in horses.**
2011 University of Sydney, Australia
Experimental study - Co-supervisor of Summer research student.

13. ***Bischofberger AS*,** Tsang A, Waschk M, Horadagoda N, Perkins N, Jeffcott L, Dart A. **Preliminary study on the effect of Protein C on distal limb wound healing in horse.**
2010 - 2011. University of Sydney, Australia
Experimental study - Supervisor of student honors thesis

12. ***Bischofberger AS*,** Horadagoda N, Dart CM, Perkins N, Little C, Jeffcott L, Dart A. **The effect of manuka honey gel on the transforming growth factor β1 and β3 concentration,**

bacterial counts and histomorphology of contaminated full thickness skin wounds in equine distal limbs.
2009 - 2011 University of Sydney, Australia
Experimental study – Primary investigator

11. ***Bischofberger AS,*** Werezska M, Hadidane I, Perkins N, Jeffcott L, Dart AJ. **Optimal tension, position and number prostheses required for maximum rima glottidis area after laryngoplasty.**
2010 University of Sydney, Australia.
Experimental study - Co-supervisor of Summer research student

10. ***Bischofberger AS,*** Hadidane I, Werezska M, Perkins N, Jeffcott L, Dart AJ. **Effect of age and prostheses on the location of the rima glottidis area in equine cadaveric larynges.**
2010 University of Sydney, Australia
Experimental study - Co-supervisor of Summer research student

9. Kwan C, Bell R, Koenig T, ***Bischofberger AS,*** Horodagoda N, Perkins N, Jeffcott L, Dart AJ. **Effects of intra-articular sodium pentosan polysulphate and glucosamine in horses on the cytology and viscosity of synovial fluid.**
2010 University of Sydney, Australia
Experimental study - Co-investigator

8. ***Bischofberger AS,*** Dart CM, Perkins N, Kelly A, Jeffcott L, Dart AJ. **The effect of short and longer term treatment with manuka honey on second intention healing of contaminated and non-contaminated wounds on the distal aspect of the forelimbs in horses.**
2008 - 2010 University of Sydney, Australia
Experimental study - Supervisor of student honors thesis

7. ***Bischofberger AS,*** Dart CM, Perkins N, Dart AJ. **A preliminary study on the effect of manuka honey on second intention healing of contaminated wounds on the distal aspect of the forelimbs of horses.**
2008 - 2010 University of Sydney, Australia
Experimental study - Primary investigator

6. ***Bischofberger AS,*** Brauer T, Gugelchuck G, Klohnen A. **Difference in incisional complications following exploratory celiotomies using antibacterial-coated suture material for subcutaneous closure: Prospective randomised study in 100 horses.**
2007 - 2008 Chino Valley Equine Hospital, CA USA
Prospective clinical study - Primary investigator

5. ***Bischofberger AS,*** Klohnen A. **Ultrasound in colic horses.**
2007 - 2008 Chino Valley Equine Hospital, CA, USA
Retrospective clinical study - Primary investigator

4. Klohnen A, Sonis J, Raffetto J, *Bischofberger AS.* **Adhesion formation rate after exploratory celiotomies in horses with and without intra-abdominal use sodium carboxymethylcellulose: a 4 year study.**

2007 - 2008 Chino Valley Equine Hospital, CA, USA
Retrospective clinical study - Co-investigator

3. ***Bischofberger AS,*** Fürst A, Auer J, Lischer CJ. **Surgical management of complete diaphyseal third metacarpal and metatarsal bone fractures: Clinical outcome in 10 mature horses and 11 foals.**
2004 - 2007 University of Zürich, CH
Retrospective clinical study - Primary investigator

2. ***Bischofberger AS,*** Ringer SK, Geyer H, Imboden I, Ueltschi G, Lischer CJ. **Histomorphologic evaluation of extracorporeal shock wave therapy of the fourth metatarsal bone and the origin of the suspensory ligament in horses without lameness.**
2004 - 2005 University of Zürich, CH
Experimental study - Dr. med. vet. thesis

1. ***Bischofberger AS,*** Konar M, Ohlerth S, Geyer H, Lang J, Ueltschi G, Lischer CJ. **Magnetic resonance imaging, ultrasonography and histology of the origin of the suspensory ligament: A comparative study of the normal anatomy in fore- and hindlimbs of 4-13 year old warmblood horses.**
2004 - 2005 University of Zürich, CH
Experimental study - Primary investigator

11 Acknowledgements

First I would like to thank **Prof. Dr. Patrick Kircher** for taking over the position of my thesis supervisor and for giving me scientific guidance whilst completing this thesis.

Further, I would like to thank **Prof. Dr. Anton Fürst** for taking over the position of my thesis co-supervisor and for his mentorship. Without his ideas and guidance this thesis would not have been possible.

Thank you to **Prof. Dr. Willy Hofstetter** for taking over the position of my PhD mentor.

I am grateful to **Prof. Dr. Sheila Laverty** for taking over the position of external co-referee. I would especially like to thank her for sharing her huge experience in the field of osteoarthritis. Her mentorship, professional motivation and study ideas helped me to come up with the study design and to complete this thesis.

Thank you to **Dr. Ann Carstens** for her valuable scientific input, her experience in the field of quantitative MRI, her motivation for this project and her kind nature helped me throughout this thesis.

Further I would like to thank:
Dr. Regula Fürst, Andrea Bachmann, Muriel Federici and **Angela Kirchmeier** for their help with the cartilage measurements and the histological scorings.

Aymone Lenisa for her valuable help in the histological processing.

Monika Hilbe und **Sabina Wunderlin** for their help in the immunohistological processing and in the supervision of the histological image analysis.

Prof. Paul Torgerson for his contribution to the statistical analysis.

Claudia Di Giovanna and **Erika Brühlmann** for the MR image acquisition and technical support.

Thank you to all my co-workers, senior clinicians, residents and interns, I have worked with on my way, for making it a memorable experience throughout.

Thank you to my family, without your encouraging and supporting excellence, I could have not achieved any of my endeavors. I feel very blessed.

20.11.2017

12 Declaration of originality

Declaration of Originality

Last name, first name: Bischofberger, Andrea

Matriculation number: 99-725-897

I hereby declare that this thesis represents my original work and that I have used no other sources except as noted by citations.
All data, tables, figures and text citations which have been reproduced from any other source, including the internet, have been explicitly acknowledged as such.
I am aware that in case of non-compliance, the Senate is entitled to withdraw the doctorate degree awarded to me on the basis of the present thesis, in accordance with the "Statut der Universität Bern (Universitätsstatut; UniSt)", Art. 69, of 7 June 2011.

Place, date Zürich, 25. Sept. 2014

Signature A. Bisch